Nuclear Science ISBN 92-64-01056-4

Accelerator and Spallation Target Technologies for ADS Applications

A Status Report

NEA No. 5421

NUCLEAR ENERGY AGENCY
ORGANISATION FOR ECONOMIC CO-OPERATION AND DEVELOPMENT

ORGANISATION FOR ECONOMIC CO-OPERATION AND DEVELOPMENT

The OECD is a unique forum where the governments of 30 democracies work together to address the economic, social and environmental challenges of globalisation. The OECD is also at the forefront of efforts to understand and to help governments respond to new developments and concerns, such as corporate governance, the information economy and the challenges of an ageing population. The Organisation provides a setting where governments can compare policy experiences, seek answers to common problems, identify good practice and work to co-ordinate domestic and international policies.

The OECD member countries are: Australia, Austria, Belgium, Canada, the Czech Republic, Denmark, Finland, France, Germany, Greece, Hungary, Iceland, Ireland, Italy, Japan, Korea, Luxembourg, Mexico, the Netherlands, New Zealand, Norway, Poland, Portugal, the Slovak Republic, Spain, Sweden, Switzerland, Turkey, the United Kingdom and the United States. The Commission of the European Communities takes part in the work of the OECD.

OECD Publishing disseminates widely the results of the Organisation's statistics gathering and research on economic, social and environmental issues, as well as the conventions, guidelines and standards agreed by its members.

* * *

This work is published on the responsibility of the Secretary-General of the OECD. The opinions expressed and arguments employed herein do not necessarily reflect the official views of the Organisation or of the governments of its member countries.

NUCLEAR ENERGY AGENCY

The OECD Nuclear Energy Agency (NEA) was established on 1st February 1958 under the name of the OEEC European Nuclear Energy Agency. It received its present designation on 20th April 1972, when Japan became its first non-European full member. NEA membership today consists of 28 OECD member countries: Australia, Austria, Belgium, Canada, the Czech Republic, Denmark, Finland, France, Germany, Greece, Hungary, Iceland, Ireland, Italy, Japan, Luxembourg, Mexico, the Netherlands, Norway, Portugal, Republic of Korea, the Slovak Republic, Spain, Sweden, Switzerland, Turkey, the United Kingdom and the United States. The Commission of the European Communities also takes part in the work of the Agency.

The mission of the NEA is:

- to assist its member countries in maintaining and further developing, through international co-operation, the scientific, technological and legal bases required for a safe, environmentally friendly and economical use of nuclear energy for peaceful purposes, as well as
- to provide authoritative assessments and to forge common understandings on key issues, as input to government decisions on nuclear energy policy and to broader OECD policy analyses in areas such as energy and sustainable development.

Specific areas of competence of the NEA include safety and regulation of nuclear activities, radioactive waste management, radiological protection, nuclear science, economic and technical analyses of the nuclear fuel cycle, nuclear law and liability, and public information. The NEA Data Bank provides nuclear data and computer program services for participating countries.

In these and related tasks, the NEA works in close collaboration with the International Atomic Energy Agency in Vienna, with which it has a Co-operation Agreement, as well as with other international organisations in the nuclear field.

FOREWORD

Under the auspices of the NEA Nuclear Science Committee (NSC), the Working Party on Scientific Issues in Partitioning and Transmutation (WPPT) was created in June 2000 to examine and provide information on the status and trends of scientific issues in partitioning and transmutation (P&T). In line with the scope of the WPPT and in order to cover a wide range of different disciplines in the P&T field, four subgroups were formed under the WPPT, each tasked with producing a state-of-the-art report in its specialised field. The four subgroups address:

- accelerator utilisation and reliability;
- chemical partitioning;
- fuels and materials;
- physics and safety of transmutation systems.

The mission of the subgroup on accelerator utilisation and reliability is to (1) evaluate the potential utilisation of accelerator-driven spallation targets as part of transmutation systems, (2) organise one or more workshop(s) of experts on accelerators, spallation targets and beam entrance windows in order to consider, evaluate and rank potential issues related to system performance and reliability, (3) evaluate expected performance of accelerators, spallation targets and beam entrance windows for applications associated with accelerator-driven transmutation systems (ADS), and (4) propose a prioritised list of issues that need to be resolved relating to the interaction of an accelerator and target system.

This present status report, produced by the subgroup on accelerator utilisation and reliability, describes different options and ongoing research concerning accelerator and spallation target technologies for ADS applications.

Acknowledgements

The Secretariat expresses its sincere gratitude to all members of the subgroup for their valuable contributions and to the authors of this report. Special thanks are conveyed to Ms. Hélène Déry for having prepared the report for publication.

TABLE OF CONTENTS

Chapter 1

INTRODUCTION

This document discusses the differing options and ongoing research in key technologies required for accelerator demonstration systems (ADS) for nuclear waste transmutation. Chapter 2 describes the two main accelerator options: linear accelerators or cyclotrons. Chapter 3 discusses the spallation target technology with details on the materials, target windows, performances, and thermo-hydraulics.

Although several technologies appear promising for industrial-scale systems, based on our present understanding of the possible technologies, a linear accelerator driving a lead-bismuth spallation target appears to be capable of providing the necessary neutron fluence and can be directly scaled from demonstrated technologies.

Chapter 2

ACCELERATOR TECHNOLOGY FOR XADS AND ADS APPLICATIONS

2.1 Introduction

Different beam performance levels are envisioned to satisfy the requirements of an XADS (experimental) facility and an ADS (industrial-scale) plant. In an XADS facility, the blanket power needs to be high enough to be representative of a full-scale ADS burner; a value between 80 MW_{th} and 100 MW_{th} is considered adequate. Nominal parameters for the accelerator driving such an XADS facility are a beam power of 5 MW to 10 MW at an energy of 600 MeV or more, so that subcritical multiplier operation over a large range of k_{eff} can be evaluated.

For an industrial-scale ADS plant, on the other hand, the nominal fission power would be about a factor of 10 greater than in XADS, on the order of 500 MWth to 1 500 MWth per burner. To minimise capital costs, several such burners could be driven by a single accelerator, as envisioned in the US Roadmap[1] for ADS development and deployment, published in 1999. In that scenario, a 1 GeV 45 MW beam would drive four 850 MW transmuters. The European ADS Roadmap,[2] published in 2001, visualises a single 1 GeV 25 MW to 50 MW accelerator driving a single large transmuter whose thermal power ranges from 500 MWth to 1 500 MWth. This arrangement would be more expensive, but likely raises fewer issues in terms of control, reliability, and safety. The ultimate beam specifications for both an XADS facility and ADS industrial systems will be dependent on the range of k_{eff} desired for operation of the subcritical assemblies.

The optimum proton energy for production of neutrons by spallation in a heavy metal target, in terms of costs, target heating, and system efficiency, lies in the range 600 to 1 000 MeV. Although specific neutron production efficiency (neutrons per unit of beam power) continues to increase up to about 2 GeV, a minimum-cost performance-optimised facility is generally obtained at somewhat lower energies due to other factors, such as the beam current, the accelerating gradient, and the accelerator electrical efficiency. For XADS power levels, the optimum energy in terms of minimising the accelerator cost would be about 400 MeV, but target considerations drive the practical lowest beam energy up to 600 MeV. At lower beam energies, the power deposition density in the spallation target is too high, and the energy loss in the beam entrance window becomes significant. For the industrial ADS plant, the range 800 MeV to 1 000 MeV is optimum, with lower energies matched to lower beam powers and vice versa.

Two completely different kinds of machines can be considered for acceleration of high currents of protons to an energy of 600-1 000 MeV: linear accelerators (linacs) and cyclotrons. For an industrial-scale ADS system, the logical accelerator choice would be a linac. The present status of

1. "A Roadmap for Developing Accelerator Transmutation of Waste (ATW) Technology", Report to Congress, DOE/RW-0519, October 1999.

2. "A European Roadmap for Developing Accelerator-Driven Systems (ADS) for Nuclear Waste Incineration", Report of the European Technical Working Group on ADS, April 2001.

cyclotron technology extrapolates to maximum beam powers and energies for a single cyclotron to about 10 MW at 1 GeV. Linac beam theory and recent technology advances have confirmed that a linac capable of delivering up to 100 MW at 1 GeV is a relatively direct extension of existing technology. Well-supported designs for this class of linac were completed several years ago at Los Alamos[3] and Saclay, and operation of a 100 mA (CW) 6.7 MeV prototype front end for such a machine has been demonstrated.[4] Another factor favouring a linac is that the system reliability and fault minimisation will lead to a design requirement that will require the accelerator operating point to be well below the maximum subsystem limits.

As the beam power requirement decreases, the competition between cyclotrons and linacs becomes closer, with pluses and minuses for each approach. A single cyclotron could conceivably satisfy the upper end of the XADS beam power requirement, although its realisation appears close to the envelope of technical feasibility.[5] The advantages of compactness and (potentially) lower cost might be great enough to warrant pushing the technology. However, if the XADS facility has the requirement to be to a transmutation plant demonstration power level, then a linac would likely be the clear choice. If designed from the beginning with an upgrade in mind, a linac could add more RF stations and/or accelerating modules to increase the beam power by factors of 3 to 5.

At lower beam power levels (1 to 3 MW), such as for experimental facilities that can be classed as "pre-XADS" (e.g. MYRRHA, TRADE), cyclotron-based systems could be preferred on grounds of compactness and cost.

For all the above applications, the requested beam performance ranges from a factor of a few to more than an order of magnitude above that of the most powerful of presently operating proton accelerators. The design challenge for XADS and ADS machines thus confronts new dimensions of power, complexity, control, and cost. In addition, there are new requirements for previously unattained levels of beam reliability and beam intensity control. These requirements are imposed by the need to limit lifetime damage to the subcritical assemblies and their fuel elements, and provide acceptable safety margins in reactor-like environments. The reduction of beam interrupts to levels that can be tolerated by the transmuters will place unprecedented demands on accelerator component and system reliability, will require fault-tolerant accelerator designs, will require for larger than presently used in practice operating margin, and will call for a significant level of component and system redundancy.

The specific accelerator reliability requirements will be dictated by the design of the selected subcritical transmuter system, and in particular the choice of fuel and coolant technology. Some transmuter designs and fuels are more tolerant to beam interrupts than others. These transmuter-dependent reliability requirements will govern the allowable number of beam interrupts per year for different interrupt time periods.

The beam operating mode of an XADS or industrial ADS accelerator will necessarily be CW (continuous wave), in order to deliver the time-averaged power, although pulsed-mode operation will likely be needed for testing and tune-up.

---

3. LANL (1997), *APT Conceptual Design Report*, Report LA-UR-97-1329, April 1997.

4. LANL (2001), *Summary of LEDA RFQ Performance*, Report LA-UR-01-2670, July; also Young, L.M. *et al.*, (2000), *High Power Operations of LEDA*, Proc. LINAC2000, 21-25 August 2000, Monterey, California, pp. 336-340.

5. Stammbach T. *et al.*, (1999), *The Cyclotron as a Possible Driver for an ADS*, OECD/NEA Proc. 2nd International Workshop on Utilisation and Reliability of High-Power Proton Accelerators, 22-29 November 1999, Aix-en-Provence, France; and *PSI Annual Report*, Annex IV, 1998.

2.1.1 Linear accelerators

Proton linear accelerators (linacs) have a very high intrinsic performance capability in terms of beam energy and current, because of their fundamental principles of operation. They consist of long chains of very similar accelerating cavities that are excited electromagnetically at microwave frequencies (300 MHz to 1 000 MHz) by RF power amplifiers. Each cavity increments the beam energy by a few MeV, so several hundred are needed in the accelerating chain. The beam passes only once through the accelerator.

In a linac, strong (alternating-gradient) transverse focusing is applied using quadrupole magnets placed at frequent intervals between the accelerating cavities. Relatively strong longitudinal focusing is produced by the high frequency of the RF cavities. These two factors set a much higher limit to the charge per bunch that can be accelerated (without significant beam loss) in comparison with the situation in a cyclotron, where both the transverse focusing and longitudinal focusing are weak. The strong focusing forces mean that (in principle) linacs could accelerate peak currents of up to several 100 mA, which is one to two orders of magnitude higher than in a cyclotron. Due to injector limitations and space-charge effects at low beam energy, the practical current limit is in the range of 100-150 mA. Because of the linear geometrical configuration, there are no problems in extracting the beam in a loss-free manner. Also, given an adequate machine length, the final beam energy is not limited on dynamical grounds or by relativistic effects (proton mass increase with energy).

Proton linacs have traditionally been constructed from normal-conducting (NC) copper accelerating cavities cooled by water. At sufficiently high beam currents ($\geq$ 50 mA), the electrical efficiency of such linacs is high because the RF power delivered to the beam considerably exceeds the RF power lost in the cavity walls. In recent years, proton linac designs and new construction, such as the SNS facility being built at Oak Ridge,[6] have replaced copper accelerating structures with liquid helium (LHe) cooled niobium superconducting (SC) structures in the high-energy section of the machine. This eliminates the wall RF power losses, significantly increasing the electrical efficiency.

A significant drawback for a linac is the fact that the beam passes only once through each accelerating structure. This leads to a long machine, with large numbers of accelerating cavities and RF-power systems. The linac length depends on the final beam energy and the accelerating gradient. SC-cavity technology can provide high average accelerating gradients, a factor of three or more greater than in NC linacs, which reduces the length dramatically compared with the present generation of machines. However, a 1 000 MeV linac is still more than 300 meters long. The length-related factors are major cost drivers. In addition to the cost of the many accelerating cavities and RF power stations, the cost of the long underground tunnel and its associated infrastructure that is required to house the accelerator and provide shielding against radiation produced by small beam losses scales in cost with length.

2.1.2 Cyclotrons

Cyclotrons are based on the principle that charged particles moving in a constant transverse magnetic field have a fixed revolution frequency, independent of the particle energy. This frequency, the cyclotron resonance frequency, is proportional to the particle charge and inversely proportional to its mass and the magnetic field value. As the particle energy rises to relativistic levels, the simple

6. Kustom, R.L. (2000), *An Overview of the Spallation Neutron Source Project*, Proc. LINAC2000, 21-25 August 2000, Monterey, California; also White, M. (2002), *Spallation Neutron Source*, Proc. LINAC2002, 19-23 August 2002, Gyeongju, South Korea.

relationship breaks down due to the relativistic particle mass increase. To address this effect, high-energy cyclotrons are designed so that the average magnetic field along the orbital path increases gradually with radius, maintaining the resonance condition; this is achieved by breaking the magnet into a small number of spirally shaped sectors. In a cyclotron, the beam executes many turns isochronously within the machine, the orbits increasing in radius as the particles gain energy. The particles pass repeatedly through a small number of large resonant accelerating cavities, which typically span the entire machine radius. These cavities, which typically have frequencies near 50 MHz, deliver a small energy gain to the beam bunches on each revolution, until the final energy is reached, and the particles are extracted from the outermost orbit.

High-energy high-intensity cyclotron systems employ two or three cascaded acceleration stages. A proton energy of 1 GeV seems to represent a reasonable upper limit for a such multi stage cyclotron design, and although a beam current of about 10 mA appears attainable, significant design challenges are expected.

A major issue for a high-energy high-current cyclotron is the beam extraction system. To limit beam losses and minimise machine activation, the deflector system that guides the beam from the outermost orbit out of the cyclotron's magnetic field, (using a special magnetic channel and a high voltage electrode), is permitted to intercept only a very small fraction of the particles. The current limit in a cyclotron is thus determined by the design requirement for producing a very clean beam at the outer radius of the machine, with a sufficiently large radial separation from the previous orbit. The orbit separation depends on the energy gain achieved per turn, which depends on the voltage capability of the RF cavities and the number of cavities.

2.2 Status of accelerator technology

2.2.1 Linacs

Most of the existing operating proton linacs are injectors for large synchrotrons, and are short-pulse low-duty-factor machines with relatively low average beam current and power. The major exception is the LANSCE linac at Los Alamos, an 800 MeV accelerator that can deliver an average beam power exceeding 1 MW, with a peak current of about 20 mA, a duty factor of up to 10%, and macropulses 0.5-1.0 ms long. Currently the most powerful proton linac in the world, LANSCE beam availability is usually > 90% during scheduled operations. All the presently operating large proton linacs were constructed with normal-conducting (NC) water-cooled copper accelerating structures; most were designed and built 20 to 30 years ago. The low-energy sections (< 100 MeV) are Alvarez drift-tube linacs (DTLs), typically operating at close to 200 MHz, and the high-energy sections (> 100 MeV) are made up of chains of resonantly coupled individual cavities operating at several times the DTL frequency.

The beam-launching stage for these linacs typically was a DC proton injector installed in a Cockroft-Walton high-voltage generator (750 kV), followed by a beam longitudinal buncher in the low-energy transport line to the linac. In the early 1980s, a major technology advance appeared, providing a radically improved solution for this challenging first acceleration stage – the radio-frequency quadrupole (RFQ). The RFQ, which consists of four orthogonally arranged vanes or rods with scalloped profiles in a resonant cavity, provides both a quadrupole transverse RF field for focusing and a longitudinal RF field for bunching and acceleration. The RFQ, at first, gradually bunches the DC beam from the injector with a high capture efficiency, and then accelerates the bunches to a few MeV. Beam tails in longitudinal phase space were greatly reduced in comparison

with the earlier situation, greatly reducing beam losses in downstream accelerator structures, and considerably higher peak currents became available.

A new generation of pulsed high-current linacs for driving neutron sources and other nuclear research facilities has been designed over the past few years, and two projects are under construction. In their execution, these new linac designs have taken advantage of technology advances that have ensued during the past three decades, including the introduction of the RFQ as the initial accelerating stage, dramatic improvements in beam simulation and understanding of beam loss, and the application of SC cavity technology to the high energy linac sections. The high-current pulsed H^- linac of the Spallation Neutron Source (SNS), presently under construction at Oak Ridge in the USA, is a 1 GeV 1.4 MW machine with 1.0 ms pulses and a peak current of 38 mA. The high-energy section of this machine is made up of superconducting (SC) niobium accelerating cavities. When it reaches its full design performance, the SNS linac will replace LANSCE as the most powerful proton linac.

The joint KEK/JAERI high-intensity accelerator complex now being built in Japan includes a 400 MeV pulsed linac (to be extended to 600 MeV) that provides an average beam power of up to 0.28 MW with 50 mA peak current. The high-energy section of this machine also employs SC cavities.

The European Spallation Source (ESS), now on hold, specifies a 1.33 GeV H^- linac delivering a beam power of up to 5 MW in 2 ms pulses, with a peak current of about 100 mA. The high-energy section of this machine was to have been a NC side-coupled linac, an updated version of the high-energy section of the LANSCE linac.

In a linac, the maximum peak current that can be accelerated is dictated largely by the charge per bunch that can be accommodated by the transverse focusing lattice and the accelerating cavity dynamics; for all the existing machines, this value has typically been much higher than the required average current, which has been 1 mA or less. For a given beam energy, the linac length depends on the representative cavity accelerating field, and the fraction of the accelerator that is filled with cavities (filling factor). The RF power required to excite each NC accelerating cavity (without beam) is proportional to the square of the accelerating field. To minimise the electric power drawn from the grid, and also the investment cost, pulsed operation has been an economic necessity for nearly all existing NC linac-based facilities. The low duty factor maintains a relatively high peak current, and thus a relatively high electrical efficiency. For very high average currents, on the order of 100 mA, a NC linac operating at 100% duty makes economic sense. In that situation, the power transferred to the beam is so high (100 MW for 1 GeV energy) that a reasonable efficiency is obtained even if several 10s of MW of RF power is dissipated in the walls of the accelerating cavities. Designs of high-power linacs for tritium production that were developed in the USA and France in the early 1990s were based on this approach. The linac designed at Los Alamos for the Accelerator Production of Tritium (APT) project was initially a 100 mA CW, 1 700 MeV accelerator consisting of an Alvarez-type drift tube linac (DTL) up to 200 MeV, followed by a LANSCE-style side-coupled linac to the full beam energy.

Because of the dramatic advances made during the 1970s and 1980s in the development of elliptical superconducting (SC) niobium accelerating cavities for electron linacs, synchrotrons, and storage rings, and in LHe refrigeration and distribution systems, SC cavity technology began, in the mid 1990s, to be considered seriously for high-current proton beam acceleration. Hundreds of CW superconducting cavities were by then in operation at CERN (LEP II), Jefferson Lab (CEBAF), and KEK (Tristan), with accelerating gradients exceeding 5 MV/m.

Owing to the very low RF losses in the superconducting regime (five orders of magnitude lower than for NC copper), the power required to sustain high accelerating fields is practically negligible,

and almost 100% of the RF power is transferred to the beam. The electrical efficiency becomes very high, even with beam currents much lower than in the 100 mA APT design. Also, because of the high accelerating gradients that are achievable in a SC CW linac, this technology permits the construction of a much shorter machine than is possible using NC technology. For example, two full multicell cavities have been built by INFN (tested at TJNAF and Saclay), reaching cavity accelerating fields of 14 to 17 MV/m.

Offsetting the reduced RF power load somewhat is the electric power needed to operate the LHe refrigeration system (cryoplant) that is required to maintain the SC cavities at their low operating temperature (2 K to 4.5 K). The refrigeration load for an SC linac depends on the total cold cavity length, the cavity gradient, and the operating temperature. Given the typical static heat load from the environment to SC-linac cryomodules, and the cryoplant efficiency, the AC power required to sustain the accelerating field in SC cavities is presently a few kW per MeV of energy gain; this is true both for LEP II cavities (4.5 K) and CEBAF cavities (2 K). Recent improvements to cryomodule design (demonstrated at TESLA) and in the quality of niobium promise significant reductions in AC power used.[7] TESLA cryomodules, with SC cavities operated at 12 MV/m, require refrigeration AC power of only 600 W per MeV of acceleration.

The final design for the APT accelerator,[8] developed in 1997 and depicted in Figure 2.1, assumed a SC linac from 211.4 MeV to 1 030 MeV, with the NC technology applied only to the low-energy section of the linac. The SC-cavity design gradient was 5 MV/m, which allowed a much shorter machine than the original all-NC design, as well as one that was electrically significantly more efficient. Additional advantages provided by the SC design included extremely low beam losses because of the very large apertures that are practical in elliptical SC cavities, improved tolerance to machine errors and faults, and better operational flexibility.

Figure 2.1. Final design of APT linac, with SC high-energy section

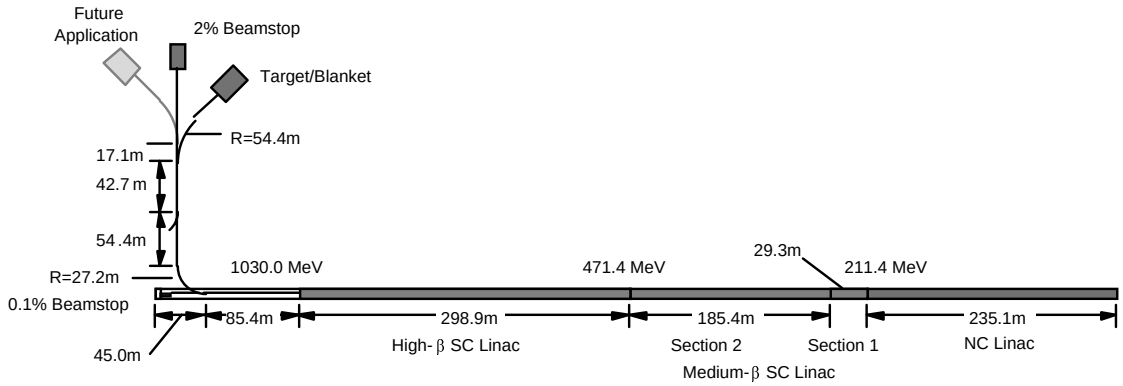

In the APT linac, two different SC cavity designs were used. Cavities corresponding to beta = 0.64 provided acceleration from 211.4 MeV to 471.4 MeV, while cavities corresponding to beta = 0.82 covered the range 471.4 MeV to 1 030 MeV. Lower beta cavities were considered for the region between 100 MeV and 211.4 MeV, but were not included in the design or the R&D program

7. Pagani, C. (1999), *Status and Perspectives of the SC Cavities for TESLA*, Proc. of the 1999 CEC-ICNC, July 1999, Montréal, Canada.

8. Lawrence, G.P. (1998), *High-Power Proton Linac for APT; Status of Design and Development*, Proc. of LINAC98, 23-28 August 1998, Chicago.

because of concerns about mechanical stability. Later, several laboratories, including KEK and Saclay successfully tested elliptical cavities at beta values near 0.5, which are suitable for this energy range. Thus, an updated APT linac design would have extended the SC part of the linac down to at least 100 MeV, and perhaps as low as 80 MeV.

2.2.1.1 Reference XADS or ADS linac architecture

Because of the technology advances described above, a present-day reference design for an XADS linac or an ADS industrial linac would be based on the use of SC elliptical cavities above an energy of about 100 MeV. The first few MeV of energy gain would be provided by an RFQ accelerator similar to the one recently developed and tested at Los Alamos in the low-energy demonstration accelerator (LEDA), or the one designed for the IPHI programme (CEA/CNRS/CERN collaboration). The next acceleration stage (from 5 MeV to 100 MeV), called either the low-energy linac or the intermediate energy part, could be made up of either NC or SC accelerating structures. Until very recently, the most likely solution for this region would have been a series of resonantly coupled Alvarez-type short DTL (drift-tube linac) sections, as in the design developed for the IPHI programme.[9] However, there have been dramatic advances in the last few years in the development of superconducting ½-wave resonators (spoke cavities), which are well suited to proton acceleration in the beta region between 0.15 and 0.5. Tests of suitable spoke cavity prototypes have been conducted by several laboratories, showing that gradients of 8 MV/m or greater can be achieved.[10] These results have encouraged linac designers to consider replacing the NC low energy portion of an XADS or ADS linac (from 5 MeV to 100 MeV) with a linac made up of several sections of spoke cavities, each section having a beta value appropriate for a different velocity range. As in the case of the elliptical cavities used for the high-energy linac, the use of SC spoke cavities eliminates RF wall losses that are present in the NC low-energy linac, along with the water cooling requirement, which is a major challenge for any low-beta CW copper structure. The overall accelerator power efficiency is improved, approaching 50%. In addition, cavity apertures can be somewhat larger than for NC structures, reducing the beam loss in the low-energy section of the linac. The use of SC cavities in this region also provides increased operational flexibility, and the potential for improved fault tolerance, which would improve beam reliability.

The high-energy SC accelerating cavities would operate in the frequency range of 600 to 900 MHz, and at a temperature close to 2 K. The low-energy accelerating structures, whether NC or SC would operate at half the frequency of the high-energy section, and would likely operate at a temperature of 4.5 K.

In the SNS pulsed linac design, the transition energy from NC to SC cavities was set at 190 MeV rather than an energy closer to 100 MeV because of concerns about Lorentz-force detuning in lower beta cavities, which is an important issue for pulsed operation, but not for CW operation. The SNS linac transition energy was also pushed to a higher (more conservative) value because of the lack of SC cavity prototyping in the lower beta range at the time the decisions were made.

The suggested ADS reference linac would thus be composed of a sequence of four different accelerating systems, as indicated below. Considerations of reliability and power efficiency have to take into account the particular characteristics of the different accelerator types. The energies chosen

9. Bernaudin, P.E. (2001), *Design of the IPHI DTL*, Proc. PAC2001, 18-22 June 2001, Chicago.

10. Tajima, T. *et al.* (2003), *Results of Two LANL Beta = 0.175, 350-MHz, 2-Gap Spoke Cavities*, Proc. of PAC2003 Conf., 12-16 May 2003, Portland, Oregon.

for the transition from one accelerator to another should be considered only as nominal, the precise value being determined by an overall design optimisation. The four accelerators are:

- DC injector: up to 100 keV.
- RFQ: up to 7 MeV.
- NC linac (DTL) or SC spoke-cavity linac: up to 100 MeV.
- SC linac (elliptical cavities): up to design energy (1 GeV).

The beam exiting the SC high-energy linac is transported to the XADS or ADS spallation target by a high-energy beam transport (HEBT) system composed of quadrupole and dipole magnets. Near the end of this transport channel, a beam expansion or rastering system generates a uniform beam on the target face with the desired shape and area. A rastering system similar to the one fully prototyped at Los Alamos as part of the APT program would likely be suitable, provided that the raster time period is short compared with the thermal time constant of the target and subcritical multiplier.

The present state of the art of the first two linac components (injector plus RFQ) sets a current limit for the accelerator on the order of 100 mA. Higher proton currents could be obtained by combining beam outputs from two low-energy linac sections (at 10 to 20 MeV) by means of funneling, a beam-combining technique proposed in the 1980s. However, the viability of this process, in terms of emittance preservation and beam stability, has not been fully established.

2.2.1.2 Proton injector

Prototypes of 100% duty proton injectors with output current $\geq$ 140 mA have been developed and successfully tested at Los Alamos and CNRS/CEA collaboration.[11,12] These are shown in Figure 2.2 and Figure 2.3 below. Both injectors employ microwave-driven ion sources of similar design, and both use solenoid lenses in the low-energy beam transport to the RFQ, with nearly complete space-charge neutralisation from trapped electrons. Measured output emittance values are about 0.2 mm-mrad at 100 mA. The LEDA injector operating voltage is 100 kV, while the IPHI injector voltage is 80 kV. In operating the IPHI injector at an output current 20% below the design value, no beam trips were observed on the test stand in weeklong runs. Extrapolating this preliminary performance data to the ADS design current level, less than one beam trip per week (due to extraction-electrode sparking) would be anticipated. Similarly encouraging results have been obtained with the LEDA injector.

From the experience gained in these two injector prototyping programs, as well as related test programs in Japan and Italy, the proton injector appears to be well understood, can clearly provide the needed XADS and ADS performance with no significant technical issues, and appears to be capable of very high reliability.

---

11. Sherman, J.D. *et al.* (1998), "Status Report on a dc 130-mA, 75-keV Proton Injector", *Rev. Sci. Instr.* **69,** 1003-8.

12. Gobin, R. (1999), *Reliability of the High Power Proton Source SILHI*, OECD/NEA Proc. 2nd International Workshop on Utilisation and Reliability of High-Power Proton Accelerators, 22-29 November 1999, Aix-en-Provence, France.

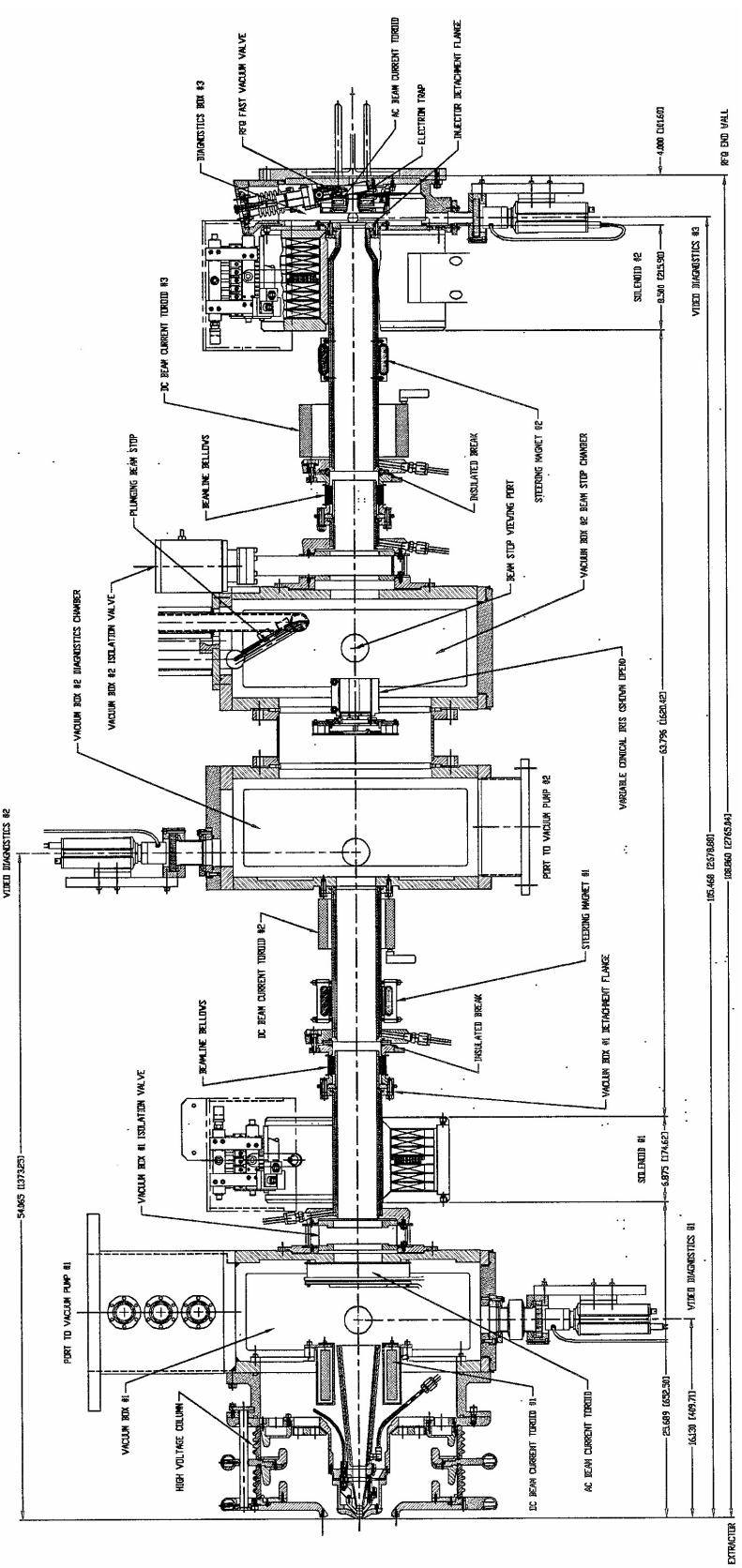

Figure 2.2. Layout of LEDA high-current proton injector

Figure 2.3. SILHI proton injector test stand operated by CNRS/CEA collaboration installed at Saclay

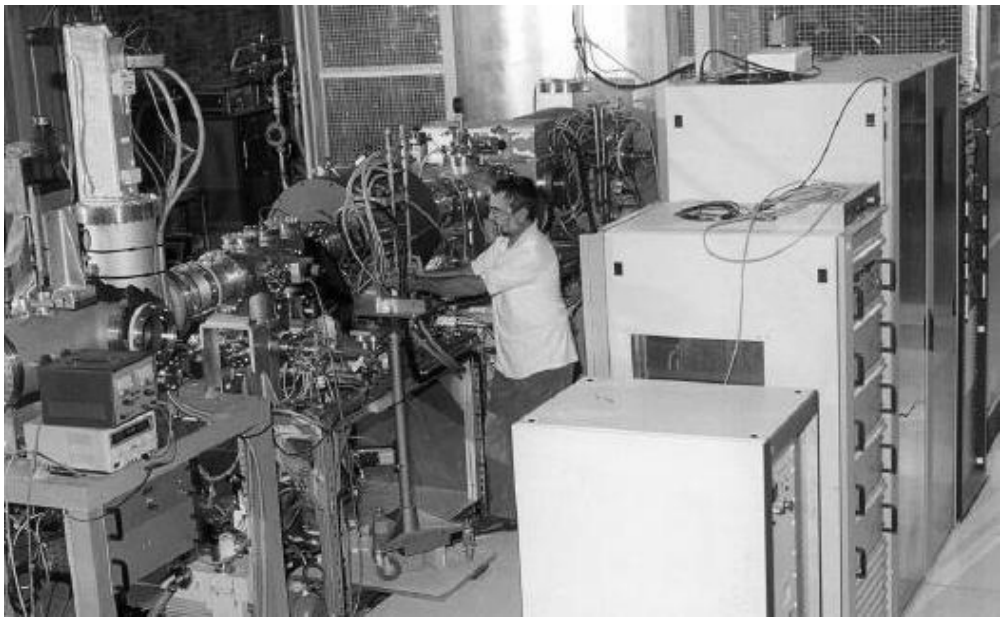

Figure 2.4. Resonantly coupled LEDA RFQ mounted in RF cavity tuning laboratory

2.2.1.3 Radiofrequency quadrupole

At Los Alamos, a 6.7 MeV RFQ prototype operating at a frequency of 350 MHz has been tested at up to 100 mA CW, as part of the LEDA project.[13,14,15] This RFQ, which is constructed from four resonantly coupled sections, is 8 meters long and is driven by three 350 MHz 1 MW klystrons. This RFQ was designed for 95% beam capture. About 1.3 MW of RF power is absorbed in the structure walls. Figure 2.4 shows the RFQ structure in the RF tuning laboratory, and Figure 2.5 shows the completed assembly installed in the LEDA accelerator tunnel, with the injector retracted. The successful LEDA RFQ beam tests at 100 mA represent a major step forward in demonstration of the technology of high-current high-power CW linacs, validating the functionality and operability of the critical lowest-energy acceleration stage, where space-charge effects are highest.

Figure 2.5. LEDA RFQ accelerating structure in accelerator tunnel, surrounded by water cooling lines, vacuum manifolds, and RF power feeds. Injector is rolled back

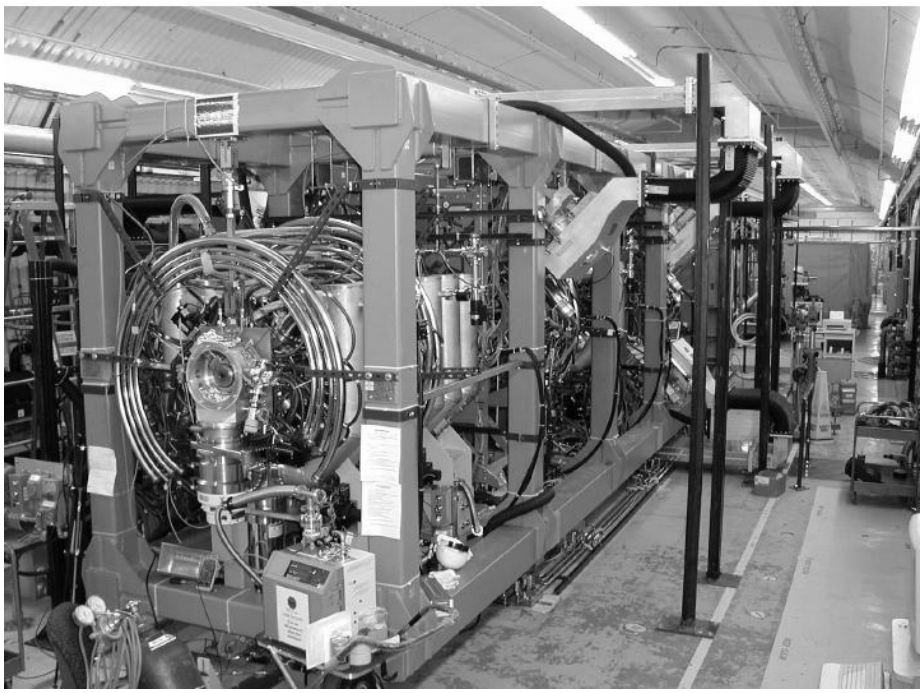

Other CW RFQs have been designed or are under constructed for operation at energies near 5 MeV and CW currents in the 50-100 mA range, at Saclay, JAERI, Legnaro (INFN), and LNL. The 5 MeV Saclay/IPHI RFQ was designed for very high beam capture (98%), using the new code Toutatis. Following the recent suspension of the IPHI programme, the Saclay RFQ (which was in fabrication), is now to be completed to 3 MeV by CERN, where it is to be used for beam injection into the PS linac.

13. Young, L.M. (1994), *An 8-meter-long Coupled Cavity RFQ Linac*, Proc. 1994 Int. Linac Conf., 21-26 Aug. 1994, Tsukuba, pp. 178-180.

14. Johnson K.F. *et al*. (1999), *Commissioning of the Low- Energy Demonstration Accelerator (LEDA) Radio-Frequency Quadrupole (RFQ)*, Proc. PAC99, 29 March-2 April 1999, New York, p. 3528-3530.

15. Smith Jr., H.V. and J.D. Schneider (2000), *Status Report on the Low-Energy Demonstration Accelerator (LEDA)*, Proc. LINAC2000, 21-25 August 2000, Monterey, California, pp. 581-3.

As a result of the recent LEDA RFQ design experience and performance tests, as well as design and modeling work carried out at other laboratories, the general impression is that this critical part of an XADS or ADS linac can be implemented as a very reliable component, assuming that there is sufficient performance margin built in. Beam interrupts in the LEDA RFQ tests appeared mainly due to reliability problems in the high power RF components, particularly the RF generators (klystrons) and the high-power RF-coupler windows.

2.2.1.4 Low-energy linac (5 MeV to 100 MeV)

The Alvarez drift-tube linac (DTL) is a venerable and well-established structure for accelerating high peak currents of protons from below 1 MeV to energies up to 200 MeV in pulsed accelerator applications, typically at a frequency near 200 MHz. It has been used since the early 1950s in injector linacs for most proton synchrotrons worldwide, and is used to 100 MeV in the LANSCE linac. In these machines, the DTL is implemented in the form of long resonator tanks each containing a large number of drift tubes, whose lengths increase in step with the increasing proton velocity. The focusing elements (electromagnet quadrupoles) are housed within the drift tubes, providing a short focal length lattice. Even the new generation of pulsed linacs, such as the SNS accelerator and the KEK/JAERI machine, continue to use the Alvarez DTL structure, although generally in shorter tanks.

2.2.1.4.1 Normal-conducting designs for LE linac (CCDTL and SDTL)

A 100%-duty version of an Alvarez DTL with parameters appropriate for XADS or ADS linacs presents new engineering challenges, chiefly in terms of removal of the large amount of RF power deposited in the accelerating structure surfaces. The thermal management problem is similar to that already solved in the development of CW RFQs, and practical 3 D computer codes now exist for joint optimisation of the electromagnetic and thermo-mechanical design. Two variations on the conventional DTL were proposed for the high-current NC low-energy linac designs in the US and French tritium programs (APT and TRISPAL). These were carried over into the early plans for XADS and ADS machines in the US AAA program and the IPHI/TRASCO collaboration in Europe.

In the reference APT accelerator, the NC low-energy linac, sketched in Figure 2.6, was designed with two types of coupled copper structures. The second section, from 96 MeV to 211 MeV, was a conventional side-coupled $\pi/2$ mode linac, with six cells per tank; quadrupoles were mounted outside the accelerating structure between tanks. The first section, from 6.7 MeV to 96 MeV, was a new concept, a coupled-cavity drift-tube linac (CCDTL), which chained together very short accelerating cells in the $\pi/2$ coupling mode, with each cell containing one or more drift-tubes, the accelerating cells were resonantly connected by means of side-mounted coupling cells. The CCDTL promised an improvement over the Alvarez DTL for CW high-current applications, because it provided very high RF stability, using a mode and coupling arrangement similar to that in side-coupled high-energy linac, and also allowed the quadrupoles to be located external to the accelerating structure between the short DTL sections, where they could be easily adjusted. However, in terms of practical engineering and implementation, several complications were encountered. Tests of CCDTL section prototypes showed significant frequency stability problems, which appear to be due to high sensitivity to small mechanical deformations, coupled with inadequate cooling channel design. Also, the horizontal coupling cells needed for a compact structure presented serious design and fabrication challenges. As a result of the now suspended development program, the CCDTL structure is viewed as a too-complex and expensive solution for a CW low-energy NC linac, although cooling design improvements or structural redesign could probably have eliminated the frequency stability problems.

Figure 2.6. Transition between CCDTL and CCL accelerating structures in APT at 100 MeV

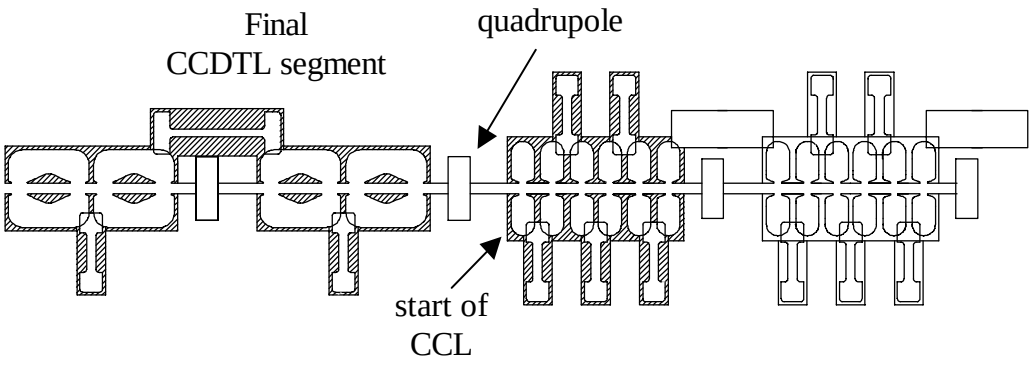

Another solution for a NC CW low-energy linac is the Saclay/IPHI scheme, which retained the Alvarez DTL idea, but implemented it as a short-tank drift-tube linac (SDTL). In this concept the low-energy CW linac was to be made up of made up of very short DTL tanks that are resonantly coupled together with side-mounted cells.[16] In this design, each DTL tank contains only a few drift tubes, and the transverse focusing and accelerating functions are longitudinally separated. The quadrupoles are located between the DTL sections, rather than inside the drift tubes. Figure 2.7 shows a photograph of the drift assembly for the prototype SDTL section. Unfortunately, the prototype was not fully completed or tested before suspension of the IPHI programme, although the quadrupoles were built and tested satisfactorily. However, because the SDTL is a basically an extension of the demonstrated Alavarez DTL design, implementation is expected to be straightforward.

Figure 2.7. Saclay SDTL prototype drift-tube assembly

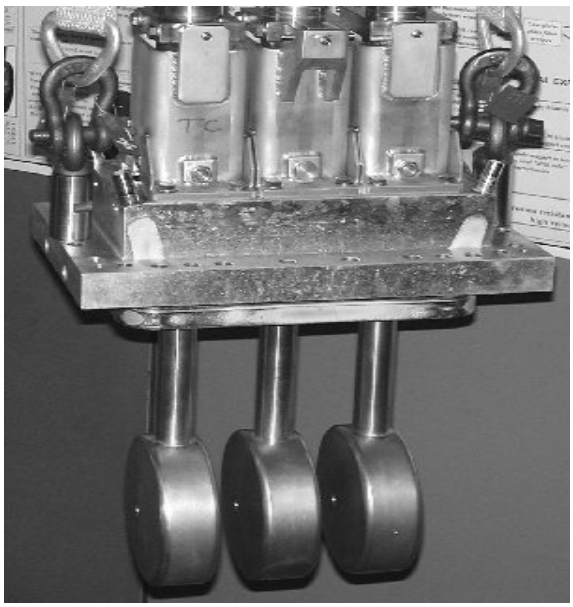

16. Bernaudin, P.E. (2001), *Design of the IPHI DTL*, Proc. PAC2001, Chicago, 18-22 June 2001.

2.2.1.4.2 Superconducting approach for LE linac (1/2-wave resonators)

An alternative approach to the LE linac for an XADS or ADS linac, which is currently being evaluated in the US, Europe, and Japan, is the use of accelerating modules made up of superconducting niobium ½-wave (spoke-cavity) resonators. Initial prototypes of such cavities were first built and tested at Argonne National Laboratory in the 1980s as part of the SDI program, and then more recently as candidate accelerating cavities for the medium-beta section of the proposed RIA (Rare Isotope Accelerator) project. Similar structures (1/4 wave resonators), integrated into cryomodules, have been in use at ANL for the Atlas accelerator since the early 1980s. One of the ANL RIA prototype cavities (beta = 0.34) was tested further at Los Alamos after improved surface preparation, and provided excellent performance. More recently, 350 MHz spoke cavities suitable for the beta = 0.175 region of an ADS linac were designed at Los Alamos, fabricated by industry, and tested at Los Alamos.[17] Figure 2.8 illustrates the design of a single-spoke (2-gap) beta = 0.175 350 MHz cavity, and Figure 2.9 shows one of the Los Alamos test cavities without its end plates. Test results, shown in Figure 2.10, show that these cavities can provide high field performance, 8 MV/m at Q (quality factor) = 1×10^9.

Figure 2.8. Sketch of β = 0.175 2-gap spoke cavity

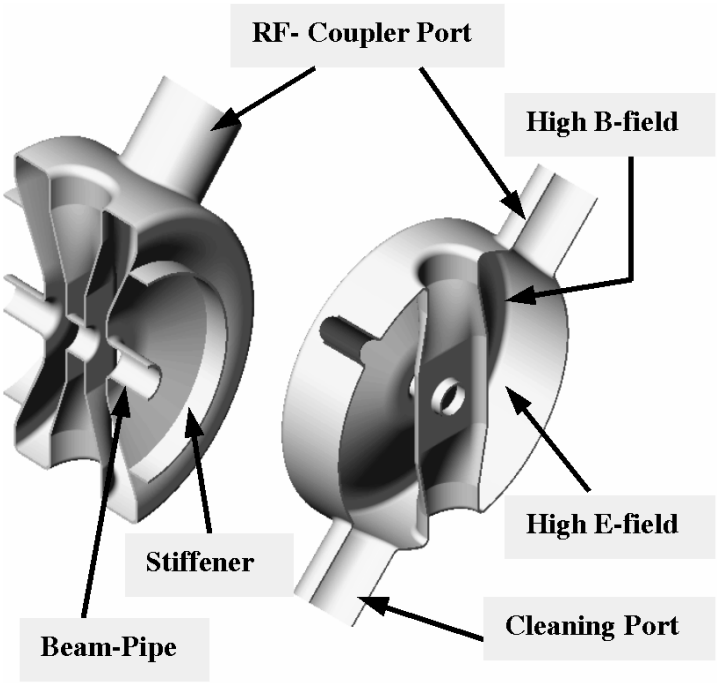

17. Tajima, T. *et al.* (2003), *Results of Two LANL Beta = 0.175, 350-MHz, 2-Gap Spoke Cavities*, Proc. of PAC2003 Conf., 12-16 May 2003, Portland, Oregon.

Figure 2.9. Niobium β = 0.175 spoke cavity before mounting end plates

Figure 2.10. Test results from two LANL β = 0.175 spoke cavities fabricated by Zanon

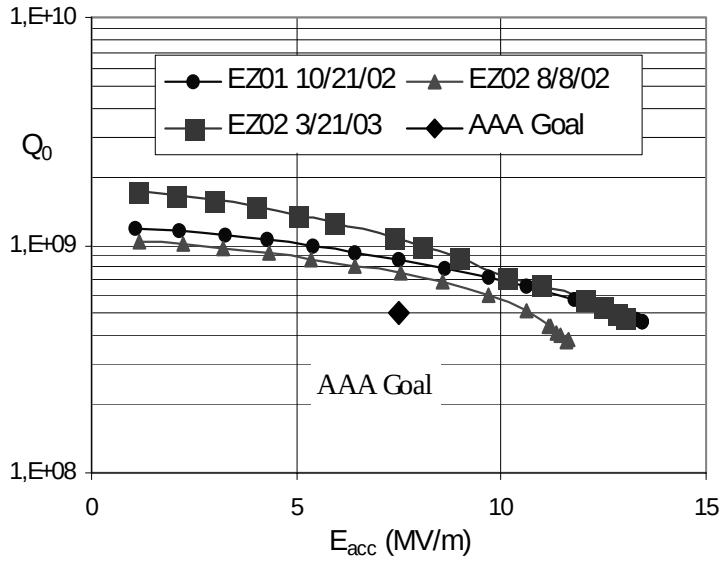

Use of superconducting spoke cavities in the low-energy section of an XADS linac would reduce the total RF power requirement for the entire accelerator by a large factor, saving on both capital and operating costs. The higher gradient attainable in SC structures also would allow the use of independently driven cavities, without sacrificing overall linac length. Independent resonators would permit fast recovery from faults by energy compensation in the rest of the linac in the same fashion as has already been considered for the high-energy SC linac. Finally, the larger apertures that can be achieved in spoke cavities would reduce the probability of beam loss in the LE linac and make it more

tolerant to imperfections in assembly or operation. In short, spoke resonators may provide significant advantages over any kind of DTL-based NC linac. Present designs have the XADS and ADS linacs made up of spoke-cavity cryomodules from the RFQ to about 100 MeV followed by beta = 0.5 elliptical cavities filling the region from 100 MeV to about 200 MeV. A remaining issue still to be addressed before full implementation of a spoke cavity architecture is testing of RF power couplers that are fully integrated into a spoke cavity.

Since the spoke cavities give good performance at 4.5 K, work is proceeding with designing the entire linac with spoke cavities. This would have the benefit of eliminating the requirement for a 2 K cryoplant with its supporting infrastructure requirements.

Several laboratories are developing and testing prototype spoke cavities, including those with more than two accelerating gaps. Figure 2.11 shows a fabricated cavity in the test laboratory, of a single-spoke (2-gap) 352 MHz cavity and Figure 2.12 shows cavity performance at 4.2 K.[18] Two cavities are planned to be installed in a single cryomodule being developed by IPN-Orsay as part of the XADS and EURISOL programs. FZJ is building triple spoke cavities for a pulsed proton neutrino generating machine.[19] Drawings and pictures of the FZJ triple spoke cavities are shown in Figure 2.13.

Figure 2.11. Two-gap prototype 352 MHz beta = 0.35 spoke cavity fixed on its insert at IPN-Orsay

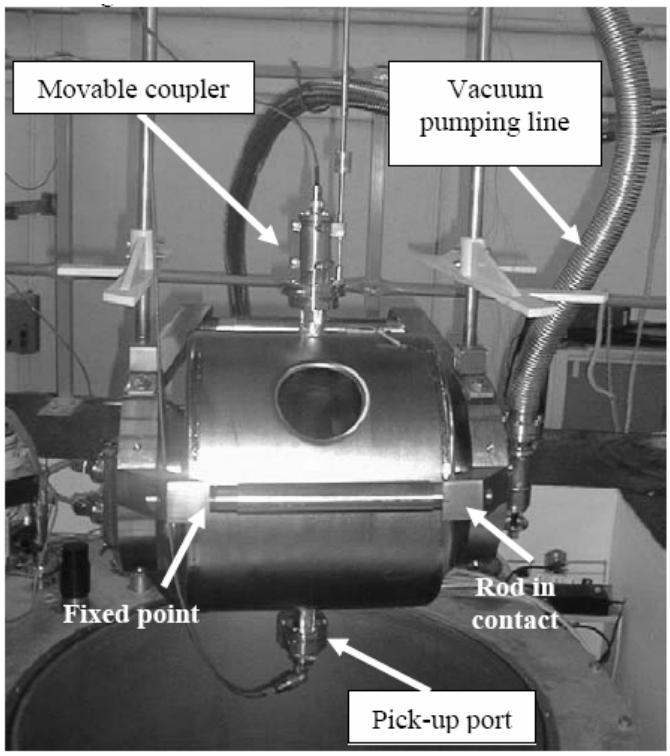

18. Olry, G. (2002), *RF Design of the Beta 0.35 Spoke Cavity AMANDA*, Workshop on the Advanced Design of Spoke Resonators, 7-8 September 2002, Los Alamos, New Mexico.

19. Zaplatin, E. *et al.* (2004), *Triple-spoke cavities at FKJ*, EPAC2004.

Figure 2.12. Q_0 vs. E_{acc} curves at 4.2 K for the 352 MHz spoke cavity

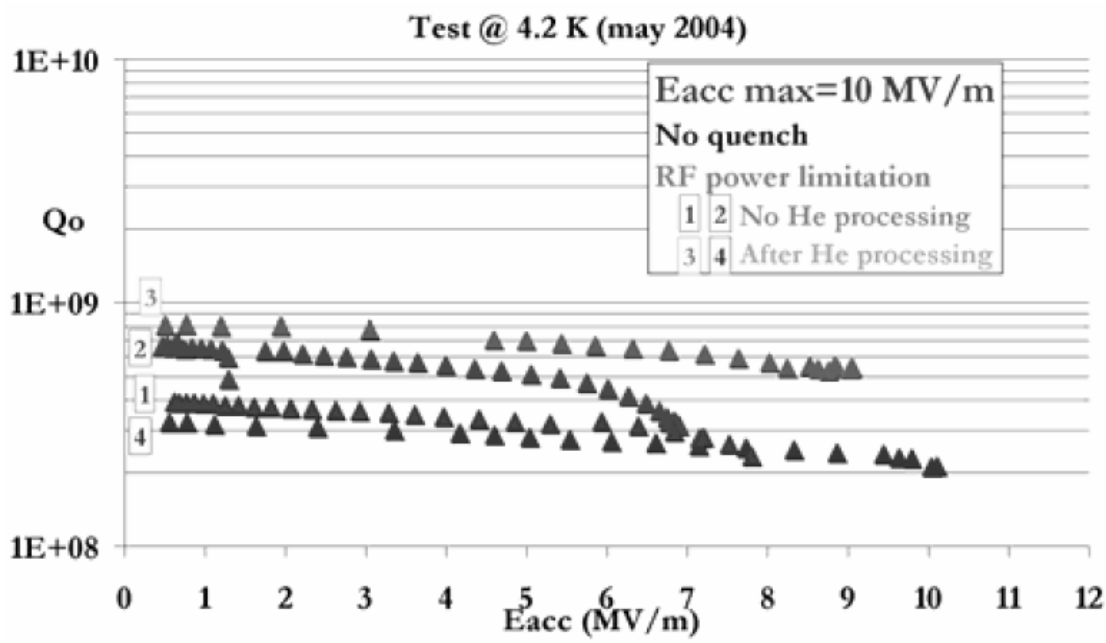

Figure 2.13. Triple-spoke cavity prototype at FZJ – schematic view, copper model and Nb parts

2.2.1.5 High-energy linac

The high-energy section of an ADS linac, from 100 MeV to the output beam energy, would be made up of a series of cryomodules containing SC niobium cavities with quasi-elliptical shapes. A superconducting HE linac provides many now well-recognised advantages over earlier NC designs, including reduced length, reduced capital and operating costs, and larger apertures. SC linacs offer improved operational flexibility, reduced sensitivity to construction and tuning errors, nearly vanishing beam losses, and intrinsically greater tolerance to faults. The last property has particular relevance for reliability. Design of the SC high-energy linac for an ADS accelerator is derived from the experience gained with elliptical SC cavities and cryomodules at CERN, JLAB, DESY, and KEK, where many high performance SC accelerating modules are in reliable operation in electron linacs and storage rings. The switch of the SNS (Spallation Neutron Source) high-energy linac design from its original NC-cavity design to SC cavity technology, in spite of a tight project execution schedule, is strong proof that the expectations of reduced capital and operating costs, as well as improved reliability are now fully realistic for this technology.

The elliptical cavities in the high-energy section of an XADS or ADS linac have shapes that are compressed along the longitudinal axis to match the reduced beam velocities in a proton accelerator, in contrast with the beta = 1 cavities characteristic of electron machines. High-energy SC linac designs call for two or three different cavity shapes, depending on the total beam-energy span, each of which is optimised to provide maximum accelerating efficiency over part of the range. A relative velocity (beta) value of about 0.5 is suitable for accelerating the beam from 100 MeV to 200 MeV, and the optimisation of the second and the third beta values depends on the linac output energy.

Figure 2.14 is a prototype beta = 0.47 intermediate energy-range cavity built for the TRASCO/ADS program. Figure 2.15 shows the performance in a vertical test cryostat of several 5 cell beta = 0.47 cavities.[20] Typical values are beta = 0.65 for beam energies from 200 MeV to 500 or 600 MeV, and beta = 0.8 or more for the highest-energy section of the linac. Figure 2.16 shows a prototype 5 cell beta = 0.64 cavity built for the APT technology development program. Test results from the beta = 0.64 five-cell elliptical cavities are shown in Figure 2.17. Figure 2.19 shows the configuration of the cavities in a cryomodule, and their relationship to adjacent focusing elements and Figure 2.20 shows the internal details of a 2 cavity cryomodule.

Figure 2.18 shows the test results on a 5 cell beta = 0.65 cavity manufactured by CERCA under the auspices of a CEA-Saclay/IPN-Orsay collaboration.[21] This works was mainly supported by the XADS and European Isotope Separator On-Line (EURISOL) programs.

20. Pierini, *et al.* (2004), EPAC2004.

21. Visentin, B. *et al.* (2004), *Performance Improvement of the Multicell cavity prototype for proton linac projects*, EPAC2004.

Figure 2.14. The TRASCO/ADS 5 cell β=0.47 cavities ready for welding of He Tank showing the stiffening rings for mechanical stability

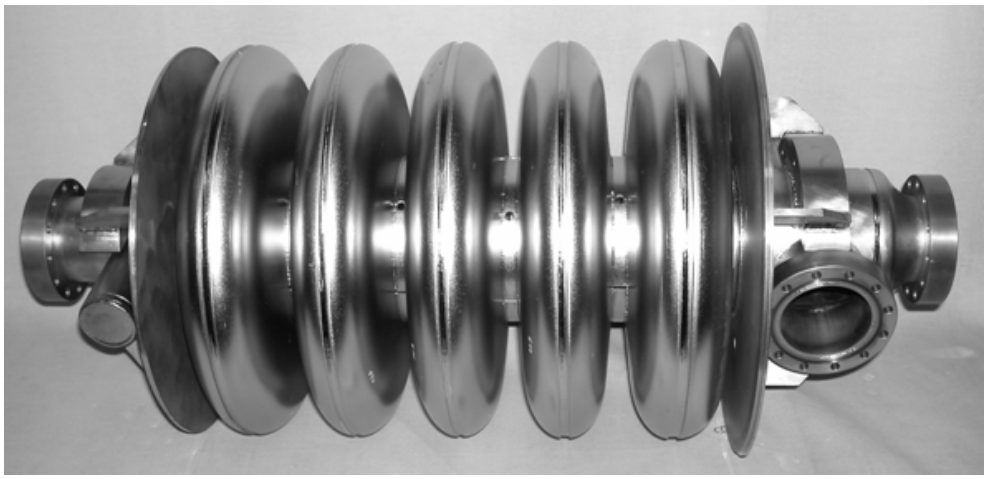

Figure 2.15. Experimental measurements of the performance TRASCO/ADS 5 cell ß = 0.47 cavities
The two cavities, named Z501 from TJNAF and Z502 from Saclay have a Ep/Eacc of 3.57, and a Bp/Eacc of 5.88 mT/(MV/M)

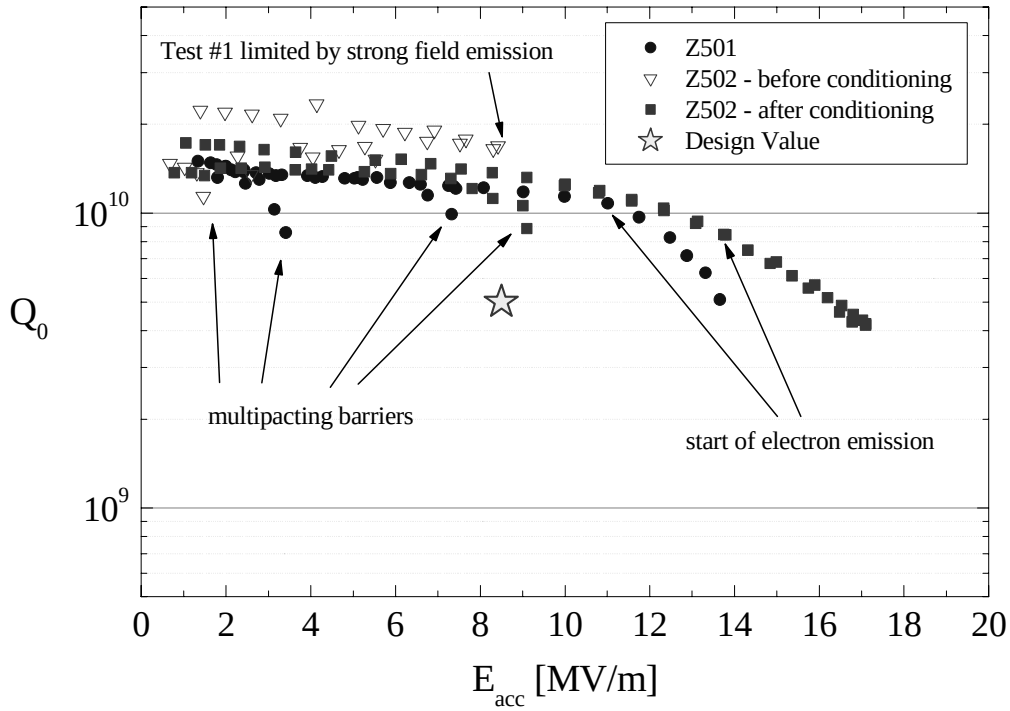

Figure 2.16. Five-cell beta = 0.64 SC cavity fabricated by CERCA

Figure 2.17. Test results from LANL beta = 0.64 five-cell elliptical cavities

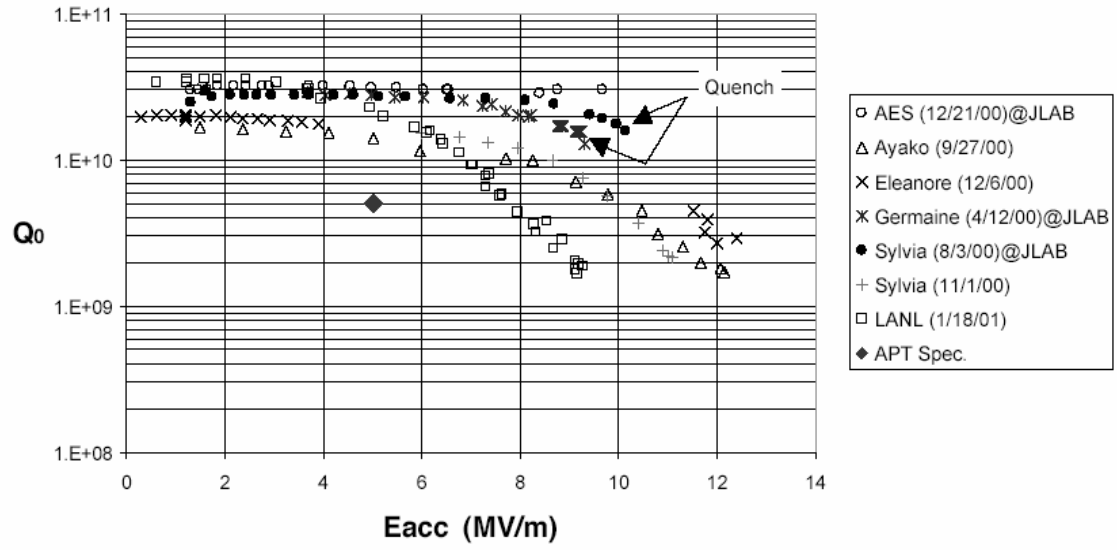

Figure 2.18. Test results from CEA-Saclay/IPN-Orasy beta = 0.65 elliptical cavities

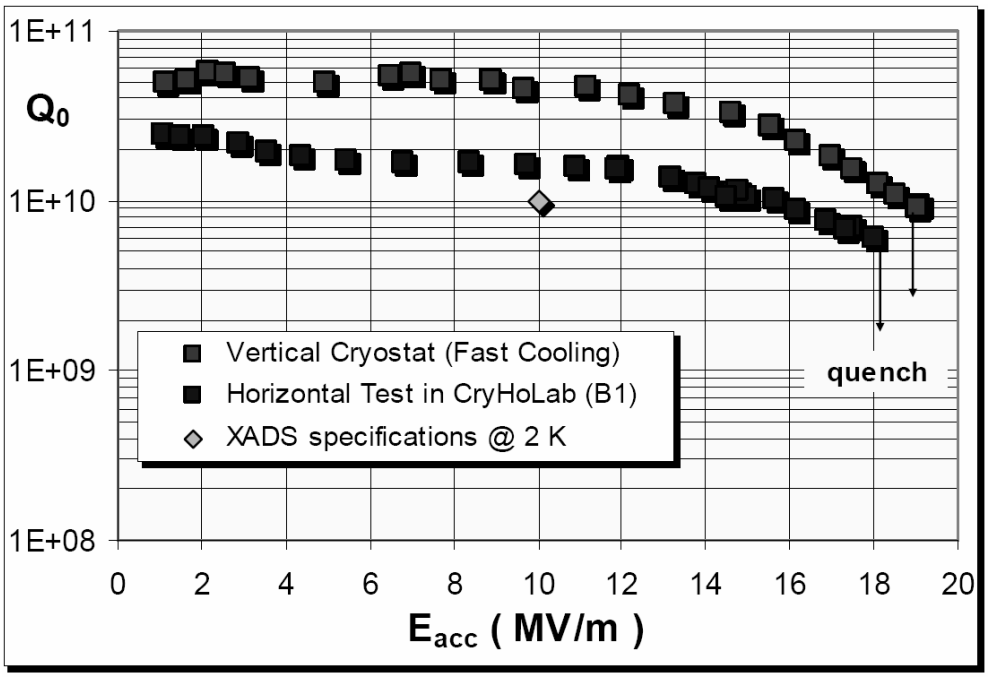

Figure 2.19. Sketch layout of APT beta = 0.64 cryomodule and quadrupole doublet in intervening warm space

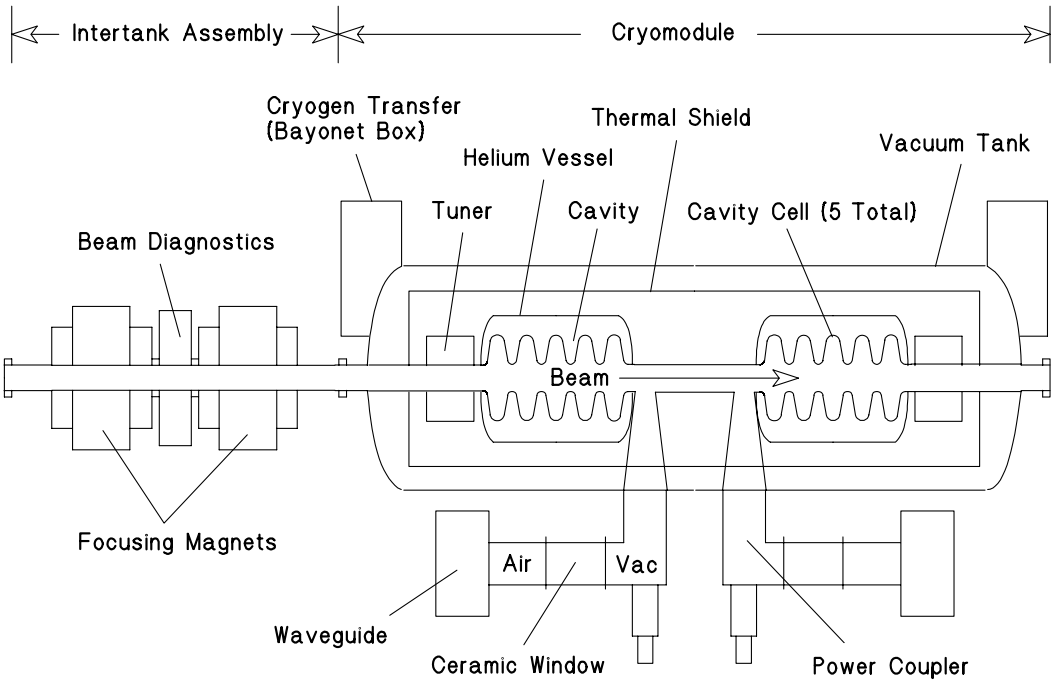

Figure 2.20. Cutaway of APT beta = 0.64 two-cavity cryomodule, showing RF couplers, tuner arrangements, and other details

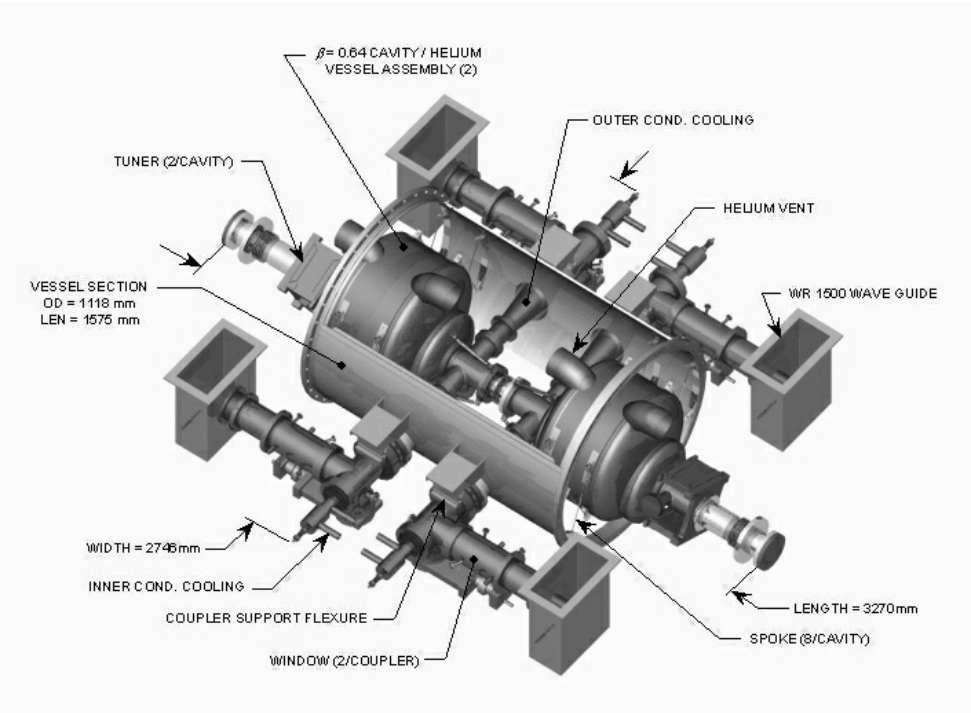

Working prototypes of axially compressed elliptical cavities with various beta values have been built and tested at several laboratories worldwide, and they behave as expected from extrapolating the beta = 1 cavity performance.[22,23,24] As a result of recent gains in SC elliptical cavity performance, resulting from better niobium material and improved surface preparation techniques, cavity accelerating gradients of 10 MV/m can now be assumed, with Q values of better than 1 x 10^{10}. Figure 2.17 shows the performance in a vertical test cryostat of several 5 cell beta = 0.64 cavities fabricated in the APT program cryomodule prototyping program.

Cavity efficiency, in terms of the electric-grid power needed for refrigeration (per MeV of energy gain) increases as beta approaches unity. From basic thermodynamic principles, considerably more refrigeration power is needed for LHe-cooling of high-frequency cavities (> 500 MHz), which operate at 2 K, than for lower frequency cavities, which can operate at 4.5 K.

Beta values significantly below 0.5 appear to be impractical for elliptical cavities because the shape compression becomes too extreme for good accelerating efficiency, and also leads to mechanical stability problems. As discussed earlier, below beta = 0.5, the SC structure of choice appears to be the ½-wave coaxial line (spoke resonator).

---

22. Chan, K.C.D. (1999), *Review of Superconducting RF Technology for High-Power Linacs*, 9th Workshop on RF Superconductivity, 1-5 November 1999, Santa Fe, New Mexico.

23. Safa, H. (1999), *Superconducting RF Linac for Waste Transmutation*, 9th Workshop on RF Superconductivity, 1-5 November 1999, Santa Fe, New Mexico.

24. Chan, K.C.D. *et al.* (2000), *Status of Superconducting RF Linac Development for APT*, Proc. of LINAC2000, 21-25 August 2000, Monterey, California.

2.2.1.6 High-energy beam transport and beam expander

From the output of an XADS or ADS high-energy linac, the full-energy proton beam will be transported to the spallation target (or targets) by a high-energy beam transport (HEBT) system composed of quadrupole and dipole magnets. Depending on the requirements of the subcritical assembly, the entrance to the target may be either vertical or horizontal. A vertical entry (from above) is straightforward to design and construct, but entails additional expense in a large vertical-plane bending magnet system to direct the beam downwards. Vertical entry also requires either a set of elevating bends in the vertical plane that would leave the target/blanket assembly at or near grade level, or placing the target/blanket assembly a significant distance below the accelerator beamline.

Near the end of the HEBT system there will be magnetic expansion elements that transform the Gaussian-profile small-diameter beam into a larger-area uniform density footprint on the face of the spallation target. The footprint may be circular or rectangular in shape, depending on the target/multiplier design. The expander can be a magnetostatic system made up of a combination of quadrupole, octupole, and possibly higher order elements, or a modulator-driven magnet system that rasters the small area beam rapidly in a pattern that uniformly fills the target area. The raster system is preferred, since it avoids the corner intensity spikes in the beam footprint as well as the undue sensitivity to exact beam conditions that is characteristic of the nonlinear static expander. Figure 2.21 illustrates the raster concept. The objective quadrupoles, shown in the figure below, act as magnifiers by projecting the desired beam profile onto the target with the required transverse dimensions.

Figure 2.21. Raster magnet system near end of HEBT

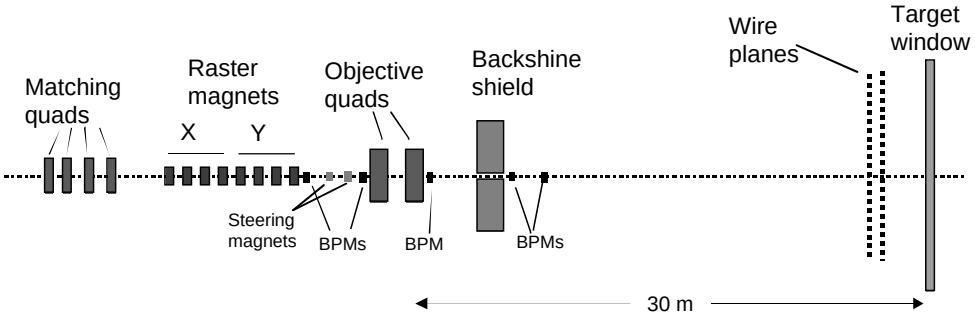

In order to avoid stressing the structural components and fuel of the transmuter, the raster pattern must be repeated within a time frame that is short compared the relevant thermal response times. This requirement implies a raster frequency in the range 1 000 Hz. A high-reliability raster magnet system that is capable of satisfying the needed amplitude and frequency requirements was demonstrated as a full scale prototype[25] as part of the APT technology development program, and is shown in Figure 2.22. Ferrite-core magnets driven, at different frequencies, with triangular waveforms by IGBT modulators deflect the beam in the horizontal and vertical planes to painted a uniformly filled distribution on the spallation target. A multiply redundant modulator fault-detector system protects the spallation target from excess beam-power density due to degradation or interruption of the sweep pattern. These modulators are supplied by uninterruptible power sources, and the magnet multiplicity limits the beam-power density increase at the target to about 33% in the event of any single-point failure.

25. *Final Report: Raster Magnet System for Expanding the APT Proton Beam*, Los Alamos Report LA-UR-99-5820, September 1999.

Figure 2.22. Full-scale prototype raster magnet system suitable for XADS or ADS application

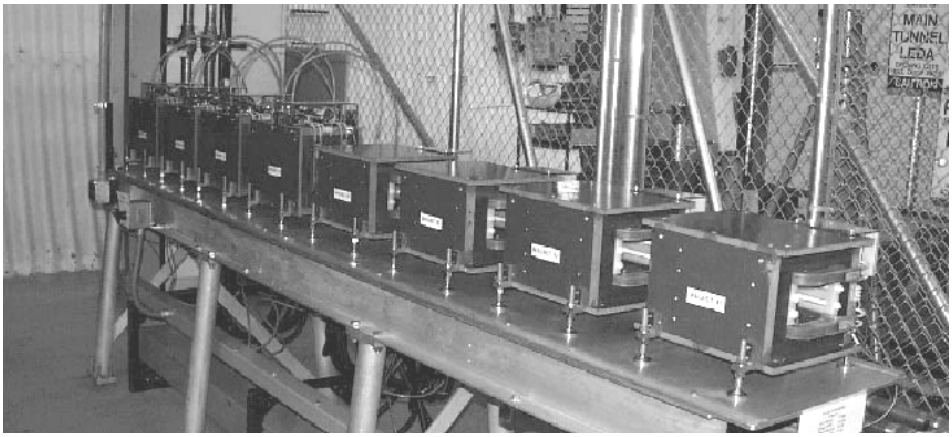

2.2.1.7 Accelerator reliability

Because of concerns about thermal cycling in the subcritical assemblies, XADS (see Section 2.5) and ADS applications impose a fundamental new requirement on the design and operation of high-power proton linacs, namely that of extremely high reliability of the beam. Beam reliability differs from availability. *Availability* is defined fraction of time that protons are delivered to the target at the specified intensity over some fixed interval, typically a year. *Reliability* has to do with the number and durations of beam interrupts in that interval.

Different transmuter concepts and technologies will have different levels of sensitivity to beam interrupts, as do different components and elements in a given type of transmuter. In liquid-metal-cooled systems, the thermal response times of the fuel assemblies is on the order of a few hundred milliseconds, so beam trips of that duration or longer cause significant thermal cycling, leading eventually to life-limiting damage. Other transmuter concepts, such as gas-cooled systems, can suffer much longer beam interrupts without significant damage to their components and fuel. For more information on accelerator reliability see, for example, reference 26.

Preliminary analysis of transmuter responses to beam trips suggests that interrupt intervals can be conveniently divided into three characteristic times, for which there are different impacts on the subcritical assembly.

- Interrupt durations on the order of up to 1 second (depending on transmuter technology) are not detrimental because the thermal transients in the multiplier are then very small. These kinds of interrupts can be said to be “invisible”.
- For longer beam interrupts, from 1 second to the order of 100 seconds, tolerance of beam trips will depend on the particular subcritical multiplier design, and the characteristic thermal response times of its elements. The fuel will likely respond on the fastest time scale (several seconds), the fuel clad and thin transmuter structures on longer time scales (tens of seconds), and thick transmuter structures on still longer time scales (minutes). In terms of life-limiting damage, preliminary analyses suggest that it will be necessary to restrict this class of beam

26. Pierini, P. (2004), *ADS Accelerator Reliability Activities in Europe*, OECD/NEA Proc. of 4th International Workshop on Utilisation and Reliability of High-Power Proton Accelerators, 16-19 May 2004, Daejeon, South Korea.

interrupt to less than 100 per year. However, if these longer beam interrupts necessitate very long restart times, then availability may be impacted as well, and the acceptable annual frequency may need to be even lower, perhaps only a few tens of times per year.

- For beam interrupt intervals greater than 100 seconds, thermal effects in the subcritical multiplier and safe re-start procedures, imply that each incident likely results in a multi-hour or even day-length downtime for an ADS plant. In order to not impact the plant's availability, such long-period interrupts would have to be restricted to a few tens per year at most.

To date, very few tolerance analyses of current ADS transmuter concepts to beam interrupts have been performed. It will be important for multiplier designers to derive tolerance response functions (i.e. allowable frequency of beam trips as a function of beam trip duration) for current and future candidate multiplier concepts. These response functions will then set general requirements for the accelerator design.

2.2.1.7.1 Influence of beam reliability requirements on accelerator design

While beam reliability requirements need more definition in terms of what is acceptable to assure satisfactory transmuter performance and acceptable component lifetimes, it is clear that a dramatic reduction of the beam interrupt rate in comparison with that in existing accelerators will be a dominant driver in the linac design. Operating proton linacs were designed with high beam availability as a key goal, but the frequency of beam interrupts was not a major issue. In fact, the design and operating emphasised the necessity of aborting the beam for almost all accelerator faults, in order to minimise damage to the machine during off-normal conditions. The interrupt rate in the LANSCE linac is typically on the order of 10^4 per year. However, a very large fraction of these are due to momentary effects, such as high-voltage arcs in RF systems, for which the beam has to be interrupted only for a very short period (<< 1 second) while the offending system is restored to operation by automated recovery systems. This leaves perhaps 10^3 annual interrupts of longer duration, which require some kind of operator intervention, as well as those that require repair or replacement of accelerator components. For a recent discussion of classes (duration and cause) of beam trips in existing linacs, and their frequency see reference 27.

Recent workshops have begun to address the way proton linacs for XADS and ADS applications can be designed to meet the new high-reliability goal.[28,29,30] Design objectives for these machines require a reduction in the total annual number of the longer beam interrupts (from current levels) by one to two orders of magnitude. One important way in which this can be accomplished is to shorten the duration of most such interrupts to the "minimal impact" region discussed above (< 300 ms). A

27. Eriksson, M. (1998), *Reliability assessment of the LANSCE accelerator system*, thesis, Royal Inst. of Technology, 1998, Stockholm.

28. Lawrence, G. (1999), *Reliability Considerations in the Design of High Power Linacs*, OECD/NEA Proc. 2nd International Workshop on Utilisation and Reliability of High-Power Proton Accelerators, 22-29 November 1999, Aix-en-Provence, France.

29. Wangler, T. (2002), *Reliable Linac Design for Accelerator-Driven Subcritical Reactor Systems*, OECD/NEA Proc. 3rd International Workshop on Utilisation and Reliability of High-Power Proton Accelerators, 12-16 May 2002, Santa Fe, New Mexico.

30. Safa, H. (1999), *Reliability: a Challenge for Superconducting Cavity Technology*, OECD/NEA Proc. 2nd International Workshop on Utilisation and Reliability of High-Power Proton Accelerators, 22-29 November 1999, Aix-en-Provence, France.

high-reliability accelerator design would include an appropriate mix of the following principles and approaches. Attaining the right balance among these that achieves reliability goals at minimum cost will be the task of trade studies during conceptual designs of XADS and ADS facilities.

- **Fault-tolerant design**. The entire linac should have a fault-tolerant beam dynamics design, meaning that beam operation can continue without interruption, and without excessive beam loss, following the failure of any single accelerating unit (accelerating cavity or RF station). Given superconducting cavities in both the HE and LE linacs, this design can be achieved by insisting that each accelerating unit increments the beam energy by an amount small enough that its absence does not prevent the beam from being adequately contained within the linac acceptance phase space. This design would likely call for each spoke cavity and each elliptical cavity to be driven by its own RF amplifier, which is likely a high-cost solution.
- **Rapid re-tuning in SC linac**. Present design strategy has the LE and HE sections of an XADS or ADS linac both constructed from SC cavities, with only a few cavities driven by each RF amplifier. If there is a small fraction of extra accelerating capacity (of order 5%) installed uniformly along the machine, the failure of a single accelerating unit can be compensated by re-tuning neighbouring and downstream accelerating units to make up for the lost in energy. Using advances made in fast digital control electrons, it should now be possible to carry out such a re-tune within < 100 ms, a time period that falls within the "no impact" range for beam interrupts. The procedure would be roughly as follows. After the control system detects an RF station or cavity (more specifically cavity window) fault that cannot be auto-corrected, beam is switched off momentarily while the cavity is rapidly detuned so that it cannot couple power from the beam into the damaged components. This can be done with magneto-strictively driven mechanical linkages. At the same time, the phases and amplitudes of the compensating accelerating units are rapidly adjusted to provide a smooth accelerating profile around the failed unit, and to provide the correct output beam energy at the end of the linac. Phases can be adjusted in < 1 ms, while amplitude adjustments would take somewhat longer. The beam is then rapidly returned to full intensity. A final tune optimisation can be carried out over the next few minutes without impacting beam continuity. The failed component would be repaired or replaced on line, if possible, or at the next scheduled maintenance period.
- **Redundancy of critical components in NC linac**. Critical equipment in the NC part of the linac (injector, RF power stations, windows, etc.), should have an appropriate level of redundancy. This should limit the beam-off time when interrupts do occur to periods on the order of a few seconds or tens of seconds, while the failed elements are switched out and the replacement elements switched in. With a very high level of component redundancy, it may be possible to ride through most faults, but the capital cost tradeoff could be considerable. If the NC low-energy linac is replaced by a SC spoke-cavity linac, then the need for redundancy is just in the injector and the RFQ RF stations and windows. For this small number of components, a high level of redundancy would be justified. For example, there should be two independent injectors, with the spare unit kept hot and ready to operate.
- **Conservative component ratings**. Critical equipment should be specified and designed to operate with parameter values (voltages, current densities, power levels, etc.) that are much lower than the tested performance envelope. These large performance margins, while building in extra cost, should provide long Mean Time Between Failures (MTBF), reducing the need for redundancy.
- **Equipment performance diagnostics**. Appropriate levels of diagnostics should be integrated into critical equipment to provide monitor its state of health, and provide advance

warning of end-of-life or impending failure. This enables the equipment to be repaired or replaced at a scheduled maintenance time, before its failure causes a beam interrupt.

- **Accessibility of critical equipment**. Equipment and components that are subject to failure between scheduled maintenance periods should be located, as much as possible, in low-radiation zones where they are accessible when the beam is on, so that they can be repaired or replaced without interrupting operation.
- **Elimination of false failures**. Spurious equipment-shutdowns due to sensitive noise-susceptible protection circuits are a major cause of beam interrupts in existing linacs. These shutdowns can be and should be reduced to a very low probability, by methods such as multiple fault diagnostics that are required to agree in their reporting of apparent equipment failures. The exact number and type of diagnostics has to be carefully evaluated lest the failure rates of the diagnostics themselves impact the overall machine reliability.

An XADS or ADS linac will likely need to employ all the above design principles to some degree or other in order to achieve the requested very-low frequency of longer beam interrupts. This frequency will depend sensitively on the equipment performance margins and on the degree of equipment redundancy, which are likely to be significant cost drivers for the accelerator. The estimated frequency of the "visible" beam interrupts that can be achieved with a linac designed from the ground up for ultra-high reliability ranges from a few tens per year to the order of 100 per year, which is a very large reduction from the interrupt rate characteristic of presently operating linacs. Detailed RAMI (reliability, availability, maintainability, inspectability) studies and cost estimates for a range of different linac architectures will be needed to estimate the attainable beam-trip rates, and how they and their cost-impacts depend on various levels of fast control, redundancy, and component performance margins.

Assuming that all the standard systems in an ADS linac would be conservatively designed and built according to strict performance specifications, the long beam trips (minutes, hours, or days) should just be those that are randomly generated by the end-of-life failures of high power components. For example, the present lifetime of high-power klystrons appears to be on the order of 25 000 hours. In a linac containing 100 such RF power generators, about 25 klystron failures per year might be expected due to end-of-life. Perhaps 75% of these incipient failures could be predicted by built in equipment diagnostics, and the affected units replaced during scheduled maintenance, leaving only 6 or so unanticipated annual failures that impact machine reliability. Similar analyses can be made for all the equipment systems or major components whose failure can cause long beam interrupts. Summing over all linac equipment systems in an appropriate manner, estimates can be made for the total annual number of beam interrupts.

2.2.1.8 Beam dynamics, beam losses, and beam halo

Beam losses in a properly designed XADS and ADS linac are expected to be very small. Multiparticle simulations (including realistic machine defects) for the APT 100 mA linac[31,32] and similar studies for TRISPAL and other high-power proton linac designs in Europe have shown that losses along the linac can be reduced to levels compatible with unrestricted hands-on maintenance.

---

31. Wangler, T., E. Gray, F. Krawczyk, S. Kurennoy, G. Lawrence and R. Ryne (1998), *Basis for Low Beam Loss in the High Current APT Linac*, XIXth International Linac Conf., August, 1998, Chicago, p. 657.

32. Wangler, T., B. Blind, S. Nath, R. Ryne and K. Crandall (1999), *Beam Dynamics Design and Simulation Studies of the APT Superconducting Linac*, 1999 Part. Accel. Conf, March 1999, New York, p. 611.

2.2.1.8.1 Losses in RFQ and low-energy linac

Measurements on LEDA in Los Alamos showed that total beam losses are limited to less than 5% in the RFQ at 100 mA output.[33] At lower current levels (80 mA) less than 2% beam losses were measured. For the IPHI RFQ design, which incorporates some improvements such as more complete capture in the bunching process, a reduction in losses by a factor of two was expected.[34] Because most of the beam losses in these RFQs are uncaptured protons at energies close to the injection energy, and because the small fraction of beam that is lost in the RFQ after acceleration still only reaches energies of a few MeV, the beam losses in this first acceleration stage do not cause a significant activation problem.

Beam simulations done for the 100 mA APT NC linac design show no beam losses above 20 MeV, and only very small losses below that energy. The low beam energy at the loss location leads to activation levels small enough for unconstrained hands-on maintenance. The low loss levels are due to several design improvements over the present generation of high-current linacs (e.g. LANSCE) including:

- replacement of the Cockroft-Walton and buncher configurations that typically are used to launch the beam in the present generation of proton linacs with a high-energy RFQ, eliminating longitudinal mismatch and greatly reducing longitudinal phase-space tails;
- use of larger apertures in the accelerating structures, improving aperture to beam-size ratios;
- strong transverse focusing, by using a high density of quadrupoles per unit length; and
- careful attention to avoiding mismatches in the focusing lattice, especially in the transitions between different linac sections, in order to minimise the formation of beam halos.

If SC spoke resonators are used in the LE linac, cavity apertures in this part of the accelerator would be even larger than are feasible with NC structures, further reducing the beam losses in this region.

2.2.1.8.2 Losses in the high-energy linac

In the superconducting HE linac, multi-particle simulations (up to a few million particles per calculation) performed by LANL, Saclay, and INFN, using different computer codes implemented for this purpose. These simulations have shown that, with proper optical matching and reasonable error tolerances, typically zero particles are lost in the accelerator and in the HEBT systems. This is true even at the 100 mA level specified for the APT linac. The extremely low beam loss levels are due to the large aperture-to-beam-size ratios afforded by the elliptical SC cavities and the relatively strong transverse focusing. The APT linac simulation results, with a full set of randomly distributed machine imperfections, are shown in Figure 2.23. These calculations confirm that the operational beam loss

33. Johnson, K.F., *et al.* (1999), *Commissioning of the Low-Energy Demonstration Accelerator (LEDA) Radio-Frequency Quadrupole (RFQ)*, Proc. PAC99, 29 March-2 April 1999, New York, 3528-3530.

34. Ferdinand, R. (1999), *IPHI-RFQ Reliability Approach*, OECD/NEA Proc. 2nd International Workshop on Utilisation and Reliability of High-Power Proton Accelerators, 22-29 November 1999, Aix-en-Provence, France.

objective desired for unrestricted hands-on maintenance along the high-energy part of the accelerator (< 0.2 nA/m at 1 GeV) should be straightforward to attain.[35,36]

Figure 2.23. RMS beam size, maximum particle displacement, and aperture radius versus beam energy in APT linac from 30 simulation runs with 100 000 macroparticles per run and random machine imperfections

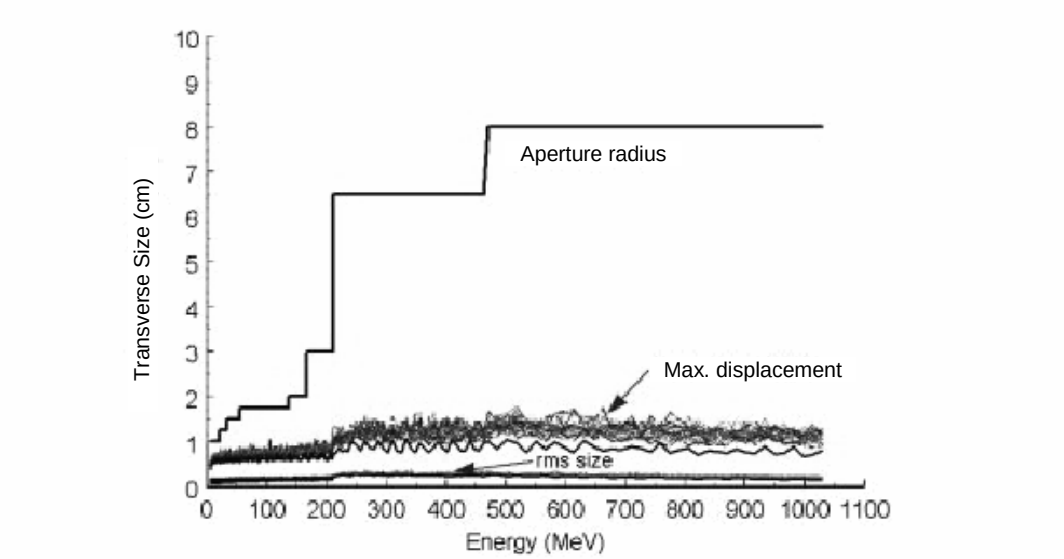

Beam halo refers to a low-density fringe of beam particles beyond 5 σ or so from the beam core. Halo is formed in high-current proton linacs by a resonant interaction between particles in the beam fringes and the space-charge field of a beam core that is undergoing envelope oscillations because of phase-space mismatch. Modelling and simulations[37] have shown that these mismatches and nonlinear space-charge forces are the main factors that produce beam-halo growth. The critical region for halo formation is the low-energy portion of the linac where the space-charge forces are high and the beam is more sensitive to mismatches. Simulations done for the APT linac show that the halo produced by the small mismatches that exist in a real machine (with imperfections) produce no significant beam loss above 20 MeV, and both analysis and simulation predict that halo formation should be negligible in the high-energy linac, assuming reasonably good matching between sections. A beam halo experiment was run on LEDA, using deliberately introduced mismatch at the entrance of a long quadrupole transport line, downstream from the 6.7 MeV RFQ. The halos measured at several stations along the beamline were consistent with the applied mismatch and an initial beam distribution that included significant tails in transverse phase space.[38] These tails were likely produced by magnetic aberrations in the injector low-energy beam transport.

35. Wangler, T., E. Gray, F. Krawczyk, S. Kurennoy, G. Lawrence, and R. Ryne (1998), *Basis for Low Beam Loss in the High Current APT Linac*, XIXth International Linac Conf., August, 1998, Chicago, p. 657.

36. Wangler, T., B. Blind, S. Nath, R. Ryne and K. Crandall (1999), *Beam Dynamics Design and Simulation Studies of the APT Superconducting Linac*, Part. Accel. Conf., March 1999, New York, p. 611.

37. Wangler, T.P. *et al.* (1998), "Particle-Core Model for Transverse Dynamics of Beam Halo", *Phys. Rev.* Special Topics – Accelerators and Beams, **1**, December, 1998.

38. Colestock, P.L. *et al.* (2001), *Measurements of Halo Generation for a Proton Beam in a FODO Channell*, Proc. of PAC2001, 18-22 June 2001, Chicago.

2.2.1.9 Power conversion efficiency

The power conversion efficiency of an XADS or ADS linac is defined as the ratio between the beam power and the power taken from the electric grid to produce the beam. This efficiency is largely determined by:

- the efficiency of the RF stations in converting the input grid power to microwave power delivered to the accelerating cavities;
- the resistive RF losses in the cavities of the NC portion of the linac; and
- the refrigeration power needed to handle cryogenic losses in the SC linac cryomodules, and the LHe distribution system.

The last two loads are current independent, so their fraction of the total required electric power decreases as the beam power increases.

Assuming a 1 GeV XADS or ADS linac, and taking 0.67 for the saturated (DC – RF) efficiency of the high-power CW klystrons, 0.97 as the AC – DC efficiency of the HVDC power supplies, allowing 10% waveguide and circulator RF losses between the klystron and the accelerating cavities, and 10% control margin, the estimated AC input power, P_{grid}, as a function of the beam power, P_{beam}, is given approximately by the simple formula:

$$P_{grid} = 1.9 \times P_{beam} + 27 \text{ MW}$$

About 15 of the 27 MW is the power deposited in the walls of the LE linac and RFQ (plus the power for water-cooling), if a NC design is used. Another 10 MW is the approximate power needed for the LHe refrigeration system, assuming the elliptical cavity performance parameters indicated above. The remaining 2 MW covers the injector, focusing magnets, vacuum systems, beam diagnostics, controls, and other auxiliary systems. As a consequence, for a beam power of 8 MW, the linac efficiency would be about 19%, while for a beam power of 30 MW the efficiency is much higher, about 36%. With a SC spoke-cavity LE linac design, about 12 MW of RF losses are eliminated, but the LHe refrigeration load increases somewhat (by about 2 MW), so the net power reduction is 10 MW. The power efficiency for a 30 MW ADS linac then increases from 36% to about 41%. These estimates illustrate the efficiency advantage of higher beam power, and also the additional efficiency advantage of using an all-superconducting linac in comparison with one whose LE section is normal-conducting.

2.2.1.10 Linac design examples

2.2.1.10.1 XADS linac design examples

Two possible XADS (see Section 2.5 on PDS-XADS) example linac designs are shown in Figures 2.19 and 2.20. Figure 2.24 is a 2001 concept done under a Memorandum of Understanding between CEA/CNRS and INFN programs. It assumes a 5 MeV 352 MHz RFQ based on the IPHI design, followed by a short 5 MeV DTL tank to bring the beam energy to 10 MeV. The low-energy linac, called the “intermediate part” is made up of sections of resonantly coupled short 352 MHz DTLs; it accelerates the beam to 85 MeV. The high-energy superconducting linac is made up of two elliptical-cavity sections, the first section with beta = 0.47 and the second having beta = 0.65. The beta = 0.47 section accelerates the beam to 185 MeV, and beta = 0.65 section accelerates it to the output energy of 600 MeV. Each cavity has four elliptical cells, and two cavities are in each

cryomodule. Quadrupole doublets in the warm inter-cryomodule spaces provide the transverse focusing. The beam current is approximately 15-20 mA.

Figure 2.24. XADS linac concept proposed by CEA/CNRS/INFN collaboration design group in 2001

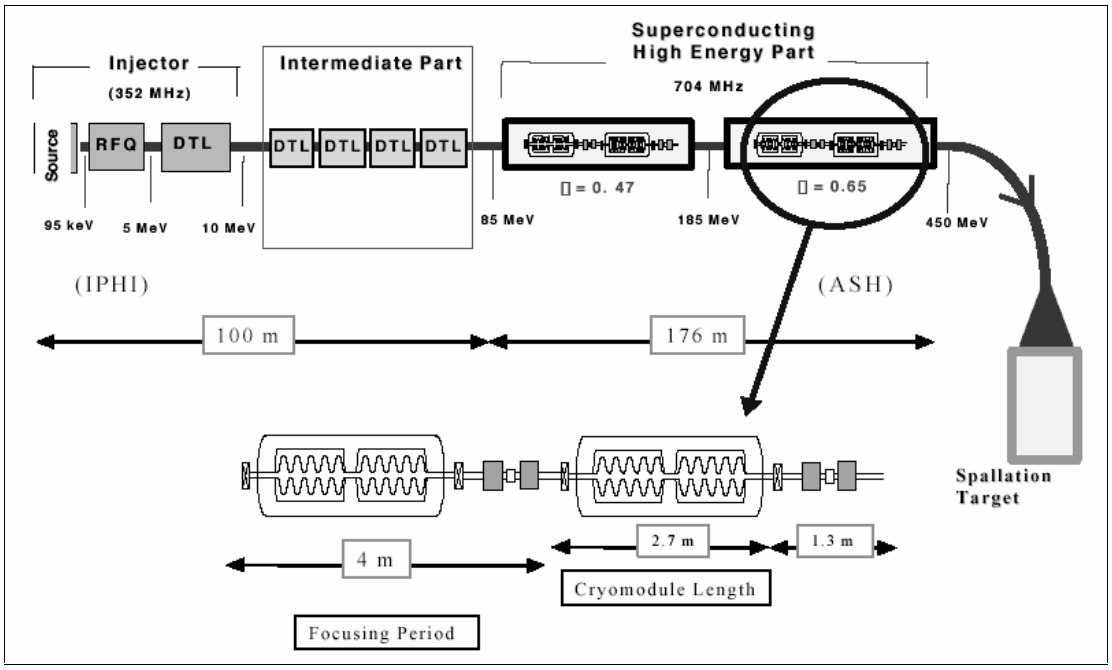

Figure 2.25 is a Los Alamos XADS linac concept (for the proposed ADTF) dating from 2001 which employs SC spoke cavities in the low-energy linac. A beam of 13.3 mA is assumed, with an output energy of 600 MeV, providing a nominal beam power of 8 MW. The protons are first accelerated to 6.7 MeV in a 350 MHz RFQ similar to that demonstrated in LEDA. The low energy linac, covering the span from 6.7 MeV to 104 MeV, consists of three sections of 350 MHz SC spoke cavities. The first section has beta = 0.175 and two accelerating gaps per cavity (one spoke), the second has beta = 0.20 and 3-gap cavities (2 spokes), and the third has beta = 0.34 and 3-gap cavities. The high-energy linac is made up of two sections of 700 MHz elliptical-cavity cryomodules; a beta = 0.50 section increases the beam energy to 211 MeV, and a beta = 0.64 section accelerates the beam to full energy. Transverse focusing is provided, in both sections of the linac, by SC solenoids located inside the cryomodules between the cavities.

Figure 2.25. Los Alamos concept for an XADS accelerator using spoke cavities in the low-energy section

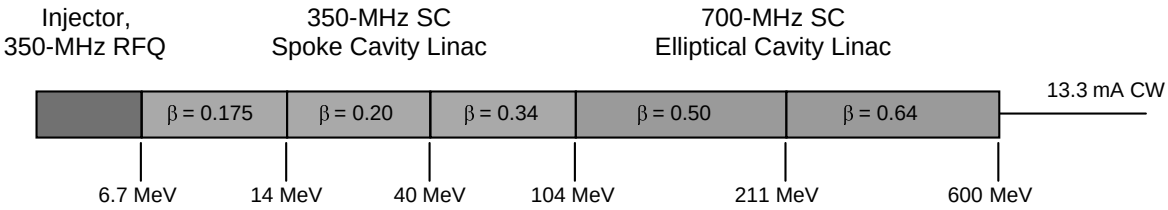

2.2.1.10.2 Industrial ADS linac design example (high reliability concept)

A Los Alamos concept for a 1 GeV, 45 mA CW high-reliability linac design for an ADS system is provided in Figure 2.26.[39] A continuous proton beam is produced in an ECR-based injector, then bunched and accelerated to 6.7 MeV by a normal-conducting RFQ similar to the one in LEDA. The RFQ would be followed by three sections of 350 MHz SC two-gap spoke resonators corresponding to geometric beta values equal to 0.175, 0.20, and 0.34, which brings the beam energy to 130 MeV. The low-energy part of the linac is followed by three sections of 700 MHz SC six-cell elliptical cavities corresponding to geometric beta values of 0.50, 0.64, and 0.82. Superconducting solenoid magnets installed in the same cryomodules as the SC cavities are used for transverse beam focusing in all sections of the linac. The design requires maximum accelerating gradients of < 7.2 MV/m, and a maximum input power-coupler capacity of 250 kW. There are 220 RF power stations, 328 SC cavities, and 82 cryomodules. The total length of the linac is 513 m. Even though the cavity gradients are high, the average (real estate) gradient is relatively modest, because of the need for a high density of transverse focusing elements, and the need to maintain a longitudinal phase advance in the LE linac below 90°. Estimated AC electric power requirements are 96 MW for the RF system, and 11 MW power for the LHe refrigerator; including 2 MW for auxiliary systems, the overall accelerator power efficiency is approximately 41%.

Figure 2.26. Industrial ADS superconducting linac design concept

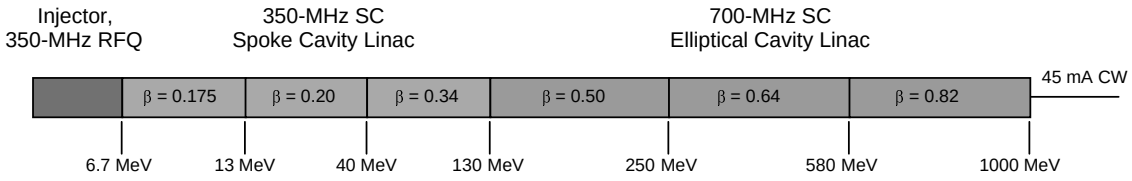

The arrangement of cryomodules and accelerating modules is shown in Figure 2.27 and Figure 2.28 for the spoke cavities and the elliptical cavities, respectively. The design specifies one cavity per accelerating module for the spoke cavities and two cavities per accelerating module for the elliptical cavities. These choices are made on the basis that the energy gain from each accelerating module is small enough that beam operation can continue following failure of a single accelerating unit. The rather large number of relatively low-power RF units that results from this choice will have a significant cost penalty. A rapid re-tuning scheme might make it possible to feed more cavities from each (larger) RF unit, which would reduce costs and maintain the desired level of reliability. Trade studies are needed to find an optimum solution.

39. Wangler, T. (2002), *Reliable Linac Design for Accelerator-Driven Subcritical Reactor Systems*, OECD/NEA Proc. 3rd International Workshop on Utilisation and Reliability of High-Power Proton Accelerators, 12-16 May 2002, Santa Fe, New Mexico.

Figure 2.27. Diagram of four spoke-cavity accelerating modules in one cryomodule

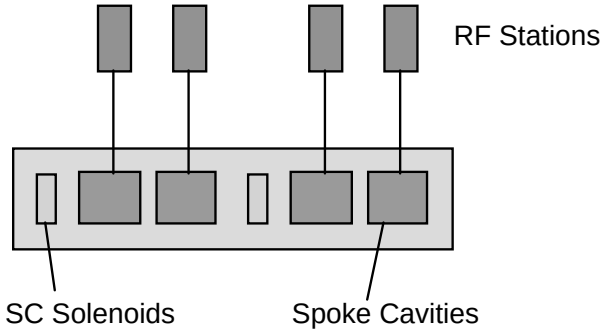

Figure 2.28. Diagram of two elliptical-cavity accelerating modules in one cryomodule

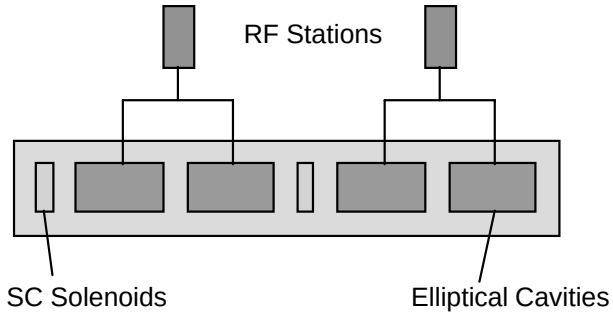

An initial beam-simulation study using 10 000 macroparticles per run shows good performance for this linac design, with substantial margin for avoiding beam losses that could cause activation in the accelerator. Figure 2.29 shows, as a function of energy, the rms and maximum beam sizes in the simulation together with the aperture radius. The high ratio of aperture to beam size indicates a very large margin for transport of the beam with minimal beam losses, which is ideal for good fault tolerance, a prime requirement in a high-reliability design. Given the present speed of micro-processors, at least an order of magnitude increase in computational speed might be required before simulations could be used to guide the linac re-tuning. Consequently, look-up tables will probably be used for the re-tuning algorithms.

Figure 2.29. Beam size (rms and maximum) from multiparticle simulations, and aperture radius, plotted versus energy for ADS all-superconducting linac concept

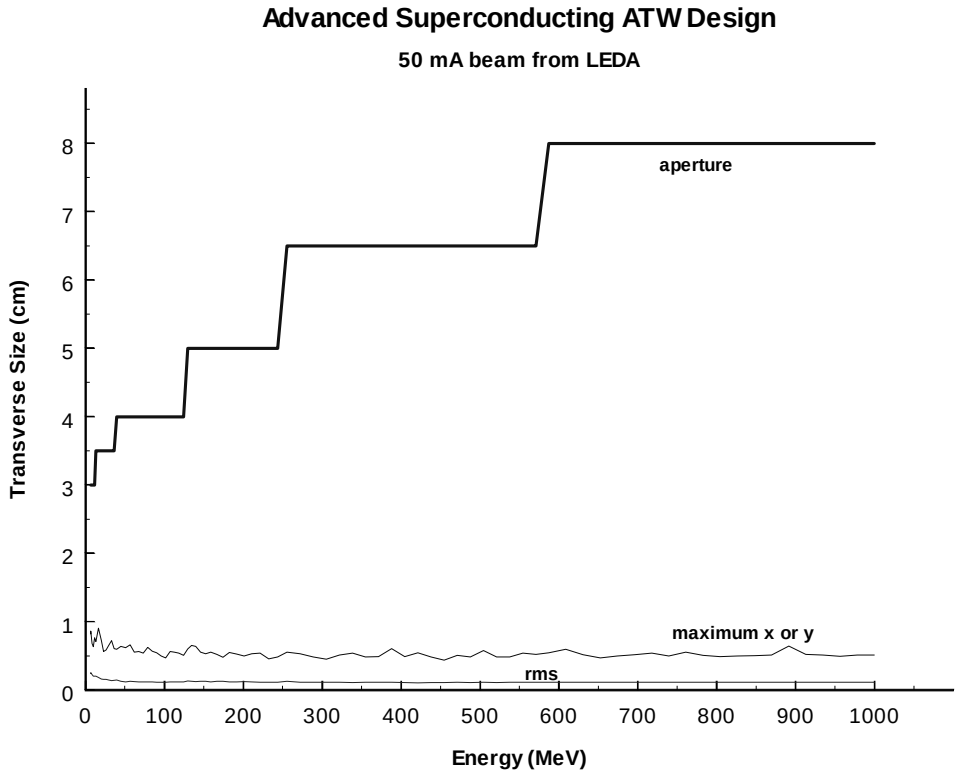

2.2.1.11 Operations and maintenance; availability

In existing large linac complexes, a short (8-24 hr) maintenance period is typically scheduled on a weekly or bi-weekly basis, and a much longer period (several weeks) once per year. This maintenance scheme reduces the number of unscheduled long beam trips induced by component failures. For an XADS or ADS linac, with proper component or system redundancy included in the design, an important operations objective would be to minimise the annual number of short maintenance periods, since they affect the overall availability of the plant. However, such maintenance periods would not contribute to transmuter thermal-cycling damage, since the beam can be turned off and then on again using a suitably slow intensity ramp. Based on experience with existing linacs, it will be challenging to operate an ADS machine for many months without the need for significant maintenance. However, the short-maintenance frequency can probably be reduced from one per week to one per month. Eventually, they might be reduced to two-to-four long periods each year, which could coincide with transmuter refueling operations. At present, the feasibility of such a maintenance framework is only a conjecture, since the required RAMI (reliability, availability, maintainability, inspectability) analysis has not been done.

As noted earlier, a major objective in design of an XADS or ADS linac is to minimise the number of long beam interrupts. A key ingredient of this program is to reduce the length of most of the interrupts that do occur to less than the transmuter thermal response time. This would be accomplished in different ways in different sections of the linac. In the SC high-energy linac, fast control electronics can enable rapid automated re-tuning to compensate for failed accelerating units. Re-tuning times are

estimated to be about 100 ms, so that equipment failures that could be compensated by re-tuning would have no impact on the transmuter lifetime. Preliminary simulations for the HE linac have been run to confirm that selected failures can be managed by such an active compensation scheme, but more work needs to be done. A similar fast re-tuning scheme could probably be applied to the LE linac if SC spoke cavities are employed. If the LE linac is built using NC cavity technology, relatively fast compensation for failed components could be provided with adequate redundancy in the RF power systems. Also, using some variant of the "supermodule" scheme that was applied in the APT linac design, failed RF units could be switched out and spare ones energised without interrupting beam for more than a few hundred milliseconds. A fast-acting high-power RF switch may be required, something that does not now exist.

A detailed analysis is required to evaluate the optimum compromise between the costs associated equipment redundancy schemes and fast re-tuning arrangements, and the desired reliability level of an ADS linac. A similar and parallel analysis must be carried out for the transmuter, in terms of the trade-offs between tolerance to thermal cycling, neutronic performance, and cost.

2.2.2 Cyclotron technology

A cyclotron-based accelerator as the proton driver for an XADS facility would be, like the linac-scheme, a multi stage system with a final energy of 600 MeV to 1 GeV. Maximum currents in the range 5 to 10 mA can be envisioned, but higher values are almost certainly prohibited by the weak focusing intrinsic to cyclotrons.

An XADS high-power cyclotron scheme would probably employ something like the following machine types and energies for the several acceleration stages:

- DC proton injector: about 60 keV.
- DC pre-accelerator (Cockcroft-Walton), or RFQ to 0.8-4 MeV.
- Injector cyclotron, 4 to 6 sectors to 80-120 MeV.
- High-energy ring cyclotron, 8 to 12 sectors to 600-1 000 MeV.

The highest-power cyclotron in the world is at the Paul Scherrer Institute (PSI) in Switzerland; this machine and its design, pictured in Figure 2.30, can be viewed as a "proof of principle" facility for the production of high power proton beams using the cyclotron approach. Following an upgrade program in 1990-1995, the 590 MeV PSI accelerator routinely produces CW beam currents of 1.5 mA to 1.7 mA, with maximum levels reaching 2.0 mA.[40] The maximum beam power is thus nearly 1.2 MW. The facility was operated at a power of about 1 MW for more than 6 000 hrs/yr in 1999, with the beam being available during 91% of the scheduled beam time. The injector cyclotron, which is fed by a Cockroft-Walton DC pre-accelerator, has an output energy of 72 MeV and two 50 MHz RF cavities, while the main (ring) cyclotron has four 50 MHz RF accelerating cavities, each having a voltage of 730 kV, producing an output beam energy of 590 MeV.

40. Stammbach, T. *et al.* (2002), *Cyclotron Performance and New Developments*, Proc. EPAC2002, 3-7 June 2002, Paris.

Figure 2.30. PSI 4-sector injector cyclotron **PSI 8-sector main (ring) cyclotron**

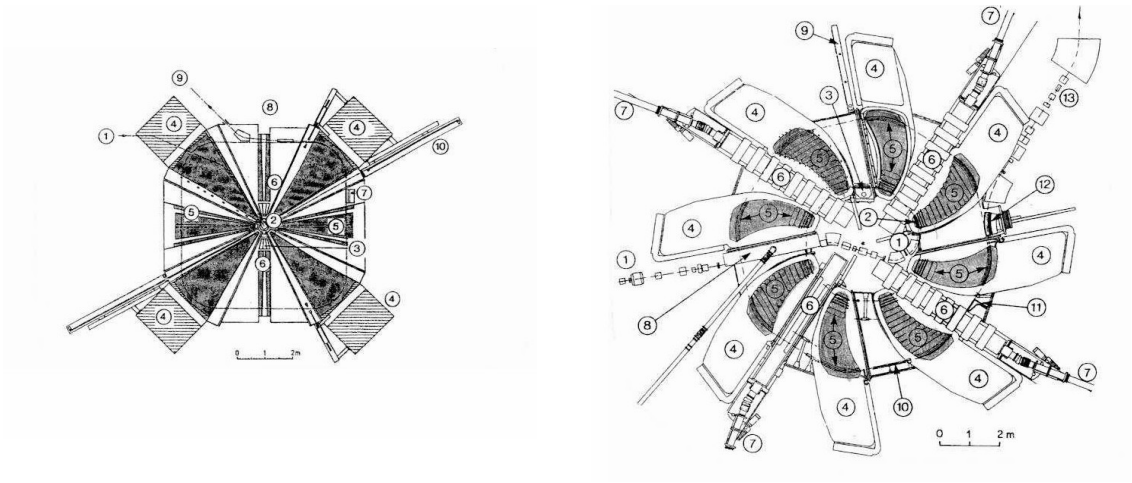

Experience with the PSI machine and reasonable extrapolation from its design suggest that a 1 GeV cyclotron facility capable of XADS performance can be built, based on existing technology. A preconceptual design of a 10 MW multi stage cyclotron has been developed by the PSI accelerator team,[41] and it is believed that the performance, efficiency, and costs of such a project can be predicted with reasonable accuracy.

A major design issue in a high-power cyclotron is the minimisation of beam losses at extraction; low loss is attained by a design that provides well-separated turns at outer edge of the final stage machine. Beam extraction from the PSI main cyclotron is achieved by an electrostatic septum followed by a magnetic channel and a septum magnet. Turn separation at extraction is 5.5 mm, about eight times the rms width of the beam, which keeps beam losses to about 200 nA (0.01% of the beam). Alternative solutions for achieving low extraction beam losses have considered the use of H^- or H_2^+ ions, and extraction by stripping[42,43] in thin foils located at the outer edge of the machine. However, both of these approaches present other difficulties. For example, the use of H^- ions requires a relatively low magnetic field, to avoid stripping during acceleration, which leads to a very large machine diameter for a 1 GeV system.

The main stage of the PSI facility is a separated-sector cyclotron (SSC) having eight sectors. The concept of separated magnet sectors was introduced[44] in order to achieve the high energy gain per turn required to minimise extraction losses. Compared to the earlier "classical" cyclotron configuration, in

41. Stammbach, T. *et al.* (1996), *The 0.9MW Proton Beam at PSI and Studies on a 10MW Cyclotron*, Proc. of the 2nd Int. Conference on Accelerator-driven Transmutation Technologies, 1996, Kalmar, ISBN 91-506-1220-4, p. 1013.

42. Craddock, M.K. (1998), *Critical Beam-intensity Issues in Cyclotrons*, Proc. of the 15th Int. Conference on Cyclotrons and Their Applications, 1998, Caen, p. 377.

43. Calabretta, L. *et al.* (1998), *Superconducting Cyclotrons for Acceleration of H_2^+*, Proc. of the 15th Int. Conference on Cyclotrons and Their Applications, 1998, Caen, p. 665.

44. Willax, H.A. (1963), *Proposal for a 500 MeV Isochronous Cyclotron with Ring Magnets*, Proc. Int. Conference on Sector-Focused Cyclotrons and Meson Factories, CERN 63-19 (1963) 386.

which “dees” (RF acceleration electrodes) are inserted between the magnet pole gaps, the magnets and acceleration structures in an SSC are split into sectors, providing space for several RF cavities. The acceleration cavities in an SSC can be much larger and more efficient than in the classical cyclotron, attaining up to 10 times greater Q-values and acceleration voltages. This high acceleration voltage results in a high energy gain per turn, which is the most important parameter for obtaining well-separated turns at extraction. The high acceleration voltage also helps to increase the beam-current limit imposed by transverse and longitudinal space charge forces, since it increases the longitudinal focusing strength. If the number of magnet sectors in the SSC is increased, more RF cavities can be inserted, achieving a further increase in the energy gain per turn. Thus, using the highest possible acceleration voltage and the maximum number of RF cavities leads to a cyclotron design with sufficient energy gain per turn to accelerate beam currents up to 10 mA, with relatively low losses at extraction. However, because of the intrinsically weak transverse and longitudinal focusing in a cyclotron (no strong-focusing quadrupole fields as in a linac, and cavity frequencies an order of magnitude lower than in a linac), it appears difficult to accelerate significantly higher currents in the separated sector concept.

2.2.2.1 Cyclotron for XADS application

Several conceptual-design studies for cascaded cyclotrons that could drive an XADS facility have been published.[45,46,47,48,49] Most of these proposals are based on extrapolation of the PSI cyclotron design, and use a 1 GeV output energy and 10 mA CW current, providing a nominal 10 MW of beam power. Higher beam currents could possibly be achieved in larger rings with more RF cavities and hence a higher energy gain per turn.[50] Also, the superconducting sector magnets in an SSC could, in principle, reduce the size and cost. SC magnets of the type and size that are roughly comparable to what would be needed in a 1 GeV proton cyclotron are under construction at the RIKEN laboratory in Tokyo (Superconducting Ring Cyclotron for the RI Beam Factory).[51] A superconducting magnet would allow construction of a particularly compact and energy-efficient SSC. However, other aspects

45. Stammbach, T., *et al.*, (1995), *The Feasibility of High Power Cyclotrons*, Proc. 4th European Conf. in Applied Research and Technology, 1995, Zurich, Nucl. Instr. and Meth. B 113 (1995) 1; and *Cyclotron-Based Accelerators for Energy Production and Transmutation*, Int. Conference on Accelerator-driven Transmutation Technologies and Applications, 1994, Las Vegas, AIP Conf. Proc. 346 (1995) 229.

46. Sarkissian, L.A. (1998), *A Layout of a 2.7 GeV and 10MW Cyclotron*, Proc. of 15th Int. Conference on Cyclotrons and Their Applications, 1998, Caen, p. 393.

47. Rubbia, C. *et. al.* (1994), Proc. EPAC, 1994, pp. 270; Fiétier, N. *et al.* (1995), *A Cyclotron-Based Accelerator for Driving the Energy Amplifier*, CERN Report AT-95-03(ET), 1995; Proc. of 14th Int. Conf. on Cyclotrons and Their Applications, 1995, Capetown, p. 598; and *High Intensity Cyclotrons for Driving Hybrid Nuclear Systems*, Proc. of 15th Int. Conference on Cyclotrons and Their Applications, 1998, Caen, p. 389.

48. Jongen, Y., P. Cohilis, (1995), *A Proton-Driven Intense Subcritical Fission Neutron Source*, Proc. of the 14th Int. Conference on Cyclotrons and Their Applications, 1995, Capetown, p. 610.

49. Tumanian, A. *et al.* (1996), *Powerful Cyclotron for ADTT*, Proc. of 2nd Int. Conference on Accelerator-driven Transmutation Technologies, 1996, Kalmar, ISBN 91-506-1220-4, p. 1065.

50. Tumanian, A. *et al.* (1996), *Powerful Cyclotron for ADTT*, Proc. of 2nd Int. Conference on Accelerator-driven Transmutation Technologies, 1996, Kalmar, ISBN 91-506-1220-4, p. 1065.

51. Yano, Y. *et.al.* (1995), *RIKEN RI Beam Factory Project*, Proc. of 14th Int. Conference on Cyclotrons and Their Applications, 1995, Capetown, p. 590.

of the performance of a high-energy SC-magnet cyclotron, such as turn separation at extraction, need to be assessed.

The space-charge current limit in a cyclotron has been shown to depend approximately on the cube of the energy gain per turn,[52,53] as seen in Figure 2.31, which plots the current attained in the PSI main cyclotron as a function of energy gain per turn. This relationship has been used to extrapolate properties and beam performance of cyclotrons for higher current levels. The current limit is reached when the extraction beam losses increase steeply as the beam size increases (from space-charge forces) to a significant fraction of the turn separation. From experience gained in the upgrade of the PSI facility, in which the peak RF voltage in the cavities was raised from 450 kV to 730 kV, it appears that such extrapolation is feasible.[54,55] Recent measurements on a 1/3-scale cavity prototype at PSI (4.2 MV/m at 150 MHz) show that voltages in excess of 1 MV can be expected for their new cavities that are now under construction.

Figure 2.31. Current limit in a proton cyclotron as a function of energy gain per turn

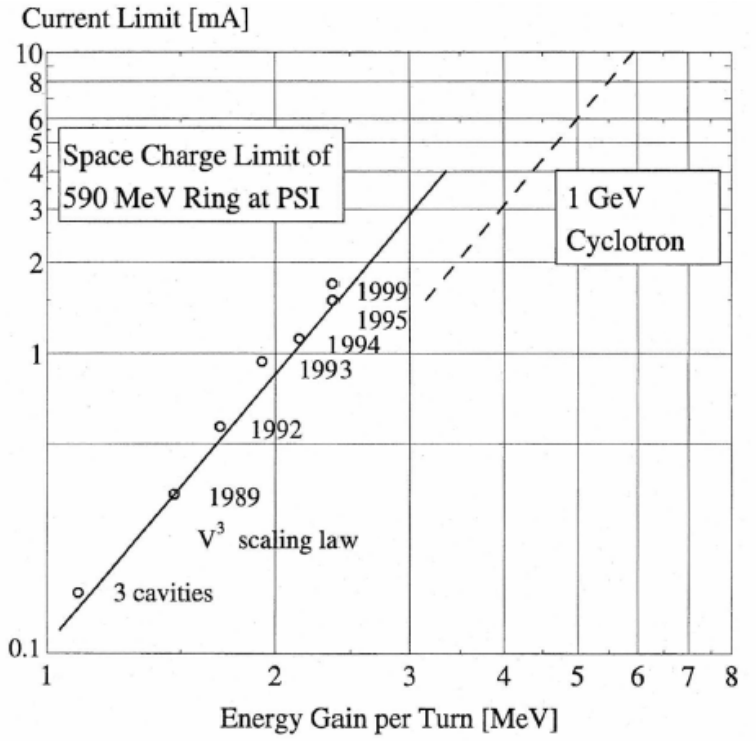

52. Joho, W. (1981), *High Intensity Problems in Cyclotrons*, Proc. of 9th Int. Conference on Cyclotrons and Their Applications, Caen, 1981, p. 337.

53. Stammbach, T. *et al.* (1998), *Cyclotron Operation Beyond Limits*, Proc. of 15th Int. Conference on Cyclotrons and Their Applications, 1998, Caen, p. 369.

54. Sigg, P. *et al.*, (1999), *Development of High Power RF Systems with Excellent Reliability*, PAC99, 29 March-2 April 1999, New York.

55. Bopp, M. *et al.*, (2001), *Upgrade Concepts of the PSI Accelerator RF Systems for a Projected 3-mA Operation*, Proc. Cyclotrons 2001 Conf., 13-17 May 2001, East Lansing, Michigan.

2.2.2.2 Ring cyclotron

The PSI XADS concept, sometimes referred to as the "dream machine" consists of a 1 GeV, 10 mA ring cyclotron injected by a 120 MeV intermediate-energy separated-sector cyclotron. Figure 2.32 shows a sketch of the ring cyclotron. The first-stage cyclotron is injected either by a Cockroft-Walton-type pre-accelerator or a low-frequency RFQ. The main cyclotron has 12 magnet sectors arranged in a ring of 15 m diameter. Its RF power system consists of eight accelerating cavities each with a peak voltage of 1 MV. The maximum magnetic field flux is 2.1 T. The proton revolution frequency (cyclotron frequency) is 7.36 MHz, and the RF cavity frequency is 44.17 MHz. The protons execute about 140 turns in the machine before extraction, and turn separation at extraction is calculated to be 9 mm.

Figure 2.32. Ring cyclotron for 1 GeV, 10 mA XADS facility proposed by PSI

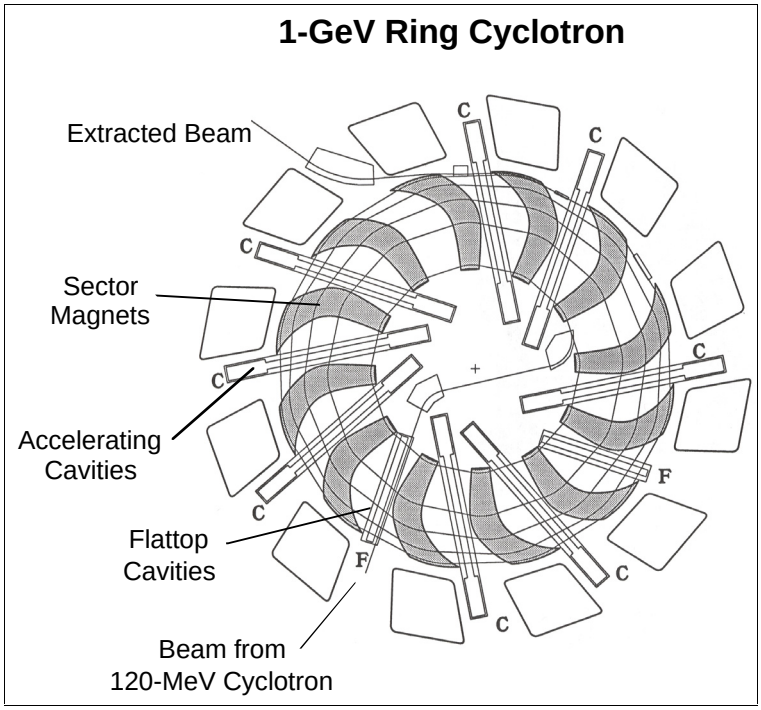

2.2.2.3 Injector cyclotron

The injector cyclotron would be a higher-energy version of the 72 MeV separated sector injector cyclotron presently operating at PSI. That machine provides a beam intensity of up to 2 mA for injection into the ring cyclotron. It is specially designed for high beam intensities, with four magnet sectors and two RF resonators (two accelerating gaps each), and a peak RF voltage of 250 kV.

The PSI injector cyclotron is operated in a special beam-dynamics regime, where the injected beam bunches are matched into a phase space volume that is stable for high space-charge forces. In this matched condition, the beam bunch is self-focused in the longitudinal and radial directions. In contrast to the situation in a high-current linac, halo particles are not spread out over the whole bucket,

but return to the matched bunch.[56,57] The injector cyclotron for an ADS facility would be operated in this same matched condition in order to reduce beam losses in the main (ring) cyclotron through better beam quality, and the fact that particles are well confined in a compact phase space volume with little tailing. The design of such a cyclotron has not yet been worked out in detail. Alternative solutions have been proposed by Mandrillon *et al*.[58] and at lower energies by Jongen.[59]

2.2.2.4 Proton injector and pre-accelerator

The DC proton source for a 10 mA cyclotron-based XADS facility would be a microwave-driven unit similar to those for the linac, and the current requirement (> 50 mA) is considerably less than what has been demonstrated in the IPHI and LEDA linac-technology programs. Thus, the injector can be considered a solved problem, and with the relatively modest performance requirement, would have very high reliability.

The pre-accelerator for the PSI injector is an 870 keV Cockcroft-Walton generator. Capture efficiency of the continuous beam from the pre-accelerator into the longitudinal bunch acceptance of the injector cyclotron is about 20%, because of the constraints imposed by space-charge forces at the low beam energy. Thus, a 10 to 12 mA DC injected beam is needed to obtain a 2 mA bunched beam in the injector cyclotron. Given this technology baseline, a major issue for an XADS cyclotron design is how to increase the injected current to 10 mA. Addressing this question, the PSI design group has shown that, using a higher bunching voltage and shorter bunching distance, a 50 mA pre-injector beam can produce a 10 mA bunched beam at the input to an XADS injector cyclotron, and within the same phase space as in the PSI system.[60]

A low-frequency RFQ might provide an alternative and more efficient solution to the existing pre-accelerator scheme, but the relevant design study and prototyping have not been carried out for the required frequency range (around 50 MHz). However, the tools for such a study exist.

2.2.2.5 Cyclotron technology development needed for XADS

Further development work and prototyping would be needed in the following areas to bring a high-power cyclotron concept to the same level of technical maturity as a high-power linac for the XADS application:

- **Low-frequency RF power systems**. Special emphasis is needed on development of high power CW amplifiers in the 50 MHz range, high power RF coupling loops, and flat-topping

56. Chabert, A. *et al.* (1975), Proc. of 7th Int. Conference on Cyclotrons and Their Applications, Zurich, 1975, p. 245; and IEEE Trans.NS 22/3 (1975) 1930.

57. Chasman, C. *et al*. (1984), Nucl. Instr. and Meth. 219 (1984) 279.

58. Rubbia, C. *et. al.* (1994), Proc. EPAC, pp. 270; Fiétier, N. *et al.* (1995), *A Cyclotron-Based Accelerator for Driving the Energy Amplifier*, CERN Report AT-95-03(ET); Proc. of 14th Int. Conf. on Cyclotrons and Their Applications, Capetown, 1995, p. 598; and *High Intensity Cyclotrons for Driving Hybrid Nuclear Systems*, Proc. of 15th Int. Conference on Cyclotrons and Their Applications, Caen, 1998, p. 389.

59. Jongen, Y., P. Cohilis, (1995), *A Proton-Driven Intense Subcritical Fission Neutron Source*, Proc. of the 14th Int. Conference on Cyclotrons and Their Applications, Capetown, p. 610.

60. Stammbach, T. *et al*. (1998), *Cyclotron Operation Beyond Limits*, Proc. of 15th Int. Conference on Cyclotrons and Their Applications, Caen, p. 369.

systems RF systems. Operating at three times the fundamental acceleration frequency, flat-topping systems permit a wider phase acceptance during the acceleration process. The flat-topping cavities act to decelerate the central region of the beam bunch, and a major issue for high beam currents is that voltage and phase stability become challenging when power absorbed from the beam exceeds the wall power in the flat-top cavities.

- **High-voltage accelerating cavities**. PSI is pursuing a project to develop and build a prototype RF accelerating cavity for > 1 MV peak voltage. Relatively simple conditioning should suffice to reach this goal; no chemical cleaning, high temperature bakeout, etc. is thought to be needed to reach the relatively modest gradient of about 3.5 MV/m.[61]
- **Extraction logistics**. Work is needed on collimation of high power beams, the design of shielding in the extraction region, and arrangements and hardware for remote handling and replacement of the highly activated parts in the extraction region.
- **High-current beam simulations**. A detailed understanding of beam behaviour at currents in the 10 mA range, where space charge forces are very strong, needs to be obtained in both the XADS injector cyclotron and ring cyclotron. Particular attention needs to be given to the longitudinal dynamics. Simulations must be carried out for a realistic distribution of possible machine imperfections. A beam-dynamics design and simulation of a candidate RFQ pre-accelerator also needs to be carried out. An advanced computer code for accomplishing these tasks is being developed in a collaboration between CERN, LANL, and PSI.
- **Injection and extraction systems**. Beam injection and extraction systems for high-current cyclotrons consist of a combination of magnetic and high voltage electrostatic components, which will need to be optimised to handle the increased beam losses anticipated at XADS power levels. The electrostatic septa must be designed explicitly for low spark rates.

2.2.2.6 Power conversion efficiency

The power conversion efficiency a cyclotron-driven XADS facility depends very much on the type of technology (NC magnet or SC magnet), on the machine size, and on the beam current. The efficiency is highest if the cyclotron is operated close to its intensity limit, i.e. at the highest possible beam power for a given accelerating voltage. Power efficiency in an XADS high-current cyclotron can be high, even without the use of superconducting technology for the magnet or the RF cavities. This is because RF losses in the cavity walls are relatively low at cyclotron RF system frequencies, and because the gridded power amplifier tubes have a high intrinsic efficiency for conversion of DC to RF power.

The PSI cyclotron is operated at relatively low beam loading, so its power efficiency of 12% is rather low. At a current of 1.7 mA, the beam power is 1 MW, for which the RF power input to the ring cyclotron is about 1.7 MW. Assuming 67% conversion efficiency from the electric grid to RF power, the total AC power input to drive the beam is 3.05 MW. The pre-accelerator, injector cyclotron and beam lines need an additional 2.6 MW, and the machine infrastructure demand amounts to about 2.5 MW, bringing the total grid power to about 8.15 MW.

61. Fitze, H. *et al.* (1999), *Development of a New High-Power Cavity for the 590-MeV Ring Cyclotron at PSI*, Proc. PAC99, p. 795.

For the proposed 1 GeV 10 mA XADS cyclotron facility, the power efficiency has been estimated to be about 36%.[62] The beam power is 10 MW, for which the RF power drive is about 14 MW. Conversion losses from the electric grid to RF power are about 7 MW. The pre-accelerator, injector cyclotron, and beam lines need about 4 MW, and the infrastructure demand has been taken as about 3 MW. The figures given are based on extrapolation from the existing PSI facility, without any consideration of power-saving technology.

2.2.2.7 Cyclotron reliability; beam interrupt rates and durations

The operation of proton cyclotrons at high beam-power levels, with the added requirements of: 1) very few long-duration beam trips per year; and 2) reducing time lost from unscheduled beam interruptions to very low levels, poses a major challenge for the designers. The design priorities for cyclotrons currently used in nuclear and particle physics have been to push the technical performance envelope to higher energies, higher currents, and higher energy resolution, while maintaining acceptable availability. High beam reliability, as in the case of linacs for similar research applications, was not a major driving function in their design.

On the other hand, similar to electron linacs medium-power cyclotrons designed for medical applications (isotope production and irradiation therapy) are faced with extreme demands for availability (> 95% of the scheduled beam time), very low unscheduled down times, and minimal time spent on maintenance (< 15% of the year). Thus, some limited experience has been gained in what design measures are effective in assuring high reliability for cyclotrons in this power regime. The design for an XADS cyclotron makes even tougher reliability and availability demands, requiring no more than a few tens to a few hundreds of beam interrupts (longer than 300 ms) per year. Hence, as is the case for linacs, existing cyclotron facilities are generally not well suited to evaluate what can be achieved with respect to reliability, as can be seen in a recent reliability summary,[62] which reports something like 100-200 beam trips/week for the PSI accelerator.

In the current generation of high power cyclotrons, the MTBF, i.e. the mean time between beam interrupts, is dominated by high-voltage arcing in the main accelerating cavities, and also in the electrostatic deflectors used in the extraction system. These sparking interrupts are relatively short in duration (typically < 1 minute), but much longer than the thermal time constants of subcritical assemblies. In the PSI facility, the beam-trip rate due to sparking is as high as 8 500/yr under good conditions.[62] This trip rate is accounted for in the design of the 1 MW spallation target (SINQ) and is not a problem at that power level. For XADS subcritical-assembly power levels, which will be two orders of magnitude greater, this rate of beam interrupts would cause a serious reduction of the transmuter lifetime. To address this specific issue, more performance studies are needed for high-gradient cyclotron cavities, both in terms of mechanisms that cause discharges, and to develop fast-recovery measures. If the probability of HV arcs can be reduced, and the accelerating field can be re-established within 300 ms, then a very large fraction of the damaging long-term beam interrupts could be eliminated. Redesigning cavities in terms of geometries that reduce field gradients at critical locations, and methods of conditioning and surface treatment are the basic measures available to reduce the spark rate.

Some of the principles of high-reliability design for a high-power cyclotron are similar to what they are in a linac. Component redundancy can be applied in some areas, such as the main RF power

62. Stammbach, T. *et al*. (1999), *The Cyclotron as a Possible Driver for an ADS*, OECD/NEA Proc. 2nd Int. Workshop on Utilisation and Reliability of HPPA, 22-29 November 1999, Aix-en-Provence; and PSI Annual Report, Annex IV, 1998.

systems, to allow fast compensation for failed elements. Also specifying component performance well below their maximum ratings envelope will greatly extend their lifetimes and MTBFs. Diagnostics embedded in critical equipment to detect the approach of a failure condition or end of life are as important in the cyclotron case as for linacs. However, there are two principles that would seem very difficult to apply, that of fault-tolerant design, and that of rapid re-tuning to compensate for failed elements.

Fault-tolerant design. Because the cyclotron has a very small number of accelerating cavities, through which the beam passes 100 times or more, there is no simple analog to the SC linac situation in which beam energy is incremented in small steps, each provided by an individual cavity, where failure of a single unit does not cause the beam to stop accelerating. If a cyclotron RF cavity fails, the beam quickly falls out of the RF "bucket" and stops accelerating, ending up as a 100% beam loss somewhere in the vacuum chamber walls until the protection system reacts to the injector.

Rapid re-tuning. Again, because the beam passes through each cavity many times, it is not possible to re-tune downstream accelerating units to compensate for a failed accelerating cavity, RF window, or RF station, as can be done in a linac. When a failure occurs in the acceleration chain, it must be repaired before beam operation can continue.

2.2.2.8 Cyclotron operations and maintenance; availability

The Mean Down Time (MDT) of high-power cyclotrons (and linacs too) is generally dominated by unscheduled interruptions of long duration lasting > 1 hr, usually due to key component failures that require repair or replacement before operation can resume. To reduce the cumulative effect of these types of failures it is necessary to focus individually on the contributions of the various accelerator systems. Suitable preventive maintenance has to be performed as needed, which in most cases adds to overall operating costs. High voltage devices, as used in beam deflectors, or RF power amplifiers are more susceptible to failure than low voltage electronics. Of great importance are: 1) integration into all critical equipment a suitable level of diagnostics that can quickly identify faults and approaching end of life; 2) availability of ready-to-operate replacement units near where they will be needed; and 3) rapid interchangeability in all critical components and devices. Lengthening the lifetimes of critical components, such as beam deflector electrodes, RF amplifiers (gridded power tubes) and RF couplers (ceramic windows) is also an important aspect of reducing unscheduled downtime.

Large cyclotron-based research facilities, such as PSI, have up to now not been seriously optimised with in terms of the above considerations, so there would seem to be considerable potential for improvement for an XADS application.[63,64] The overall operating costs of cyclotrons (including annual power consumption, operating staff, and maintenance), became a more-urgently addressed issue when cost effectiveness was first analysed in terms of commercial applications, such as isotope production, rather than research applications.

There is the same need to reduce weekly or bi-weekly maintenance periods as in the linac case, discussed earlier, and the objectives would be similar. The major goal would be to reduce scheduled

63. Sigg, P. *et al.* (1999), *Development of High Power RF Systems with Excellent Reliability*, PAC99, 29 March-2 April 1999, New York.

64. Sigg, P. *et al.* (1998), *Reliability of High Beam Power Cyclotron RF-Systems at PSI*, OECD/NEA Proc. 1st Int. Workshop on Utilisation and Reliability of HPPA, 1998, Mito, Japan.

accelerator maintenance to a very few week-long periods distributed evenly throughout the year, timed (if possible) to coincide with transmuter refueling operations

2.2.2.9 Cyclotron beam losses

In terms of losses in an XADS cyclotron system, beam extraction from the 1 GeV ring cyclotron is the most critical operation and location. Good separation between orbits at the extraction radius is mandatory in order to achieve high extraction efficiency. In the nominal 10 MW beam facility, the ring cyclotron radius and number of turns have been chosen so that turn separation at the outer edge is larger than in the existing 590 MeV cyclotron at PSI. The year-averaged extraction efficiency achieved in routine operation of that machine is as high as 99.98% (implying 0.02% beam losses or 340 nA at 1.7 mA output). Roughly the same extraction efficiency is projected for a 10 MW facility, so the actual beam loss amount would increase by a factor of five, to about 1.7 microamperes. The output beam-energy increase is a factor of 1.7, so the total power increase in the beam lost at the extraction point is nearly an order of magnitude. Thus, the extraction hardware logistics (shielding, replacement of highly activated components, remote handling arrangements, etc.) will be significantly more challenging than in the present PSI operation.

The limiting factor for allowed beam losses in a high-power cyclotron is the radiation dose imposed on the personnel involved in repair and maintenance. This dose is difficult to estimate, because it depends not only on the actual beam losses in the cyclotron, but to a larger degree on the design of the equipment, the installation of local shielding, on provision for quick and remote removal of activated components into shielded boxes, and the use of manipulators.[65] It also is affected by preventive measures, such as the concentration of activation products in specially designed beam catchers, optimised material selection, and the management of the personnel who handle activated components to achieve minimal dose levels. From the experience at PSI during several decades of operation and steady beam-power upgrades, the serviceability of activated areas or components appears to be more a function of their design and their environmental configuration than simply of the amount of beam lost at a given location. In the PSI facility, annual beam production has increased by three orders of magnitude over the past 25 years, while the annual dose to maintenance and operations personnel has been halved. PSI designers are confident that, with the appropriate remote-handling design and strategies for dealing with activated equipment, a 10 MW cyclotron facility can operate with acceptable radiation doses to personnel (assuming that the beam transmission is comparable to that in the PSI cyclotron).

2.3 Status of current high-power proton accelerator projects

2.3.1 Japan

JAERI and KEK in Japan have jointly proposed a multi-purpose complex called the High-Intensity Proton Accelerator Project,[66] which will serve high-energy physics, spallation neutron science, and transmutation research. Phase 1 of this project is under construction. It includes:

- a 400 MeV normal-conducting linac;

65. Mariani, E. *et al.* (1998), Fig. 3 in *An Electrostatic Splitter for the PSI 590-MeV Beam*, Proc. EPAC98, 1998, Stockholm; and U. Schryber *et al.* (1995), Fig. 2 in *High Power Operation of the PSI Accelerators*, Proc. 14th Int. Conf. on Cyclotrons and Their Application, 1995, Capetown, p. 32.

66. Yamazaki, Y. and M. Mizumoto (1999), *Accelerator Complex for the Joint Project of KEK/JHF and JAERI/NSP*, Proc. PAC99, 29 March-2 April 1999, New York.

- a 3 GeV proton synchrotron at 1 MW;
- a 50 GeV proton synchrotron at 0.75 MW;
- a major part of a 1 MW spallation neutron source; and
- a portion of a 50 GeV high-energy physics experimental facility.

The total budget for Phase 1 is 133.5 billion yen, and the schedule calls for its completion within 6 years. Phase 2 of the project will comprise construction of an XADS facility, including adding a 200 MeV superconducting linac section to the 400 MeV linac to increase the beam energy to 600 MeV, upgrade of the spallation source to 5 MW, construction of a neutrino beam line, and upgrade of the 50 GeV experimental facility. R&D on elliptical SC cavities for the proton linac has been underway at JAERI since 1995. Performance tests have been conducted on beta = 0.5 and beta = 0.89 prototype 5 cell cavities, achieving surface fields of 23 MV/m and 31 MV/m respectively at 2 K.[67,68] Fabrication of a prototype cryomodule, which includes two 5 cell cavities (beta = 0.60) was accomplished in 2001.

2.3.2 Europe

Two projects in Europe have been of interest in terms of the design and construction of a future XADS facility. These are IPHI (Injecteur de Proton Haute Intensité) in France (Saclay/CEA-CNRS), and TRASCO (TRAsmutazione SCOrie) in Italy (INFN). A collaboration (CEA-CNRS-INFN) between these two projects was established so that some important design choices were made in common, providing the maximum profit from the investments.

2.3.2.1 IPHI project, France

The IPHI project, which has been suspended due to changes in program direction, was initially thought to be a 10 MeV 1 MW demonstration linac that could prototype the front end of a high power proton linac suitable for XADS or ADS applications. IPHI was to consist of:

- a 95 keV, 140 mA proton injector that included an ECR proton source (SILHI, Source d'Ions Légers Haute Intensité) operated at 2.45 GHz with an axial magnetic field of 875 Gauss, and a solenoid-based low-energy beam transport system;
- a 352 MHz proton RFQ able to deliver a 5 MeV 100 mA CW beam (500 kW) using the SILHI injector as input;
- a short DTL tank (first tank of the NC low-energy linac), which would increase the proton energy to 10 MeV.

The SILHI proton injector was built and tested, including the low energy transport line. It demonstrated the design beam performance, and also very high beam reliability when operated at 80% of the design rating. The design of the RFQ was completed, and its construction was well underway when the IPHI programme was suspended. The present plan is for the RFQ to be completed

67. Ouchi, N. *et al.* (1999), *Superconducting Cavity Development for High Intensity Proton Linac in JAERI*, Proc. 9th Workshop on RF Superconductivity, 1-5 November 1999, Santa Fe, New Mexico.

68. Mizumoto, M. *et al.* (2000), *Development of Superconducting Linac for the KEK/JAERI Joint Project*, Proc. LINAC2000, 21-25 August 2000, Monterey, California.

(but to a somewhat lower energy) by CERN, most likely for use in the Proton Synchrotron injector linac. The construction of the short DTL tank was not completed, although a prototype three-drift-tube assembly was built, and prototype drift-tube quadrupoles were built and tested.

2.3.2.2 TRASCO programme, Italy

The TRASCO programme objectives include:

- conceptual design of a 1 GeV 30 mA proton linac suitable for an ADS system;
- design and construction of a proton source and a 5 MeV, 352 MHz CW RFQ;
- study of alternative designs for the low-energy linac (5 MeV to 100 MeV);
- design of the SC high-energy linac, based on elliptical accelerating structures, as well as the construction and testing of SC cavity prototypes.

The conceptual design of the proton source, the 352 MHz RFQ, and a short DTL section has been completed. The nominal accelerated current is planned to be about 30 mA. The proton source has been built and has been commissioned. Detailed design and engineering of the 352 MHz RFQ has begun. A 3 m long aluminum model has been built, and RF stability tests carried out. The first section of the RFQ is under construction. Preliminary studies of an ISCL (independently phased Superconducting-Cavity Linac), which could be used for the low-energy linac instead of the traditional Alvarez DTL, have been done. The conceptual design of a 352 MHz SC linac, which would accelerate the beam from 100 MeV to 1 700 MeV, was worked out. However, the TRASCO programme was redirected in 2000 from the 352 MHZ LEP frequency to the 704 MHz bulk-niobium technology that has matured due to the extensive TESLA effort. The original 352 MHz design is based on axially compressed versions of the elliptical cavities used in the CERN LEP II project. Single-cell and multi-cell Nb-sputtered copper beta = 0.85 cavity prototypes were built and tested in the CERN superconducting-cavity development laboratory, under a collaboration agreement between CERN and INFN. Only the beta = 0.85 (five cell) structure was made at 352 MHz, performing as expected (i.e. identical to LEP II performances in terms of peak fields, as reported in the Santa Fe HPPA meeting). Four single cells and two 5 cells at beta = 0.47 were then made in bulk niobium at 704 MHz. The latest design reflected this technology switch and uses only elliptical cavities at 704 MHz, after the RFQ and intermediate acceleration stage at 352 MHz.

2.3.3 United States

2.3.3.1 Los Alamos (LEDA project and other linac technology development)

The low-energy demonstration accelerator (LEDA) at Los Alamos, illustrated in Figure 2.33, was built and tested[69] as a major element of the technology development and demonstration effort associated with the APT project, and later the AAA program. Its successful full-power operation and testing in 1999-2001 confirmed the feasibility of the lowest-energy stage of a high-power proton linac, the most challenging portion of such a machine. At present, LEDA is in cold shutdown. All the equipment remains in place, and it is capable of being quickly restarted for use in future applications, including the front end of a possible XADS linac. A 600 MeV, 8 MW linac-based XADS facility using LEDA for its initial stage was proposed in 2001-2002 as the ADTF (accelerator driven test

69. Smith, Jr., H.V. and J.D. Schneider (2000), *Status Report on the Low-Energy Demonstration Accelerator (LEDA)*, Proc. LINAC2000, 21-25 August 2000, Monterey, California, pp. 581-3.

facility). In its present configuration, LEDA is a 100 mA CW, 6.7 MeV proton accelerator consisting of a 75 keV H^+ injector coupled to a 350 MHz radio-frequency-quadrupole (RFQ) linac.

Figure 2.33. Low-energy demonstration accelerator (LEDA), shown with 6.7 MeV RFQ + injector

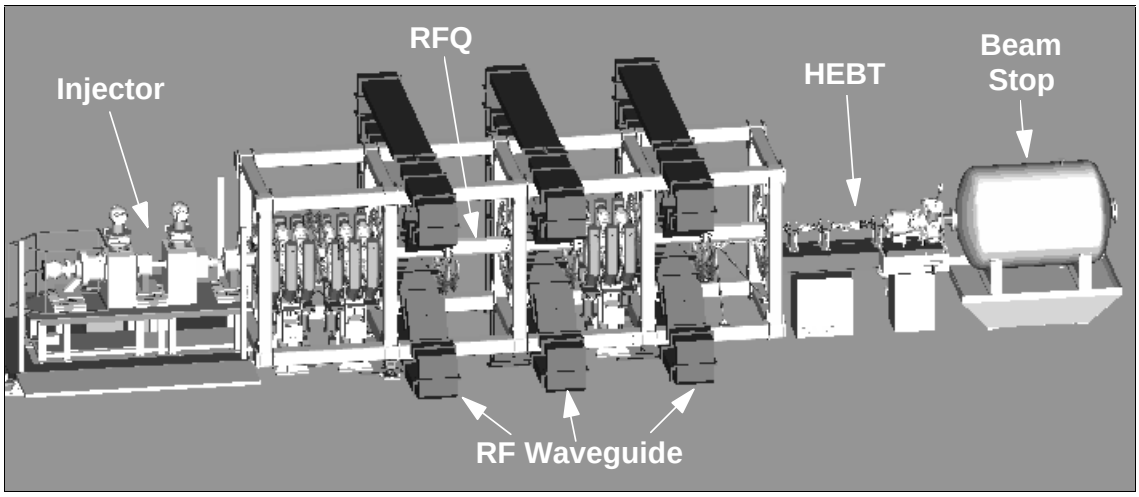

Another important element of the APT/AAA technology program was the SC-cavity and cryomodule development effort that supported the design of the HE superconducting linac. Several 5 cell elliptical beta = 0.64 were fabricated and tested.[70] Initial gradient and Q results satisfied the APT design requirements (5 MV/m and 3×10^9). Later, improved surface preparation was applied to these cavities, resulting in more than a factor of 2 improvement in performance. A complete 2 cavity beta = 0.64 cryomodule was partly constructed, but was suspended at termination of the APT and AAA programs. Prototype high-power 700 MHz RF couplers were developed for the cryomodule, including ceramic windows; these were bench tested under cryogenic conditions with more than 1 MW CW of transmitted RF power.[71]

2.3.3.2 Spoke cavity development

In the past three years, a major thrust of accelerator technology with application to XADS and ADS machines has been the development and testing of prototype spoke cavities for use in the low-to-medium beta sections of an all-superconducting linac. Several laboratories, including Los Alamos, Argonne National Laboratory, Orsay, Legnaro, and JAERI/KEK have been engaged in this R&D effort, examples of which were noted earlier in this report. A workshop held recently at Los Alamos provides a fairly complete view of worldwide activity in this field.[72] Prototype spoke cavities have been built and tested covering the beta range 0.175 to 0.43. Preliminary indications are that single-spoke and multi-spoke cavities can be built that have gradients > 10 MV/m, and Q values > 1×10^9,

70. *Medium-Beta Superconducting Cavities for High-Energy (APT) Linac*, APT Report TPO-E41-R-TNS-X-0041, June 2001.

71. *Development and Performance of Superconducting-Cavity Power Couplers (for APT)*, APT Report TPO-E42-R-TNS-X-0049, August 2001.

72. Proc. of Workshop on the Advanced Design of Spoke Resonators, Los Alamos, New Mexico, 7-8 September 2002, LANL Report LA-14005-C.

which exceeds the performance requirements for a SC low-energy proton linac. These cavities would form the building blocks of a low-energy SC accelerator that could replace the normal-conducting (DTL, CCL) linac design previously assumed for XADS and ADS applications. There would be several advantages, including lower operating costs, a greatly improved match to reliability schemes, and lower beam losses. Suitable prototype RF power couplers for spoke cavities (in a high-power application) have also been designed. Next steps in spoke-cavity R&D programs will involve building and testing complete cryomodules, including SC focusing elements, power couplers, and tuners.

2.3.3.3 All-spoke-cavity superconducting linac study

At Los Alamos, a straw man 600 MeV 20 mA CW linac design suitable for XADS has been investigated,[73] in which the entire superconducting linac is constructed only from spoke cavities, eliminating the elliptical-cavity high-energy section. This concept appears to offer significant advantages in comparison with the earlier design for the ADTF machine, including shorter overall length and operation of all the SC cavities and cryomodules at 4.2 K, which provides simplification and lower capital and operating costs for the LHe refrigeration and distribution system.

The LANL all-spoke-cavity linac study, which assumes the use of the LEDA 6.7 MeV RFQ as the injector, divides the SC linac into four 350 MHz sections, designed for beta values of 0.175, 0.34, 0.48, and 0.64. Each section has different numbers of cells per cavity, different numbers of cavities per cryomodule and RF driver unit, and different accelerating gradients. Transverse focusing in all sections is provided by SC solenoids located inside the cryomodules. Nominal cryomodule layouts for each section are sketched in Figure 2.34, and Table 2.1 summarises the key parameters.

Maximum cavity gradient is 7.7 MV/m, which is a conservative choice based on prototype beta = 0.175 spoke cavity tests conducted at LANL, and tests conducted on higher-beta spoke-cavity prototypes at other laboratories.

73. Garnett, R. *et al*. (2004), *An Improved Superconducting ADS Driver Linac Design*, OECD/NEA Proc. of 4th Int.Workshop on Utilisation and Reliability of High-Power Proton Accelerators, 16-19 May 2004, Daejeon, South Korea.

Figure 2.34. Schematic cryomodule layouts for each SC spoke-cavity linac section

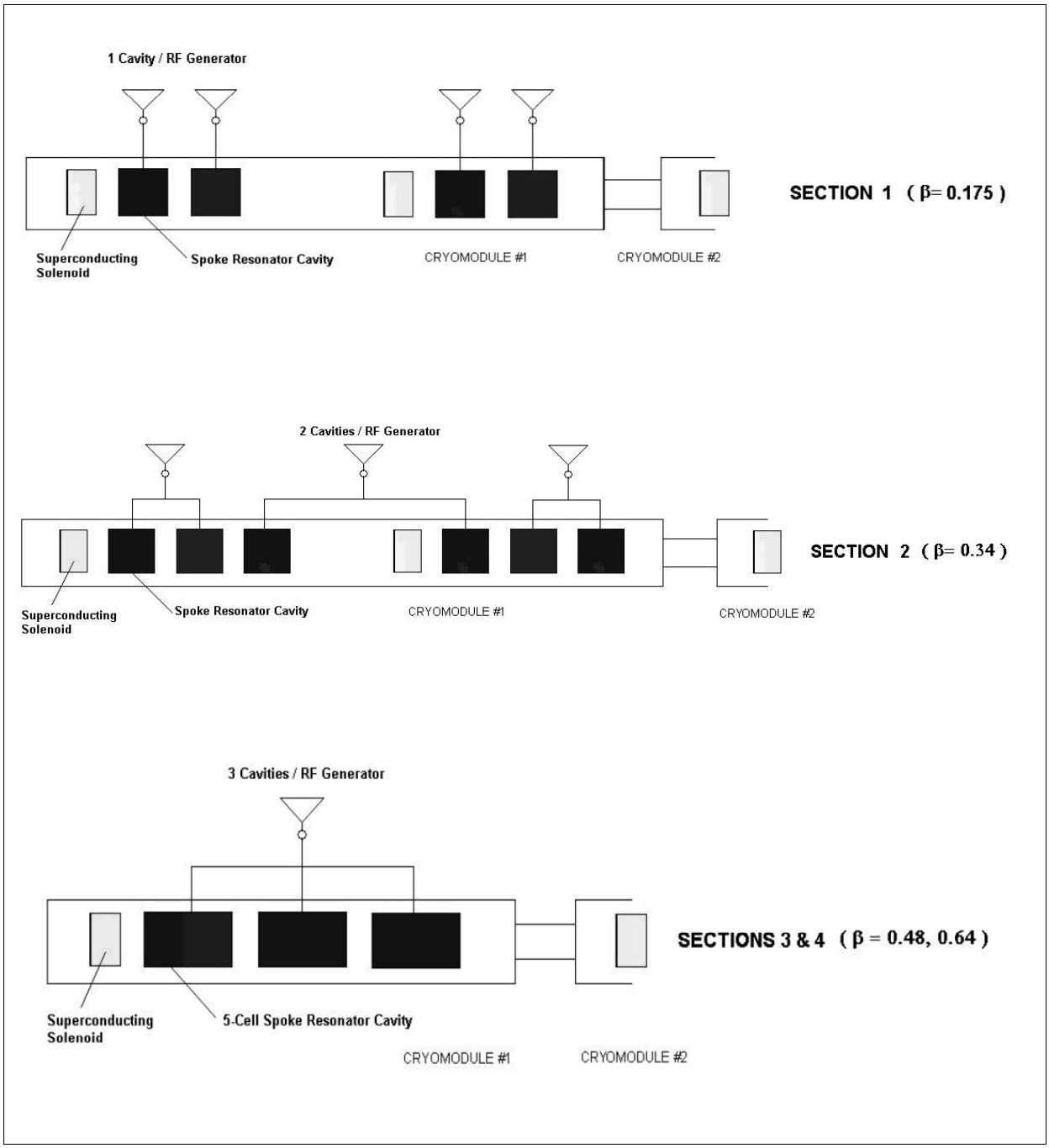

Table 2.1. SC linac design parameters

	Section 1	Section 2	Section 3	Section 4	Total
No. of gaps per cavity	2	3	5	5	–
Cavity beta	0.175	0.34	0.48	0.64	–
Bore radius (cm)	2.5	3.0	3.0	3.0	–
Cavity length (m)	0.200	0.433	1.101	1.371	–
Solenoid length (m)	0.150	0.150	0.250	0.400	–
Cryomodule length (m)	4.226	6.624	5.266	6.226	–
Focusing period (m)	2.263	3.462	6.679	7.639	–
Cavities per cryomodule	4	6	3	3	–
No. of cryomodules	20	6	7	13	46
ΔW/cavity (MeV)	0.08-0.64	0.48-2.1	4.2-6.8	8.8-9.3	–
Synchr. phase (deg)	-45 to -32	-32 to -28.4	-28	-28	–
E_oT (MV/m)	1.1-7.5	1.7-7.5	4.6-7.5	7.2-7.7	–
W_{in}/W_{out} (MeV)	6.7/43.1	43.1/112.0	112.0/239.3	239.3/600.0	–
Section length (m)	90.5	41.5	46.8	96.3	278.1
Max. coupler power (kW)	12.7	42.9	136.0	187.0	–
No. cavities per RF unit	1	2	3	3	–
No. RF units per section	80	18	21	39	158
Solenoid field (T)	1.5-3.3	3.8-4.4	4.0-4.9	4.2-5.6	–
Avg. RE gradient (MV/m)	0.40	1.66	2.72	3.63	2.13

Phase and accelerating-gradient ramps are used to adiabatically capture the RFQ output beam, and to make the transitions from section to section in the spoke-cavity linac as current insensitive as possible. The RF power system is based on the use of inductive output tubes (IOTs) for sections 1 and 2, and klystrons for sections 3 and 4. In section 1, each cavity is driven individually by its own low-power (1.5 to 13 kW) IOT. In the other sections, each RF generator powers two or three cavities. The maximum power required per cryomodule is 408 kW in section 3, and 560 kW in section 4. Figure 2.34 shows a 3 way power split between cavities in these cryomodules.

Table 2.1 shows that the use of 5-gap spoke cavities in the last two sections of the linac provides a high real-estate (RE) accelerating gradient. Compared with previous designs using 700 MHz elliptical cavities in this region, a gradient improvement of a factor of 2.4 is achieved. This is primarily due to the increased active cavity length at the lower operating frequency.

Using 10 000 particle runs, beam simulations were carried out for the straw man accelerator design specified in Table 2.1, both for the ideal linac case and for the case including errors. The assumed errors were of the same type, magnitude, and distribution as those employed in the APT linac design studies. Except for some matching challenges at the transition between the RFQ exit and the first spoke cavity section, the beam dynamics of the linac design are relatively straightforward. Figure 2.35 shows the maximum transverse beam amplitude compared with the machine aperture as a function of beam energy. Both the ideal case amplitude and the distribution of amplitudes for the error cases are plotted. A small fraction of the simulations revealed small beam losses (10^{-4} level) in section 1. No particles were lost in the simulations in the higher-energy sections. The transverse beam emittance was found to be well-behaved, with a growth of approximately 30% due to random errors.

Further work is needed to improve the transition between the RFQ and section 1, but the overall beam-dynamics picture indicates that an all-spoke-cavity 20 mA SC linac can be designed with adequately low beam losses.

Figure 2.35. Maximum beam amplitude as a function of energy for 20 mA current; solid line presents ideal linac; points represent linac with different error sets

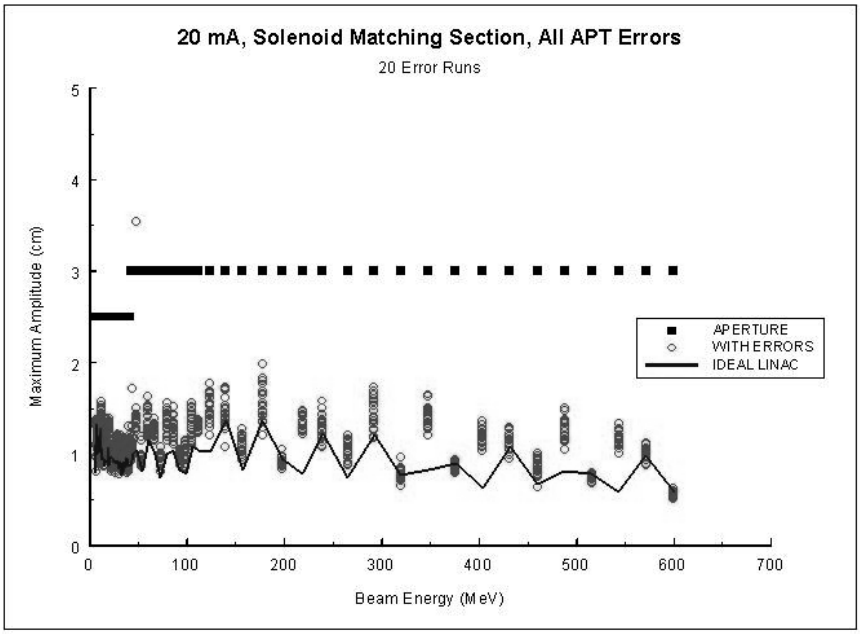

A preliminary design of 5-gap 350 MHz SC spoke-resonator cavities was carried out for both beta = 0.48 and beta = 0.64. The design study included shape optimisation and parameter adjustment to simultaneously minimise the peak electric and magnetic fields. Figure 2.36 shows a cutaway realisation of a 5-gap beta = 0.48 cavity and its axial peak RF electric field profile. The active length of this cavity is 0.83 m, the transit time factor is 0.82, and the ratio of peak electric surface field to average field (E_0T) is 3.5.

Figure 2.36. 5-cell model of β = 0.48 spoke resonator, with on-axis E-field profile

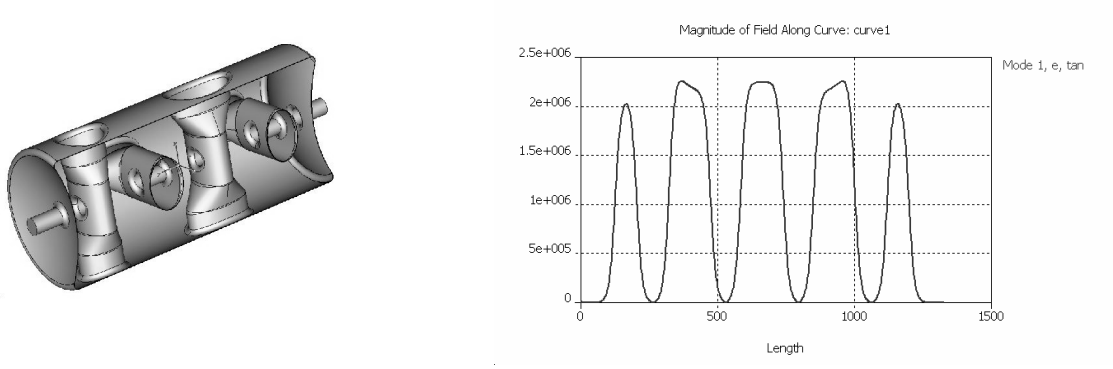

In future iterations, the 5-gap cavity design could be improved by employing some approaches used by the groups that are developing SC spoke cavities for the proposed rare isotope accelerator (RIA).

2.4 The path forward

In the US, only linear accelerators have been considered for XADS and ADS applications. Most of the design and technology development work has been concentrated at Los Alamos, within the context of the APT and AAA programs. A preliminary study of a 600 MeV, 8 MW linac was put together as part of a US XADS proposal (ADTF) in 2001-2002, along with a cost estimate for different options and approaches. One option was to extend and upgrade the capability of the existing LEDA facility at Los Alamos; this was compared in the cost analysis with building an ADTF at a green-field site.

2.5 PDS-XADS project

A recent summary of the European view on XADS accelerators has been given within the context of the (PDS-XADS Project) Preliminary Design Studies of an Experimental Accelerator-Driven System[74] sponsored by the European Commission. The accelerator part of this study, which derives from the European ADS Roadmap study, is led by CNRS-INPN (France). The perspective of this study, in terms of the accelerator for XADS and ADS applications is summarised below.

The linear accelerator, with elliptical SC cavities in the high-energy section, is presently seen as the "solution of choice" for both the XADS and ADS high-power accelerator applications, for power levels that exceed 2 to 3 MW. Such a linac is schematically depicted in Figure 2.37. The main reasons are that: 1) such a linac makes a perfect match to the required energy and power regime; and 2) its inherent modularity provides an easy upgrade path to whatever energy and beam power are finally needed for industrial transmutation. In addition there are two key aspects in which the linac appears to provide the best solution: 1) reliability, availability, and maintainability; and 2) cost and performance optimisation.

74. Deliverable DEL-02-009 of PDS-XADS is dedicated to the preliminary accelerator design (requirements and technical answers).

Figure 2.37. European concept for XADS proton accelerator

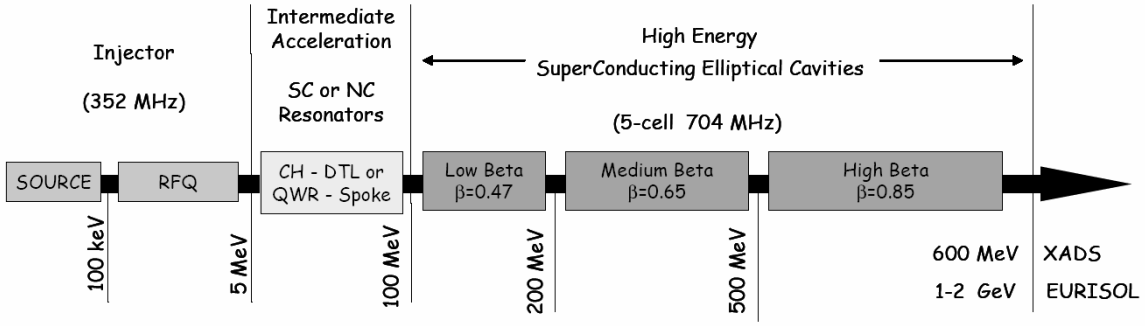

In terms of reliability, a SC linac design allows several typical machine failures to be addressed through an appropriate design philosophy, as follows.

The very high accelerating gradients now attained in elliptical SC cavities (> 25 MV/m) allow the use of a conservative design for the high-energy part of the linac, where gradients no higher than 10 MV/m would be used (without making the accelerator too long). Present studies are investigating how to extend this philosophy into the conservative design of other key linac components, such as power couplers, and RF amplifiers.

The SC high-energy linac is well adapted to design with a high degree of component modularisation. This favours the use of component redundancy and a “spares on line” capability, leading to a highly fault-tolerant design, and therefore to high accelerator reliability and maintainability. An associated fast control-system will allow rapid re-tuning of cavities downstream from a fault, in order to maintain a high-quality beam. Beam simulations are presently under way to quantitatively assess this attractive reliability measure.

Extending the concept of modularity to lower energies, it is envisioned that the intermediate and low-energy sections of the linac could be constructed from independently driven SC cavities (either re-entrant resonators, or spoke cavities).

The high-degree of modularisation will enable a cost-effective spare parts policy, which would be actively coupled with preventative maintenance measures.

Beam dynamics calculations show that SC cavities, with apertures that are large compared with the beam size, will permit linac operation at XADS and ADS current levels with extremely small beam losses, making accelerator maintenance straightforward and uncomplicated.

With regard to cost/performance optimisation it is clear that the over-design philosophy expressed above will likely incur additional capital expense in the linac construction. On the other hand, the high level of modularisation is expected to provide cost-savings because it permits assembly line manufacturing for many of the electronic and mechanical components. The use of SC-cavity technology, starting from an as low an energy as possible, will maximise the power efficiency of the accelerator, and reduces operating costs.

Although the SC-linac solution is thus considered the baseline option for an XADS or ADS accelerator, cyclotron technology should continue to be assessed. A preliminary conclusion is that a

600 MeV cyclotron may be technically feasible at the beam-current level needed for an XADS machine. However, beam extraction schemes that use electrostatic deflectors or H^- stripping should be excluded for reasons of accelerator reliability and maintainability, which would eliminate designs based on an extrapolation of the PSI machine or on a scaled-up version of TRI-University Meson Facility (TRIUMF). The remaining cyclotron concept for the XADS intensity regime would therefore be a machine that accelerates H_2^+ beams, with extraction via stripping. However, the required magnetic rigidity would lead a cyclotron about twice the diameter of the PSI machine, or to a technically very challenging SC cyclotron. In either case there are significant manufacturing challenges, and it is not clear that the cost advantage that lower-intensity cyclotrons have with respect to linacs would remain valid. Nevertheless, further definitive consideration should be given to the cyclotron option, including an assessment of the potential for reliability improvements.

PDS-XADS is in its ending phase (scheduled to end 31 October 2004), and a program is starting in the 6th Framework Program of the EC (named IP-EUROTRANS).

2.6 Santa Fe HPPA workshop

The recent workshop on the Reliability and Utilisation of High-Power Proton Accelerators reached the following conclusions regarding accelerator technology for XADS and ADS applications.

2.6.1 Technology options

There are two options for a high power proton driver: a cyclotron and a linac. The two options both have advantages and disadvantages, but they are quite different and the choice depends on the application. A consensus was achieved on the following general considerations and statements:

2.6.1.1 Cyclotron

For high power proton cyclotrons the only suitable reference machine is the PSI accelerator complex, delivering a 1.2 MW proton beam at 600 MeV. No major R&D programs are under way to sensibly extend this performance, except for the new RF system for the PSI ring that would enhance the power to about 2 MW. A preliminary design has been proposed for a 1 GeV 10 MW machine. However, one disadvantage is that the cost (of the magnet) for a higher energy machine appears to scale nearly quadratically with the output beam energy.

The reliability and availability of the PSI machine is high, but its further improvement in the direction of the basic XADS/ADS requirements (namely, very few unscheduled beam interrupts per year) appears to be very difficult. The basic machine concept does not permit the application of the concepts of redundancy and online spares, which are considered crucial for the reliability demands of a full-scale XADS demonstrator.

2.6.1.2 Linear accelerator

For high power proton linacs, a worldwide R&D effort has been in progress for a number of years, and both the high potential value and the feasibility of these machines have been proven. Different programs have driven this effort: tritium production, spallation sources and ADS. Proton injectors and RFQs with beam capability up to 100 mA have been built and successfully operated,

defining the front end technology up to about 7 MeV. The well-developed and highly efficient elliptical SC-cavity technology is the technology of choice above 100 MeV. For intermediate energies, both NC-cavity and SC-cavity solutions are considered viable. The NC option is already available in terms of design and engineering, although it has not been fully demonstrated under high-current CW conditions. The SC option requires a significant R&D effort. In the linac, the capital cost per MeV decreases with energy.

Apart from the front end (injector plus RFQ), which could be duplicated, an all-superconducting linac has an intrinsic high degree of modularity, which increases with energy. The machine can be designed on the basis of a properly apportioned redundancy in order to permit the use of the online-spares concept. Moreover, maintenance of key components such as the RF amplifiers (klystrons) can be envisioned during machine operation.

2.6.1.3 Recommendations

Cyclotrons of the PSI type should be considered as the natural and cost effective choice for preliminary lower power XADS experiments (such as MYRRHA and TRADE) where availability and reliability requirements are not necessarily among the driving functions.

CW linear accelerators will be the baseline technology for XADS demonstration facilities and full-scale industrial ADS plants, because of their high potential for achieving the required level of beam reliability and availability, and also because of their power upgrade capability.

2.7 R&D on accelerators

Future accelerator technology development efforts should be focused on:

- Reliability analysis of components and subsystems.
- Design analysis of different linac schemes on the basis of reliability performance.
- Working prototypes of new major components to set reliability numbers.
- Development of fast controls and switching devices for taking advantage of component redundancy and online-spares arrangements.
- Development of fast beam-turn-off systems for fail-safe protection of the subcritical assembly.

An R&D effort of a few years, with adequate funding, is required both on accelerator components and accelerator system analysis before it is possible to build a linac fulfilling the XADS and ADS requirements.

Chapter 3

SPALLATION TARGETS FOR ADS APPLICATIONS

3.1 Introduction

At the heart of an accelerator driven system (ADS) is the spallation target. It is the neutron source providing the primary neutrons that are multiplied by the surrounding subcritical core or blanket, in which the transmutation reactions take place. These primary neutrons are produced by spallation reactions of heavy target nuclei bombarded by high-energy protons that are generated by a suitable accelerator.

3.2 Design issues

The number of spallation neutrons per incident proton depends on the beam energy and on the mass of the target nuclei. Due to their high atomic number, heavy metals such as lead, mercury, uranium, tungsten, tantalum, or eutectics such as lead-bismuth are the most appropriate choices for the target material. Moreover, because of the requirement to minimise the size of the target in relation to the core dimensions (to provide good neutron economy); the target design is driven to maximum power density. For the very high power densities reached in a spallation target (several hundred kW per liter for proton beam powers of several MW), a flowing liquid metal target material provides the best option for practical removal of the heat by convection. The use of a heavy liquid metal (HLM) also significantly reduces the damage caused by intense radiation to the target itself and the structural materials.

However, the use of HLM gives rise to problems of erosion, corrosion, and liquid metal embrittlement (LME) of structural materials that are in contact with the circulating metal at its characteristic high temperatures and high fluid velocities. In addition, difficulties concerning the confinement of volatile spallation products and the separation between the proton beam vacuum and the liquid spallation target must also be addressed.

Lead-bismuth eutectic (LBE) is today the reference target material for ADS applications. Both lead and lead-bismuth exhibit very low neutron capture making them good candidates from a neutronic standpoint. Lead (Pb) might at first appear a better target choice than LBE, because of its considerably lower production of ^{210}Po (a migratory α-emitter) under neutron bombardment. However, lead has the critical disadvantage of a higher melting point (327°C compared with 123.5°C), which presents severe thermo-mechanical design challenges for the target structural materials. The ^{210}Po release problem in LBE is mitigated by the fact that Po forms a chemical bond with Pb to form metastable Pb-Po, which has an emanation rate (vapour pressure) 1 000 times lower than that of Po by itself.

Mercury (Hg) has also been considered as a spallation target material because of its low melting point (-38.9°C) and the absence of the ^{210}Po problem. However, its high volatility would seriously complicate the confinement of its radioactive isotopes, and its low boiling temperature would make its use in ADS difficult due to the high working temperature of the target and also of the subcritical

multiplier. In addition its high neutron capture cross section degrades the leakage and therefore the neutron efficiency of the target.

With regard to the separation between the proton beam vacuum and the HLM, two types of spallation target configurations can be considered: a *window* concept where physical separation is provided by a material (metal) window and a *windowless* concept where the HLM is in direct contact with the beam vacuum, and the proton beam directly impinges on the liquid heavy metal.

Configurations using a metallic beam window have the problems of: 1) cooling the window; 2) cyclic thermal loading of the window under creep conditions; 3) a very corrosive environment; and finally 4) the radiation damage induced by the protons and fast neutrons in the window material. It has been estimated that an ADS target beam window will have to be replaced at least every 5-6 months.

A windowless target poses the issue of compatibility with the beam-transport vacuum. Evaporation from the target surface must be minimised in order to avoid degradation of the beam vacuum, and also in order to avoid migration of radioactive spallation products into the beam pipe. These problems can be solved by appropriate design of the liquid target, as well as the terminus of the beam transport line. The target surface temperature should be held below 450°C, which minimises liquid metal evaporation and gas emanation, reducing the load on the vacuum pumping system. Another issue is the definition and the stability of the free liquid metal surface in normal and transient (e.g. beam trip) conditions. For a window target design, concerns about beam vacuum degradation and radioactive spallation product release should also be taken into account to deal with the case of a window rupture. Appropriate safety measures should be taken for both the window design and windowless design.

For cooling of an ADS spallation target, two options can be considered: cooling by means of the subcritical reactor primary system coolant, or cooling via an independent loop. In order to limit the window operating temperature to tolerable values (< 550°C), it is likely that the window target design will need an independent loop. In the case of the windowless configuration, the target can be cooled by the primary coolant because window integrity is not an issue.

In order to prevent contamination of the coolant, the HLM target containing the spallation products has to be kept confined within the target unit and separated from the primary cooling loop. In the case of a gas-cooled ADS target, the target unit has to be designed for high outside pressures. For both HLM and gas cooled systems, the target needs to be designed as a removable unit, because its lifetime is anticipated to be considerably shorter than the subcritical reactor lifetime, due to the intense radiation and high local thermal stresses. The structural materials for the target unit should be compatible with the HLM and able to resist the mechanical loads on the target window at the relevant operating temperatures and under intense proton and neutron irradiation.

3.3 Ongoing design projects and support programmes

3.3.1 Europe

Within the 5th Framework Program of the European Commission, the ADS design efforts have been concentrated within the PDS-XADS project.[75] Here, three ADS system designs were studied: two

75. Carluec, B. (2003), *The European Project PDS-XADS, Preliminary Design Studies of an Experimental Accelerator-Driven System*, Proceedings of the International Workshop on P&T and ADS Development 2003, ISBN 9076971072, SCK•CEN, Mol.

LBE-cooled concepts (an 80 MW system and a compact 50 MW system), and one 80 MW gas-cooled concept. Each concept has its specific spallation target designs.

80 MW LBE-cooled[76]

LBE is chosen for the spallation target, which is bombarded with a 600 MeV, 6 mA CW proton beam. About 70% of the beam power is deposited as heat in the target material (2.6 MW_{th}).

The LBE target material, in which spallation products are produced by the beam, is kept confined within the target unit in order to prevent the contamination of the primary LBE coolant. The elements of the target unit are the proton beam pipe, a heat exchanger, and the LBE circulation system. The latter can be designed for forced or natural circulation, depending on whether a window or windowless target is employed.

The window target, schematically shown in Figure 3.1, features a thin metallic sheet as a barrier between the LBE target and the beam-transport vacuum pipe. The window and most of the target unit are made of ferritic-martensitic $_{9}Cr_{1}Mo$ steel. The heat generated by the spallation reactions is removed by natural circulation of the LBE. The use of a diathermic fluid as secondary coolant provides high flexibility in the choice of the thermal cycle; in particular, it permits the temperature of the hottest part of the window to be held below 500°C. The LBE flow velocity is kept below 2 m/s to limit corrosion and erosion problems. The design lifetime of the window is expected to be significantly smaller than the other structures of the target unit (about 3 to 6 months).

In this ADS system design a windowless target concept, such as that shown in Figure 3.2, is also considered. In the windowless target unit, the proton beam impinges directly on the free surface of the liquid target. To avoid local boiling of the LBE, the power density deposited by the beam is reduced by scanning it over the target surface in a direction orthogonal to the main flow motion; in this way, the maximum LBE temperature is constrained to < 450°C. Again, 2 m/s is set as the upper limit for the LBE flow velocity. Natural circulation is not practical for this design because the heat source is at the top of the circuit. The heated LBE must be thus driven downwards to the heat exchanger by some means, in this concept two mechanical pumps in series. A stream of primary LBE is bypassed from the cold plenum to the heat exchanger to serve as a cooling medium.

In the windowless target unit option, no structural material is exposed to direct proton bombardment, which leads to lifetimes similar to the handling intervals of the fuel assemblies (estimated to be about 3 years).

80 MW gas-cooled[77]

Again, LBE is chosen for the spallation target which is bombarded with a 600 MeV, 6 mA proton beam.

---

76. Cinotti, L. *et al*. (2003), *Status of the Studies performed by the European Industry on the LBE cooled XADS*, Proceedings of the International Workshop on P&T and ADS Development 2003, ISBN 9076971072, SCK•CEN, Mol.

77. Giraud, B. (2003), *Preliminary Design Studies of an Experimental Accelerator-Driven System, Overall description of the gas-cooled system*, Proceedings of the International Workshop on P&T and ADS Development 2003, ISBN 9076971072, SCK•CEN, Mol.

Figure 3.1 Window target (80 MW LBE-cooled)[76]

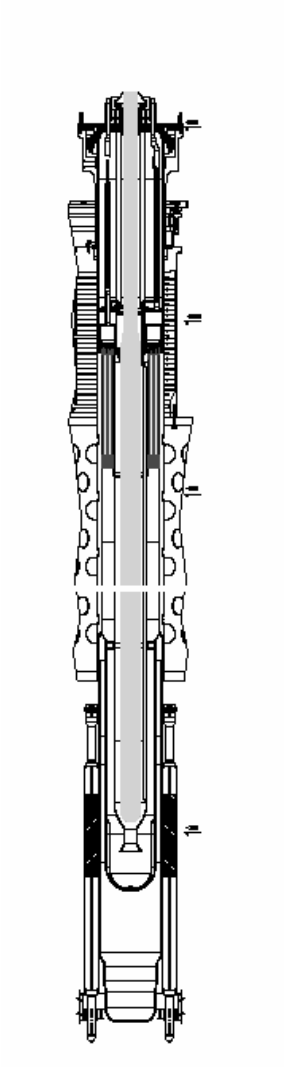

Figure 3.2. Windowless target & Proton beam scanning (80 MW LBE-cooled)[76]

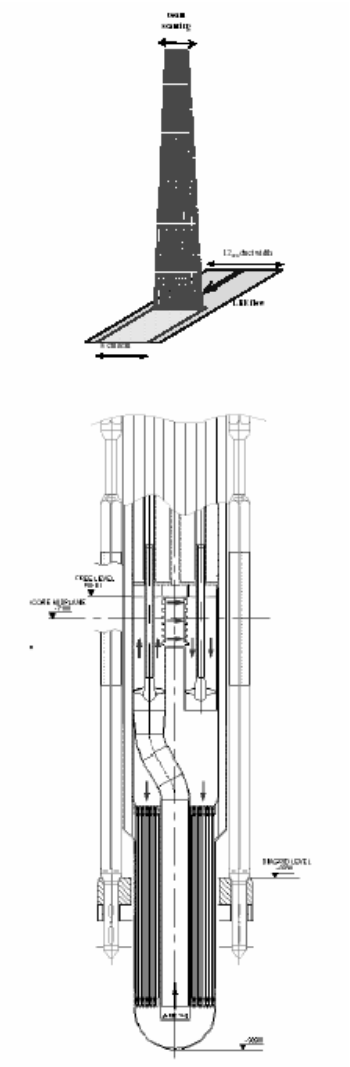

Separation of the target LBE from the primary coolant is realised by the main target unit shell; the reactor thimble acts as a second barrier, protecting the main shell from the 60 bar primary coolant system pressure. The beam tube and integral beam window (both made of ferritic-martensitic $_{9}Cr_{1}Mo$ steel), constitute the physical barrier between the target LBE and the beam line vacuum (see Figure 3.3.).

The LBE is circulated by electromagnetic pumps and cooled by an external heat exchanger (with low pressure water, pressurised water or diathermic fluid) located in the target cooling room outside the reactor vessel. The same limits on LBE temperature and velocity apply as in the LBE cooled case.

Figure 3.3. Spallation zone (80 MW gas-cooled)[77]

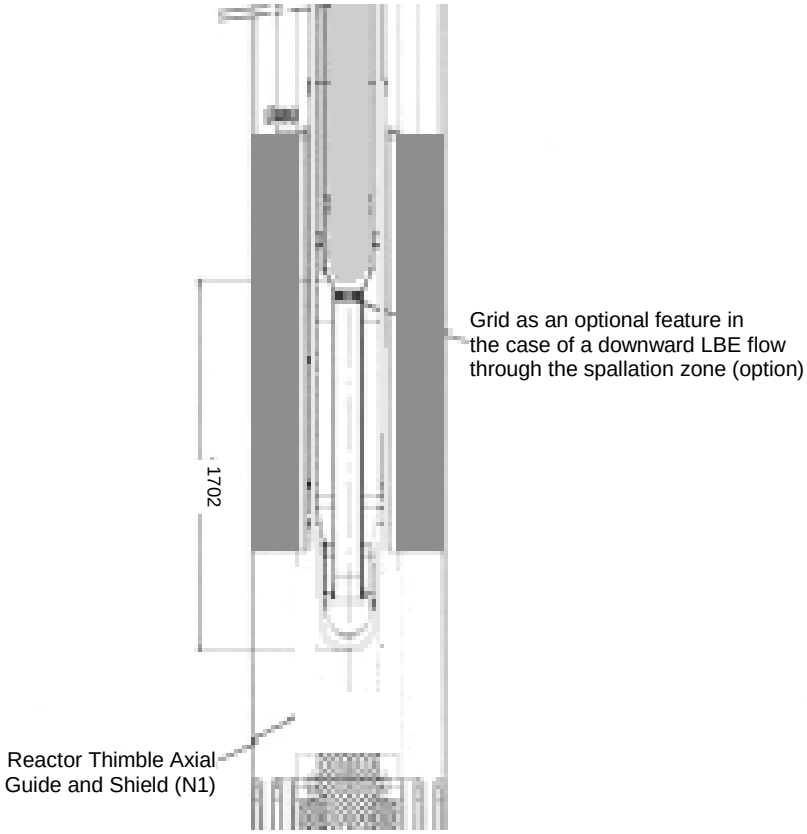

50 MW LBE-cooled (MYRRHA)[78]

For the spallation target of the MYRRHA ADS under development at Mol, Belgium, LBE has been chosen as the spallation target material (Figure 3.4). A windowless target design was chosen, mainly for reasons of space restrictions in the high-performance subcritical core. The current density of the 350 MeV, 5 mA proton beam exceeds 150 μA/cm^2 at the window, which is at least a factor of 3 higher than for any window that has been attempted.

The deposited beam power is removed by forced convection (mechanical pump + auxiliary electromagnetic pump) and transferred to the reactor primary system LBE coolant in a liquid metal – liquid metal heat exchanger. The target unit is made of ferritic-martensitic $_9Cr_1Mo$ steel. Surface temperatures are kept below the maximum of 450°C in order to limit LBE vapor evaporation, by minimising recirculation zones and scanning the proton beam in such a way that it matches the flow pattern. LBE flow velocities are kept below 2.5 m/s to limit corrosion and erosion.

78. Aït Abderrahim, H. *et al*. (2003), *MYRRHA, A Multipurpose Accelerator-Driven System for R&D. State-of-the-art of the project at mid-2003*, Proceedings of the International Workshop on P&T and ADS Development 2003, ISBN 9076971072, SCK•CEN, Mol.

Figure 3.4. A schematic view of the MYRRHA windowless spallation target loop

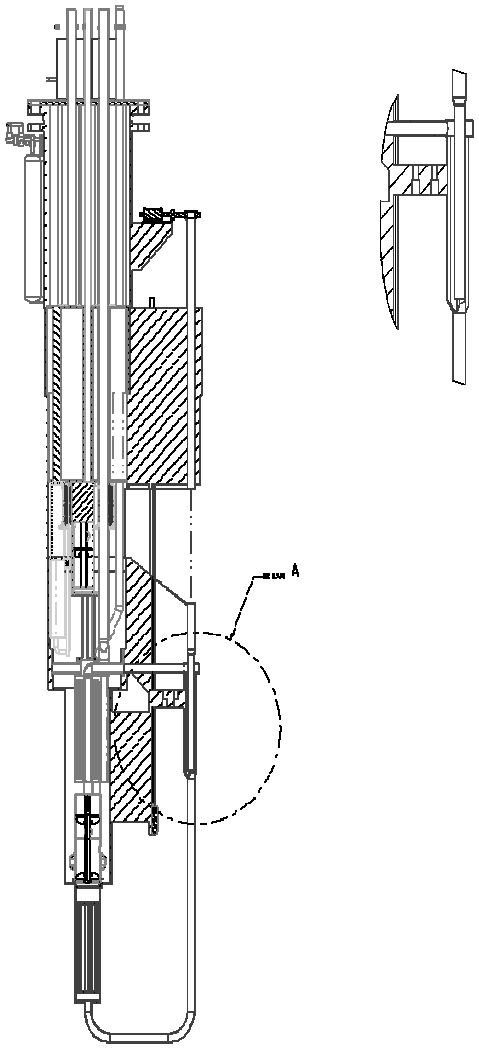

The R&D programs that support the spallation target design are grouped within the Technological Support for Transmutation (TESTRA) cluster of the Thematic Network on Advanced Options for Partitioning and Transmutation (ADOPT) network of the 5th EC Framework Program: SPIRE[79] investigates the effect of neutron and proton irradiation on steels, Technologies, Materials and Thermal-Hydraulics for Lead Alloys (TECLA)[80] studies materials corrosion in contact with LBE as well as thermal-hydraulics for LBE, Assessment of Computational Fluid Dynamics Codes for Heavy Liquid Metals (ASCHLIM)[81] deals with computational fluid dynamics for HLM, and Megawatt Pilot Target Experiment (MEGAPIE)-Test[82] for LBE spallation target.

These design-support and R&D activities will be continued within the 6th EC Framework Program within the Integrated Project EUROpean Research Programme for the TRANSmutation of High Level Nuclear Waste in an Accelerator Driven System (IP-EUROTRANS). Here, the LBE windowless target is put forward as the reference concept, and the window target is considered as the backup solution. Supporting R&D on HLM technology that is relevant in some areas to the design of an ADS spallation target will be performed within the DEvelopment and assessment of structural materials and heavy liquid MEtal technologies for TRAnsmutation systems (DEMETRA) sub-project.

The MEGAPIE[83] is a joint initiative by six European research institutions (PSI, CEA, CNRS, ENEA, FZK, SCK•CEN), joined now by DoE (USA), JAERI (Japan) and KAERI (Korea), to design, build, operate and evaluate an LBE spallation target at the level of 1 MW of beam power. This experiment makes use of the existing 590 MeV, 1.8 mA proton beam of the SINQ spallation neutron source at PSI, Switzerland.

As shown in Figure 3.5, MEGAPIE has a window target cooled by a pumped bypass flow of LBE next to the main LBE cooling flow. Electromagnetic pumps have been selected for the main and the bypass LBE cooling flow. The structural material for the target is martensitic steel (T91) for the lower, active part. For the upper part, austenitic (316L) steel is used.

The goal of MEGAPIE is to explore the conditions under which an ADS spallation target system can be licensed, to accrue a design database for liquid lead-bismuth targets and to gain experience in operating such a system under the conditions of present day accelerator performance. Design validation of the target through extensive monitoring of its operational behaviour and post- irradiation examination of its structural components are integral parts of the project. Parts of these activities are performed within the 5th Framework Program of the EC in the MEGAPIE-Test program.

---

79. Alamo, A. *et al.*, (2003), *Overview of SPIRE project*, Proceedings of the International Workshop on P&T and ADS Development, 2003, ISBN 9076971072, SCK•CEN, Mol; and "Irradiation effects in Martensitic Steels under Neutron and Proton Mixed Spectrum SPIRE", European Commission 5th Framework Program Contract N° FIKW-CT-2000-00058.

80. Benamati, G. *et al.*, (2003), *TECLA Project: Technologies, materials and thermal hydraulics for lead alloys*, Proceedings of the International Workshop on P&T and ADS Development 2003, ISBN 9076971072, SCK•CEN, Mol; and "TECLA Progress Report Annual Scientific and Technical Report", European Commission 5th Framework Program Contract N° FIKW-CT-2000-00092.

81. Arien, B. (2003), *ASCHLIM: a 5th FP Project for the Assessment of CFD Codes applied to Heavy Liquid Metals*, Proceedings of the International Workshop on P&T and ADS Development 2003, ISBN 9076971072, SCK•CEN, Mol.

82. Fazio, C. *et al.* (2003), *MEGAPIE-TEST*, Proceedings of the International Workshop on P&T and ADS Development, 2003, ISBN 9076971072, SCK•CEN, Mol.

83. Bauer, G.S. *et al.* (2001), "MEGAPIE, a 1 MW Pilot Experiment for a Liquid Metal Spallation Target", *Journal of Nuclear Materials*, Volume 296, Issue 1-3.

Figure 3.5. Schematics of the MEGAPIE target[84]

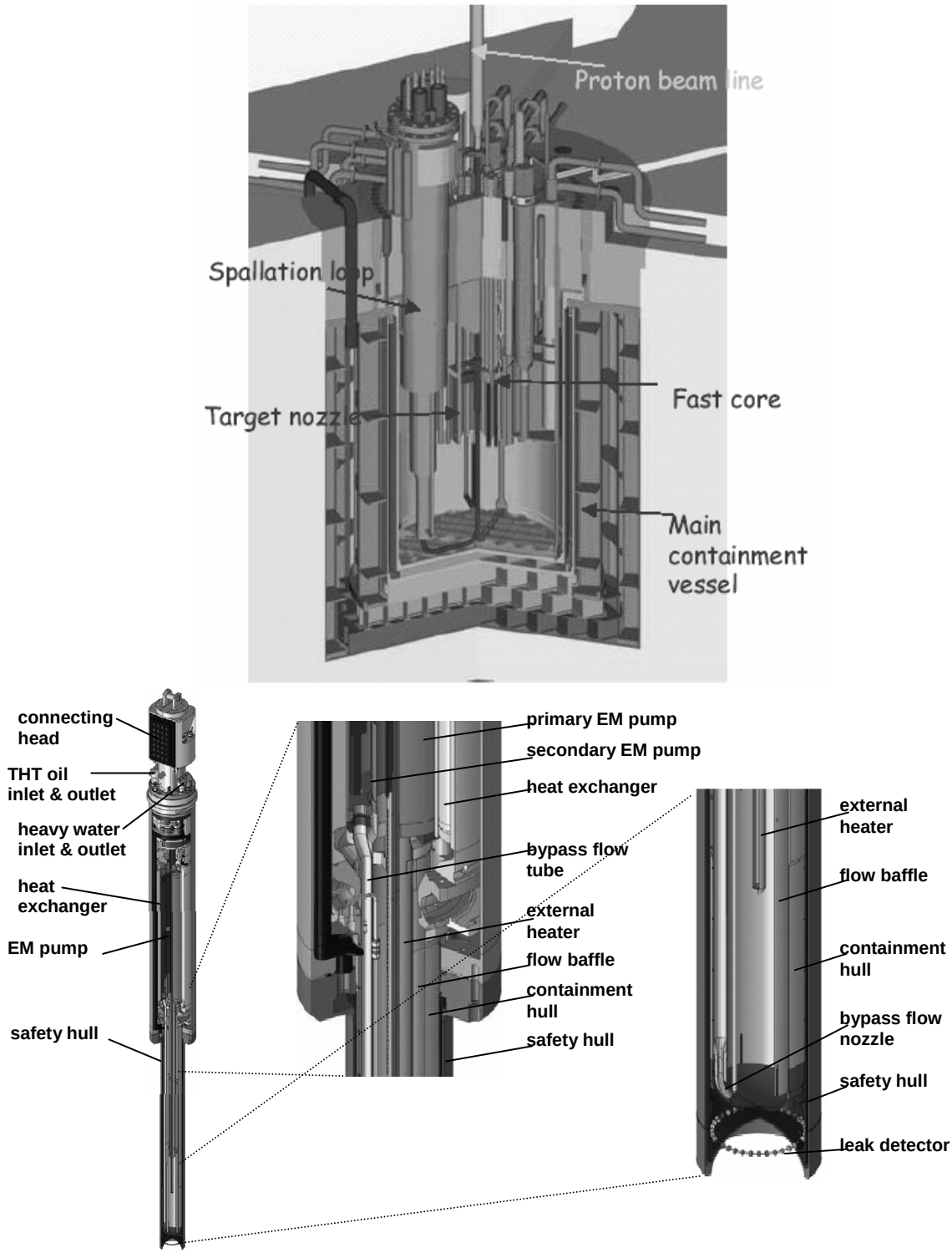

84. Fazio, C. *et al.* (2003), *The MEGAPIE-TEST Project*, Proceedings of the International Workshop on P&T and ADS Development 2003, ISBN 9076971072, SCK•CEN, Mol.

3.3.2 Korea

KAERI is developing a 1 000 MW_{th} fast spectrum ADS concept called HYPER (HYbrid Power Extraction Reactor). In this design, a 1 GeV, 20 mA proton beam is directed at an LBE target with a window.[85] The window material is chosen to be $_9Cr_2VWTa$ (Optifer) steel, an advanced ferritic-martensitic alloy. To limit corrosion and erosion, the temperature of the LBE is fixed at 500°C and its velocity at 2 m/s. A value of 600°C is chosen as the maximum allowable temperature for the beam window, and the stress intensity is not allowed to exceed 1/3 of the yield strength of the window material (480 MPa at 600°C). Static corrosion tests in LBE have been performed and a dynamic corrosion loop has been designed.

3.3.3 Japan

In their ADS program, JAERI is studying the design and technology of an 800 MW_{th} system with a 1.5 GeV, 15 to 25 mA proton linac.[86] LBE is selected as the first candidate for the window spallation target material. Several target structural materials are being considered (austenitic JPCA and martensitic F82H). An R&D program studying the corrosion of structural materials, the thermal-hydraulics in the beam window, and the behaviour of radioactive impurities has been set up.

To demonstrate ADS feasibility, a Transmutation Experimental Facility (TEF) is planned within the framework of the J-PARC project. The construction of TEF is scheduled to start in 2006, and it consists of two buildings, the Transmutation Experimental Facility for Physics studies (TEF-P) and a Target Test Facility (TEF-T). TEF-P is a zero-power critical facility to research the subcritical reactor physics. TEF-T is a materials irradiation facility that can handle a 600 MeV, 330 μA (200 kW) proton beam incident on an LBE spallation target.

3.3.4 United States

The Advanced Fuel Cycle Initiative (AFCI) Program Series II aims at developing and demonstrating nuclear waste transmutation through advanced reactors (Gen IV LFR) and ADS.[87] An ADS concept using an LBE spallation target and coolant is under evaluation and development. LBE technology development has been supported by AFCI (including the predecessor programs ATW and AAA) and is now jointly supported by GEN IV LFR.

An ADS R&D program is set up that includes material corrosion and erosion, thermal-hydraulics, thermodynamics, radiation effects, and instrumentation tests. The primary facility to be used to study the materials and thermal-hydraulics of lead and lead-alloy systems is the DEvelopment of Lead-alloy Technology Applications DELTA loop at LANL (Figure 3.6). A program to measure target material

85. Cha, J.E. *et al*. (2003), *Preliminary Design of Dynamic Corrosion-Facility for Lead-Bismuth Eutectic and Test in Static Corrosion Facility*, Proceedings of the International Workshop on P&T and ADS Development 2003, ISBN 9076971072, SCK•CEN, Mol.

86. Oigawa, H. (2004), *A Review of Research and Development on Accelerator-Driven System for Transmutation of Long-Lived Nuclear Waste*, Proceedings of the IAEA Technical Meeting on the "Review of National Programs on Fast Reactors and Accelerator Driven Systems (ADS)", Technical Working Group on Fast Reactors, IAEA, Vienna, (to be published).

87. Roglans, J. (2004), "Status of the U.S. Activities in Fast Reactors and Accelerator Driven Systems", oral presentation at the IAEA Technical Meeting on the "*Review of National Programs on Fast Reactors and Accelerator Driven Systems (ADS)*", Technical Working Group on Fast Reactors, IAEA, Vienna.

properties under irradiation in a high-energy proton beam is under way at Los Alamos using the 800 MeV, 1 mA LANSCE proton linac. Also, a proposal is under consideration for construction of a new experimental facility at LANSCE for testing ADS target materials and fuels. This facility, the LANSCE Materials and Fuels Test Station (MFTS), would irradiate target materials at prototypic AFCI flux levels and temperatures and test target design concepts.

Figure 3.6. Schematics and picture of the DELTA loop at Los Alamos National Laboratory

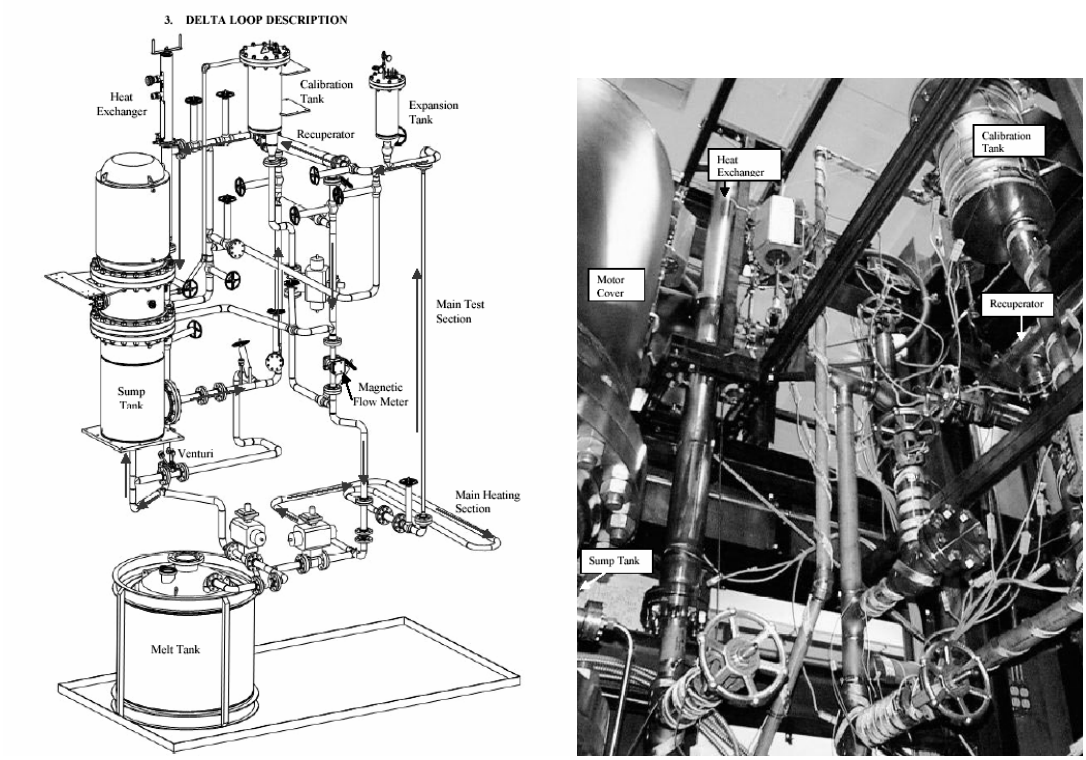

3.3.5 India

A five-year plan (2002-2007) has been initiated that will set up and use facilities to demonstrate key technologies needed for ADS development.[88] As part of this program, the thermal-hydraulics of both window and windowless target configurations are being investigated by modeling and experiments. For this purpose, a mercury circulation loop is being assembled at BARC (Bhabha Atomic Research Centre) in Mombay. The basic process system design of an LBE loop has been completed and its components are being ordered. Beam heating simulations are being planned. The loop will also be used for the study of material compatibility with regard to corrosion and erosion by heavy metals. Materials considered are SS 321, T91 and tungsten-rhenium alloys.

88. Nema, P.K. *et al.* (2004), "Status of activities in India on Development of Accelerator Driven System", Proceedings of the IAEA Technical Meeting on the *Review of National Programs on Fast Reactors and Accelerator Driven Systems (ADS)*, Technical Working Group on Fast Reactors, IAEA, Vienna, (to be published).

3.3.6 China

A five-year conceptual study of ADS ended in 1999. A new five year program of basic research has been launched in 2004.[89] The research activity is focused on nuclear database and material studies supporting ADS. This includes the simulation of window and target radiation damage and material compatibility.

3.3.7 Russia

R&D work in the area of ADS is carried out in various Russian research centers on their own initiative or under international contracts.[90] The largest program has been carried out at the State Scientific Research Centre of the Russian Federation – Institute for Physics and Power Engineering (SSRC RF-IPPE, Obninsk, Russia), which dealt with the development and construction of the first spallation target complex (TC-1) in the world to use LBE coolant. This target was intended to be irradiated by the LANSCE 800 MeV proton accelerator at Los Alamos. The equipment was delivered to LANSCE in 2002. Because of compatibility issues, the target system is being assembled at UNLV for engineering testing without proton beam.

3.4 Target technology

3.4.1 Structure materials

The reference spallation target material in the present designs of accelerator driven systems is liquid lead-bismuth eutectic (LBE).[91] As discussed above, the eutectic has clear advantages over other candidates (e.g. Pb and Hg) regarding operating temperature. However, LBE is potentially highly corrosive for most common construction materials, due to the high solubility of the alloying metals (mainly Ni and Fe) in LBE.

The process of liquid metal corrosion is initiated by the interaction of the liquid metal with the surface of the structural material.[92] This damages the protective outer layer and exposes the alloying elements in the bulk material to solution in the LBE. In addition, there is the possibility of the reaction of the structural material with non-metals that are dissolved in the LBE. For rapidly flowing pumped LBE systems, in contrast with systems using stagnant eutectic, the corrosion rate is increased because of the higher diffusion rate and the contribution of erosion. Furthermore, mass transfer processes of the dissolved material along temperature gradients in the target vessel (where compound elements are dissolved in hot zones and deposited in cold zones) maintain the corrosion. The mechanism also poses

89. Haihong, X. *et al*., (2004) "The progress of Researchs on ADS in China", Proceedings of the IAEA Technical Meeting on the *Review of National Programs on Fast Reactors and Accelerator Driven Systems (ADS)*, Technical Working Group on Fast Reactors, IAEA, Vienna (to be published).

90. Poplavsky, V.M. *et al.* (2004), "Russian Fast Reactors in 2003 and Their Prospects", Proceedings of the IAEA Technical Meeting on the *Review of National Programs on Fast Reactors and Accelerator Driven Systems (ADS)*, Technical Working Group on Fast Reactors, IAEA, Vienna, (to be published).

91. Cinotti, L. *et al., Technical specification and target unit interface (LBE and gas cooled concepts, window and windowless options)*, PDS-XADS Workpackage 4.3, deliverable 02/070.1. Available at http://www.sckcen.be/ADOPT.

92. Sapundjiev, D. *et al.*, "Liquid metal corrosion of T91 and A316L materials in Pb-Bi eutectic at temperatures 400°C-600°C", submitted for publication in *Corrosion Science*.

an operational hazard, due to accumulation of slag in critical components like heat exchangers. Liquid metal corrosion changes the structure and appearance of the materials surface, leading to a possible deterioration of heat transfer efficiency. Finally, corrosion will obviously influence the mechanical properties of the structural materials.

Figure 3.7. The different phases of corrosion of unirradiated T91 in LBE that depend on the temperature and oxygen concentration

From left to right: the formation of a stable oxide layer, the transition mode in which the oxide layers are attacked by the LBE and finally the dissolution of Fe and Ni into the LBE.[92]

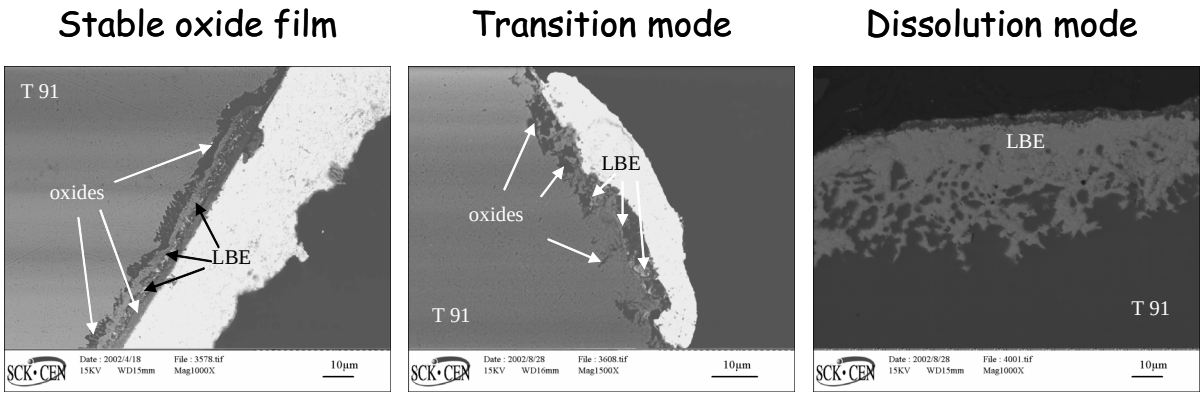

In terms of material corrosion and degradation, conditions are even more severe within the spallation target itself. First, the high-energy protons and neutrons produce various spallation and fission products via nuclear reactions with the target material. These products can modify the chemical composition of the liquid metal, and consequently the corrosion potential, in a very significant way. In addition, the attack on structural materials and target window is enhanced by the thermal load due to the proton beam and the radiation burden due to the high-energy protons and the intense neutron field, with the latter causing irradiation embrittlement and swelling. In view of these considerations it is clear that the reference materials for the construction of a spallation target must be chosen with due care. The selected substance should meet the following criteria:[91]

- a proven manufacturing process should be available for all target components;
- the material must have the right physical characteristics to be employed in the construction of nuclear components;
- the material should have sufficient strength and be capable of withstanding high thermo-mechanical stresses and loads; and
- the material must have good resistance to LBE corrosion, irradiation by an energetic proton and neutron spectrum, and possible synergies arising from the combination of both effects.

At high temperatures (> 400°C), unprotected high-nickel austenitic steels are known to be susceptible to severe corrosion in LBE. Ferritic and low-alloy steels, on the other hand, in principle have a higher resistance to liquid metal corrosion because of the absence of alloying elements that have a large solubility in LBE. At lower temperatures however, high-chromium austenitic steels show better resistance because of the higher stability of the chromium-oxide protective layer. The current state of corrosion research indicates that for a mid-term exposure to flowing LBE (1 m/s) containing dissolved oxygen the operational temperature limits are about 535-550°C for both ferritic-martensitic and austenitic steels, if the oxygen activity is controlled at oxidising conditions (for in-situ oxidation

and self-healing of the oxide layer). Adding Si to austenitic steels at a percentage not higher than 5%, prevents dissolution of Ni and penetration of the Pi/Bi eutectic at 550°C. The use of proper coating, such as Al-alloying with different techniques, has been demonstrated to provide a good corrosion resistance even at 600°C.

In highly irradiated parts there is also a minimum requirement for the temperature since results from the Spallation Induced Radiation Effects (SPIRE) project indicate that hardening and embrittlement under helium production would be reduced significantly above 400°C.[79,93] In almost all situations, an active control of the oxygen concentration in the liquid metal is of paramount importance. The concentration range is defined by the requirement that it must be high enough to allow a stable Fe-Cr-oxide layer to be formed, while the precipitation of oxides formed with Pb or removed from the metal surface by erosion, should be avoided.

Further R&D efforts supporting the materials choice for ADS spallation targets must be aimed at the understanding of the physical and technological aspects of corrosion/erosion behavior of structural (and window) materials that are exposed to flowing LBE under irradiation by high intensities of high-energy protons and a hard intense neutron spectrum. On the one hand, investigations should be concentrated on the nickel-free 9%-12% Cr type of ferritic-martensitic steels, work that may benefit from the development of low-activation martensitic steels in the fusion-materials program. On the other hand, high-chromium/high-nickel austenitic steels should be considered as well because of their high-temperature strength. In most of current design projects involving a megawatt ADS spallation target, T91 (9% Cr, 1% Mo with traces of V, Nb, N, Si and Mn) and SS 316L (16%-18% Cr, 10%-14% Ni, 2%-3% Mo) have been selected as reference materials for both types of steel respectively because of the availability of some data from irradiation tests in fission reactors. To optimise the integrity of the materials used in the spallation source the following topics should be covered.

Susceptibility to LBE corrosion, liquid metal embrittlement, and fatigue

As noted above, the present state of research into the reference spallation target materials shows that LBE corrosion should not pose a problem in the relevant temperature range for ADS operation, provided that proper control of the oxygen concentration is established. Also, small additions of Si (< 1%) to 12 Cr ferritic/martensitic steels (such as HT-9) have shown beneficial effects on improving corrosion resistance in LBE. Alloys such as EP-823 developed in Russia have shown superior corrosion resistance, although irradiation results show an embrittling effect from the Si for irradiations at temperatures below 450°C.

Overall, the data on liquid metal embrittlement (LME) are not conclusive. Experiments on SS 316L did not show any LME in the relevant temperature range. For T91 there is some concern for LME to occur in situations predetermining the embrittlement. This may point to a possible synergy between the effects of irradiation/He-formation damage and LME.

Fatigue experiments on T91 have shown that normal cycle fatigue is not significantly altered by the presence of LBE. Low cycle fatigue, on the other hand, is affected by LBE (Figure 3.8). Data taken at 375°C using a 1-10 Hz cyclic load between 50% and 150% of the yield stress have shown a lifetime reduction of 25%-30% in LBE, compared with the same experiment done in air. This result is independent of the frequency.

93. Turroni, P. *et al.*, *Evaluation of candidate material properties under irradiation (p,n) and corrosive conditions to relevant target unit structures (LBE and gas cooled concepts)*, PDS-XADS Workpackage 4.3, deliverable 04/29. Available at http://www.sckcen.be/ADOPT.

Figure 3.8. Reduction of low cycle fatigue life of T91 in LBE as compared to T91 in air
The diminuation is 25-30% at low stess, (half of the yield stress) while at high stress (twice the yield stress) the reduction of the fatigue life goes up to 70%.[94]

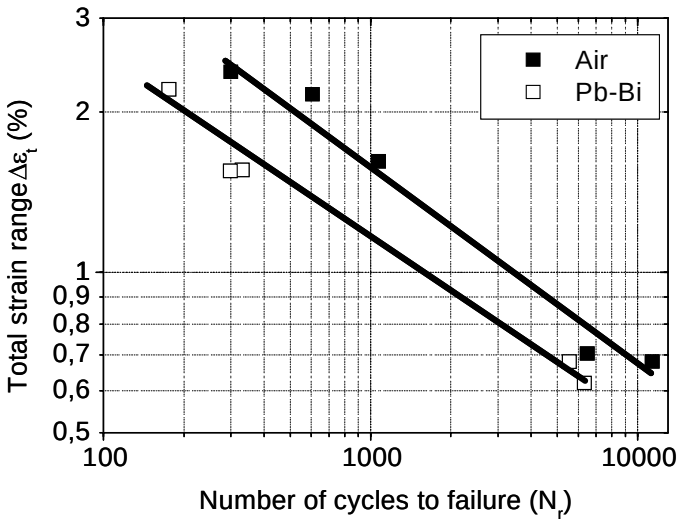

An important concern in this research, which focuses on the validation of reference materials for use in structural components of an ADS spallation source, is that the influence of LBE depends on the morphology of the material surface after manufacturing of the component. This means that in principle not only samples with a standard surface but also "realistic" components (after forging, drawing, rolling, machining, welding, etc.) should be investigated. Furthermore, all experiments have been performed using pure lead-bismuth eutectic while in the real situation, contaminating elements, in particular spallation products, may be present. In view of these uncertainties the development of protective coatings and surface treatment to augment the corrosion resistance is highly relevant. Finally, the tools required to guarantee the assumed conditions of oxygen control must be developed. This argumentation leads to the following, non-exhaustive list of research issues that need to be addressed:

- Long-term stability of oxide layers and scales that are formed on the reference materials by pre-oxidation in air.
- Influence of manufacturing process on the surface morphology and corrosion susceptibility.
- Chemical-physical effects of inhibitors in LBE.
- Influence of spallation products on the corrosion of reference materials in LBE.
- Development of protective coatings to augment corrosion resistance.
- Development of an integral oxygen control system with the inclusion of stable and reliable oxygen sensors.

94. Vogt, B. *et al.* (2003), *Liquid metal promoted fracture of T91 steel*, Proceedings of the III[rd] International Workshop on Materials for Hybrid Reactors and Related Technologies, 15 October 2003, Rome.

Susceptibility to radiation

The susceptibility of the reference SS 316L has been investigated extensively via experiments performed in fission reactors while some data on T91 are also available. Measurable material characteristics that are most relevant to structural design analyses are the tensile stress-strain curve, ductility (and the ductile-to-brittle-transition temperature) and cycle fatigue.

Displacement (dpa) hardening/embrittlement

Present data indicate that radiation-hardening embrittlement under irradiation occurs for both reference materials, in particular for irradiation below 400°C. The temperature dependence is due to annealing effects in the lattice. Experimentally, the reduction of final elongation under tensile tests, which acts as a measure for the ductility, is found to depend on the irradiation temperature. It seems to reach a maximum for irradiation at 250°C but data between 250°C and 400°C are scarce. Yet, even at doses up to 50 dpa there is still some ductility (5%-6%). To fill the gap between 250°C and 400°C, a new irradiation at 325°C has been committed in the fast neutron reactor BOR 60.

He/H hardening/embrittlement

While being exposed to the radiation field, the structural materials are involved in the spallation reaction, giving rise to a range of new isotopes in the metallic matrix. Helium and hydrogen are among the most produced and both cause material hardening and embrittlement. The material degradation due to the presence of alien elements is in principle independent and supplemental to the contribution coming from displacement damage. The concentration of the induced elements in the lattice depends on the production rate and their mobility in the matrix up to the outgassing surface. This is the reason why helium, although it is produced less than hydrogen, is expected to be more damaging. The mobility factor is, together with the annealing effect, responsible for the observed temperature dependence. As before, low temperature can cause higher susceptibility. The temperature range indicated above for displacement damage is valid here as well.

Swelling and creep

Investigations in the fields of advanced fast reactors and nuclear fusion form the basis of the knowledge regarding swelling and creep behavior of T91 and SS 316L under irradiation. Actually, the basic reason for selecting T91 as the martensitic steel reference material is the improved behavior concerning swelling and creep effects under irradiation, compared with the behaviour of austenitic steels like SS 316L under the same conditions. Irradiations at 400°C, up to 49 dpa, have shown that swelling is small (<0.01%/dpa) for T91 while for SS 316L much higher values have been measured. It should be noted however, that for a high energy (600-1 000 MeV) mixed proton and neutron spectrum, the nuclear reaction chain is quite different and its effect on swelling and creep must be investigated.

Susceptibility to LBE/radiation synergy

Up to now, there is no clear evidence on the effect of the synergy between the degrading effects on the structural material caused by exposure to LBE and those originating from proton/neutron irradiation exist. Solid information can only be achieved by performing irradiation experiments of

materials exposed to LBE. These studies are planned within the IP-EUROTRANS project and also in fully prototype target tests as MEGAPIE.

3.4.2 Window versus windowless spallation target design issues

As mentioned above, an important consideration in present designs of megawatt spallation targets for ADS is the difference between window and windowless design approaches. In the first option, a physical separation between the accelerator beam line and the target zone is provided by a metal window. The window forms a cutoff between the transport beam line vacuum and the target material, and defines the position and shape of the target surface. The most difficult technical challenge for this design option is to ensure the integral stability and reliably of the metallic target under very harsh conditions. These combine cyclic thermal loads, exposure to (potentially) highly corrosive liquid LBE eutectic, and a very hard and intense mixed proton/neutron field including direct impingement of the accelerator beam. As a result of these factors, window embrittlement and lifetime is a major concern.

Radiation damage calculations were performed within the PDS-XADS initiative for the window target option in the gas cooled reactor.[95] These calculations indicate that for the envisioned 600 MeV, 6 mA proton beam impinging on an LBE target, the target window will suffer damage at the level of 210 dpa per year. The bulk of this value (about 85%) is due to neutrons. It should be noted, however, that He effects (embrittlement, void swelling, and creep) are yet to be added to the analyses. If one uses an estimated operational limit for existing ferritic/martensitic steels of about 80 dpa, as was done in this assessment, it turns out that the target window should be replaced at least every 5-6 months.

Identifying and testing suitable materials for use in a spallation target window is one of the important tasks in the EC FP5 SPIRE project that is presently underway. Preliminary results indicate that the ferritic/martensitic steels (like T91) seem to be adequate. In addition, oxide dispersion strengthening, which is expected to increase the window lifetime, is being investigated. In any case, a definite assessment must await the final analyses of the materials after full completion of the irradiation program.[19]

In the windowless design option, the absence of a physical barrier implies that the beam line and target material share a common vacuum, and that confinement of volatile spallation products must be incorporated as an integral property of the vacuum system. Assuming a vertical beam insertion geometry, the target material itself is kept in place by gravity while the target surface is defined by the free liquid metal flow.

In principle, vacuum compatibility of the interface between the beam line and the target is achieved when the proton beam can reach the target material without significant interference or degradation. The maximum pressure that is tolerable in the region above the target surface is 10^{-4} to 10^{-3} mbar. Above this pressure, plasma would be formed from the interaction of the proton beam with the gases and vapors evolving from the spallation target. The concern is that a destructive positive feedback process could occur, because the plasma electrons and ions have enough energy to induce desorption of atoms from the beam line wall. These, in turn would generate more plasma, and a run-away effect could take place. Also, an intense plasma would cause sputtering of the structural materials in the beam-entry region, producing an additional thermal load on the beam pipe walls. The

95. Abanades, A. *et al.* (2004), *Heat Deposition and Materials Damage in the Window target of the Gas Cooled Reactor Core*, PDS-XADS Workpackage 4.3, Deliverable 04/61. Oral presentation at the 6th Technical meeting on PDS-XADS Workpackage 4.3, 24 March 2004, Karlsruhe.

need to avoid plasma formation requires that the pumping speed at the beam line/target interface must be sufficient to maintain the pressure below the critical region.

The contributors to the atmosphere above the target are the outgassing of dissolved elements, evaporation of the liquid metal, and emanation of volatile spallation products. Experiments combined with calculations on this topic performed at SCK•CEN in Mol, Belgium and at the polytechnic university of Milan, Italy have shown that at 400°C, the outgassing of LBE can be reduced to a level where it is comparable to the liquid metal evaporation rate. The estimated production rate of spallation products in the target is not sufficient to cause any difficulties as far as the vacuum interface is concerned.[96]

The absence of a target window removes the containment barrier that prevents radioactive spallation products evolving from the target face from migrating up the beam line. To eliminate this migration, the vacuum system at the end of the beam line must contain suitable trapping arrangements. A possible solution is a scheme in which the vacuum above the spallation target is maintained by cryopumping, with each of the cryopumps periodically regenerated by a turbopump that is backed by a small getter pump. The getter pump may then be treated as radioactive waste. For safety reasons, a similar vacuum engineering solution will likely be required even in the case of a window target design. In order to develop the design of the beam line/target interface vacuum system, rates of LBE evaporation and deposition, the evolution rates of volatile spallation products, and the gas dynamics of the beam line geometry have to be thoroughly understood.

In a windowless spallation target the liquid-metal surface is formed, not by a physical shape, as in the window target situation, but by the free flow of the LBE through a properly designed nozzle. In order to avoid excessive evaporation at the target surface, surface temperatures should be kept low (< 450°C for LBE). To accomplish this, the target nozzle should be designed to optimise convective removal of the heat deposited by the beam. Heat deposition in recirculation or stagnant zones should be minimised, as it would lead to the formation of hot spots. This is accomplished by excluding or minimising such zones in the design of the liquid-metal flow guide. In addition, the time-averaged beam profile can be tailored to avoid them, either by a beam rastering system or by non-linear optics near the end of the beam line. In addition to controlling target-material evaporation, the release of HLM droplets from the surface should be prevented by design. For a vertical target flow, which is the most sensitive in terms of creating recirculation zones and emitting droplets, a possible mitigation procedure might be to add a few percent of swirl to the flow for stabilisation.[97]

Radiation streaming (mainly by neutron flux) occurs from the core towards the reactor roof, through the beam pipe. In order to limit the streaming inside the beam pipe, its overall size must be kept as small as possible.

The results of the neutron streaming with a proton beam pipe of 200 mm diameter for the European LBE-cooled ADS show that in normal operation no access is possible at reactor roof level and that with reactor at shutdown and after some days of cooling access is possible, but limited to few hours.

---

96. Schuurmans, P. *et al.* (2003), *VICE, R&D support for a Windowless Spallation Target in MYRRHA*, Proceedings of the International Workshop on P&T and ADS Development 2003, ISBN 9076971072, SCK•CEN, Mol.

97. Van Tichelen, K. *et al.* (2003), *The MYRRHA Windowless Target: R&D on Thermohydraulics*, Proceedings of the International Workshop on P&T and ADS Development 2003, ISBN 9076971072, SCK•CEN, Mol.

In the case of the windowless target unit the beam pipe cross-section can be fairly small (from 5 x 4 cm^2 at the top to 12 x 5 cm^2 at the LBE bottom), significantly improving the accessibility at eactor roof level after shutdown for refueling and handling operations.

3.5 Target performance

3.5.1 Neutron yield and energy deposition

The main purpose of the high power spallation target in an ADS is to provide the primary neutron flux for driving the fission process in the surrounding subcritical core. For this reason the neutron yield is an important consideration in selecting the energy and current parameters of the proton beam. Experimental data, Figure 3.9, show that in the energy range relevant for ADS (300-1 000 MeV) the neutron yield per incident proton (n/p) scales approximately as $E_{proton}^{3/2}$ (with E_{proton} in MeV). Thus, for a given neutron yield, lower beam current is required at higher beam energy. An advantage of higher beam energy is greater penetration depth in the target, leading to lower axial power densities. The reduced relative importance of the Bragg peak (compared with meson production) shifts the beam heating profile towards the target surface, but does not cause a problem except at lower energies. Although the energy deposition at the surface per proton increases at higher energies, this effect is compensated by the reduced current requirement. In addition, a lower fraction of the total beam power is deposited as heat in the target at higher proton energies. However, a penalty for higher beam energy and lower current may be increased accelerator cost.

Figure 3.9. A compilation of thick-target n/p values for p + Pb & Pb-Bi at intermediate energy

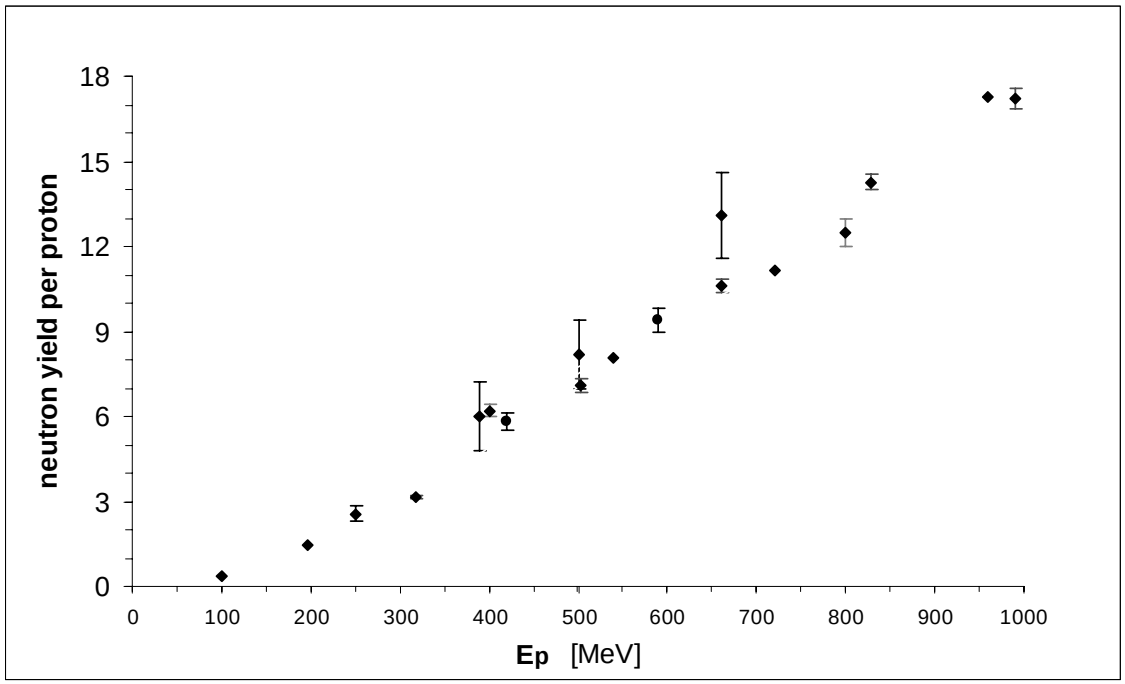

3.5.2 Spallation products and radiotoxicity

Radiotoxic nuclides are produced directly from spallation reactions in the target LBE, and bombardment of the target by spallation neutrons as well as neutrons produced in the subcritical core. These nuclides build up in the LBE target material during operation. Theoretical calculations were performed in the framework of the PDS-XADS initiative for a 600 MeV, 6 mA proton beam impinging on an LBE target, assuming an operational period of 20 years. They show that the major long-term contributors to the radiotoxicity of the spallation target are: ^{210}Po, ^{194}Hg, ^{207}Bi, ^{204}Tl, ^{90}Sr, ^{3}H, ^{210m}Bi, ^{205}Bi, ^{206}Bi, ^{210}Bi and ^{197}Hg.[98]

During operation, ^{210}Po provides the largest single contribution to the total target radiotoxicity. During the first eight years after shutdown, ^{210}Po remains the dominant radiotoxicity source, although its strength is reduced by five orders of magnitude. The volatile isotope ^{194}Hg takes over during the decay period from 10 to 1 000 years after shutdown. After that time, ^{210}Po again dominates the radiotoxicity curve, for a period of more than 1 million years. In this time period, the ^{210}Po is produced by decay of the long-lived isomer ^{210m}Bi. Care must be taken when calculating radiotoxicity levels since the theoretical assessment of ^{210}Po production rates suffers from a large uncertainty (up to a factor of two) in the relevant cross sections.

3.5.3 Spallation neutron spectrum

Figure 3.10 displays the overall neutron spectrum of a primary spallation-source along with the components of this spectrum from various birth channels: the intra-nuclear cascade (INC), the pre-equilibrium and the evaporation neutrons for a 350 MeV proton beam fired upon a Pb-Bi target.[99] For higher proton energies, similar curve shapes are obtained.

A typical fission neutron spectrum is shown in the same figure. The spallation neutron spectrum is not very different from a typical fission neutron spectrum with most neutrons emerging with energies between 1 and 2 MeV. However, a very distinct difference is found in the presence of a tail of high-energy neutrons with an energy over 20 MeV that reaches up to full energy of incident protons. The contribution of the high energy tail is about 10 % of the total spectrum.

Finally, the evaporation neutrons constitute the major part (70%) of the total number of neutrons and show a fission-like energy spectrum.

98. Cetnar, J. *et al*. (2004), *Analyses for radiotoxicity assessment of the target module*, PDS-XADS W.P. 4.3, Deliverable 04/060.2, 2004. Available at http://www.sckcen.be/ADOPT.

99. Malambu, E. *et al*. (2002), *Status of neutronics analysis of the MYRRHA ADS*, SCK•CEN report R-3593, SCK•CEN, 21 March 2002, Mol.

Figure 3.10. Spallation neutron spectrum (E_{proton} = 350 MeV, Pb-Bi target) vs. fission spectrum

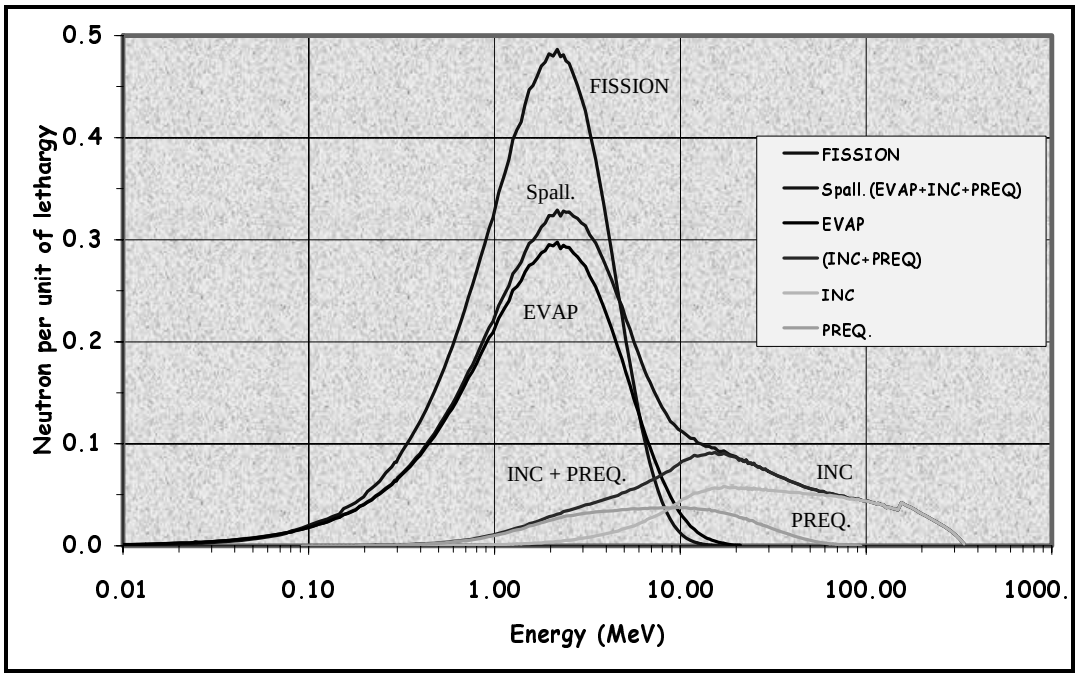

3.6 Thermal-hydraulics

3.6.1 Cooling

The power generated by spallation reactions in the target must be removed to prevent overheating of the target coolant, primary coolant or structures. The method of heat removal from the target coolant will depend on the design chosen for the target unit and the primary coolant.

For the window target option, the heat generated by the spallation reactions can be removed by natural convection and forced circulation. For the first case, special attention has to be paid to the start-up procedure. For windowless target concept, a natural circulation pattern in the cooling circuit is not feasible because the beam line vacuum represents an interruption of the spallation loop which prevents natural circulation. In case of a LBE cooled ADS, the reactor primary LBE can be used as coolant for the target LBE, on the condition that window and surface temperatures can be kept sufficiently low. In most window designs, this condition cannot be fulfilled. In this case, an independent cooling circuit for the target Pi-Bi is necessary. This is also the case for all gas cooled ADS. Generally, a diathermic fluid is preferred. Low-pressure water and pressurised water can also be considered.

3.6.2 Hydraulics and heat transfer

In order to correctly estimate the cooling capacity of an HLM heat exchanger, or to predict the temperature at a target window or free target surface, reliable correlations predicting the heat transfer coefficients are needed. To generate these correlations, appropriate experiments have been conceived, and these are planned to be carried out within the framework of IP-EUROTRANS, following the assessment in the 5th FP ASCHLIM[7] initiative, but a substantial effort is still needed in this field.

Existing computational fluid dynamics codes have shortcomings in terms of how they model HLM turbulent heat transfer as well as modeling of free-surface and two-phase flows. However, these problems are addressed in several on-going and future research programs.[100]

3.7 Safety

In an ADS, the power level is mainly controlled by the accelerator. The ability to shut down the beam rapidly and reliably on demand is essential for safety aspects in the subcritical reactor. Several means of shutting down the proton beam can be provided, such as:[101]

- inhibiting operation of key accelerator system components, such as the injector;
- use of dipole magnets to divert the beam in the transport line to a beam dump;
- introduction of a physical barrier in the transport line to block the beam;
- shutting off electric power to the accelerator as a whole.

Any system provided to perform one of these roles would be expected to be a high quality safety-class system with multiple redundancy. It is essential that there would be adequate monitoring devices to measure relevant target parameters, and provide automatic initiation signals for shutdown. Development of a passive fail-safe system that trips the beam automatically in cases of abnormal and dangerous evolution of subcritical core parameters would increase confidence in shutdown reliability and is a necessary requirement.

The proton beam is a source of activation of the target structures and target material (e.g. ^{210}Po from Bi by proton irradiation), which has to be taken into account in the radiological protection of the ADS facility workers. The radioactive spallation products generated within the target must be kept confined within the target unit to prevent contamination of the primary coolant and the accelerator beam pipe.

For the window target concept, the window forms a physical barrier between the target LBE and the beam vacuum. However, since it necessarily is relatively thin, the window is a weak point of the containment, and the possibility of rupture must be taken into account.[102] A window rupture would produce a situation similar to that which exists continuously in the windowless target concept. Thus, all designs must include features that inhibit migration of radioactive material along the beam line. The barrier for prevention of contamination of the beam-transport line and ultimately the accelerator must include trapping systems in the beam line vacuum (as noted above), as well as fast-acting valves that are triggered when a target anomaly is sensed.

Heat removal from the ADS target coolant is required during normal operation at power, and in incidental or accidental conditions because of the spallation and activation products decay-heat in the

100. Proceedings of the IAEA Technical Meeting on "Theoretical studies of Heavy Liquid Metal Thermal Hydraulics", FZK, 28-31 October 2003, Germany (to be published).

101. Peers, K. *et al.* (2003), *System Classification*, PDS-XADS Project, Workpackage 2.3, Deliverable 03/21, 5th Framework Program of the European Commission, 2003.
Available at http://www.sckcen.be/ADOPT.

102. Ehster, S. *et al.* (2003), *The Integrated Safety Approach – Goals – Principles, Rules for Assessment, Safety Design and Criteria*, PDS-XADS Project, Workpackage 2.1, Deliverable 03/006, 2003. Available at http://www.sckcen.be/ADOPT.

target. Failure of this safety function would threaten the target unit integrity and could lead to release of spallation products. Target-coolant heat removal would be challenged by a loss of coolant circulation or coolant, or by a fault with the secondary cooling system. Because the amount of afterheat is small (less than 1% of the full power level), the target cooling issues in this faulted condition is manageable. A target cooling system using natural circulation can be considered as inherently safer against a loss of decay heat removal.

Chapter 4

CONCLUSIONS AND RECOMMENDATIONS

The optimum proton energy for production of neutrons by spallation in a heavy metal target, in terms of costs, target heating, and system efficiency, lies in the range 600 to 1 000 MeV. Two completely different kinds of machines can be considered for acceleration of high currents of protons to an energy of 600-1 000 MeV: linear accelerators (linacs) and cyclotrons. Cyclotrons of the PSI type should be considered as the natural and cost effective choice for preliminary lower power XADS experiments where availability and reliability requirements are not necessarily among the driving functions. CW linear accelerators will be the baseline technology for XADS demonstration facilities and full-scale industrial ADS plants, because of their high potential for achieving the required level of beam reliability and availability, and also because of their power upgrade capability. Linac beam theory and recent technology advances have confirmed that a linac capable of delivering up to 100 MW at 1 GeV is a relatively direct extension of existing technology.

For ADS applications involving a few tens of megawatts, HLM is the target-material of choice at present. This selection is principally driven by the need for high-neutron yield per proton, the high power deposition densities reached within the target, and compatibility of the target material with structural materials. Both window and windowless target concepts are currently being investigated in ongoing ADS design projects worldwide. However, the constraints introduced by a window in terms of the required subcritical-core working temperature, the need of frequent window replacement, and/or the need for an extra cooling loop for the spallation target have raised major design challenges for this approach. These concerns are reinforcing an R&D effort aimed at solving key design issues for the windowless target concept, namely compatibility of the beamline vacuum and target outgassing, and control of spallation products evolved from the target, and of HLM evaporated from the target surface. These R&D efforts are not dedicated exclusively to supporting the windowless target concept, but also address the safety issues arising from a possible window rupture in the window target case. Therefore, it is recommended that there should be a strong and sustained R&D effort in this area. The development of structural materials that are resistant to HLM corrosion at high temperatures is also an important R&D area, as well as R&D leading to development of corrosion-inhibiting surface. This kind of materials R&D is very open to a broad international collaboration, as the key issues are common to ADS, fusion reactor technology development, and the development of next generation advanced fission reactors.

LIST OF CONTRIBUTORS

Chair

Richard Sheffield	(LANL, USA)

Scientific Secretary

Byung-Chan Na	(OECD/NEA)

Chapter 1: Scientific Secretary

Richard Sheffield	(LANL, USA)

Chapter 2: Accelerator Technology for XADS and ADS Applications

Richard Sheffield	(LANL, USA)
George Lawrence	(LANL, USA)
Kemal Pasamehmetoglu	(LANL, USA)
Paolo Pierini	(INFN, Italy)
Guillaume Olry	(IPN, France)
Alex C. Mueller	(IPN, France)

Chapter 3: Spallation Targets for ADS Applications

Paul Schuurmans	(SCK•CEN, Belgium)
Katrien Van Tichelen	(SCK•CEN, Belgium)
Luciano Cinotti	(Ansaldo, Italy)

Chapter 4: Conclusions and Recommendations

Richard Sheffield	(LANL, USA)

Reviewers

Richard Sheffield	(LANL, USA)
Luciano Cinotti	(Ansaldo, Italy)

MEMBERS OF THE SUBGROUP

BELGIUM	
AIT ABDERRAHIM, Hamid	SCK•CEN
FRANCE	
LAFFONT, Guy	CEA-Cadarache
LAGNIEL, Jean-Michel	CEA-DAM
MUELLER, Alex	Institut de Physique Nucléaire
GERMANY	
BAUER, Guenter S.	ESS
KNEBEL, Joachim U.	Forschungszentrum Karlsruhe GmbH
ITALY	
CINOTTI, Luciano	Ansaldo Nucleare
PAGANI, Carlo	INFN-University of Milano-LASA
PICARDI, Luigi	ENEA
PIERINI, Paolo	INFN-University of Milano-LASA
JAPAN	
HASEGAWA, Kazuo	Japan Atomic Energy Research Institute (JAERI)
OUCHI, Nobuo	Japan Atomic Energy Research Institute (JAERI)
KOREA (Republic of)	
SONG, Tae-Yung	Korea Atomic Energy Research Institute (KAERI)
SWEDEN	
ERIKSSON, Marcus	Royal Institute of Technology
SWITZERLAND	
SIGG, Peter	Paul Scherrer Institute (PSI)
UNITED STATES	
CAPPIELLO, Michael W.	Los Alamos National Laboratory (LANL)
FINCK, Phillip J.	Argonne National Laboratory (ANL)
LAWRENCE, George	Los Alamos National Laboratory (LANL)
LI, Ning	Los Alamos National Laboratory (LANL)
LYNCH, Michael T.	Los Alamos National Laboratory (LANL)
MALOY, Stuart	Los Alamos National Laboratory (LANL)
PASAMEHMETOGLU, Kemal	Los Alamos National Laboratory (LANL)
PITCHER, Eric	Los Alamos National Laboratory (LANL)
SHEFFIELD, Richard (Chair)	Los Alamos National Laboratory (LANL)

TALEYARKHAN, Rusi P.	Oak Ridge National Laboratory (ORNL)
WANGLER, Thomas	Los Alamos National Laboratory (LANL)

INTERNATIONAL ORGANISATION

NA, Byung Chan (Secretary)	OECD Nuclear Energy Agency (NEA)

OECD PUBLICATIONS, 2 rue André-Pascal, 75775 PARIS CEDEX 16
Printed in France.